TAMPEREEN TEKNILLINEN YLIOPISTO
TAMPERE UNIVERSITY OF TECHNOLOGY

Esa J. Saarinen

# Optical Pulse Generation with Semiconductor Disk Lasers

Julkaisu 1056 • Publication 1056

Tampere 2012

Tampereen teknillinen yliopisto. Julkaisu 1056
Tampere University of Technology. Publication 1056

Esa J. Saarinen

# Optical Pulse Generation with Semiconductor Disk Lasers

Thesis for the degree of Doctor of Science in Technology to be presented with due permission for public examination and criticism in Tietotalo Building, Auditorium TB103, at Tampere University of Technology, on the 21st of June 2012, at 12 noon.

Tampereen teknillinen yliopisto - Tampere University of Technology
Tampere 2012

ISBN 978-952-15-2868-2 (printed)
ISBN 978-952-15-2882-8 (PDF)
ISSN 1459-2045

# Abstract

Optical pulses are used as bits to transmit information. Controlled pulse generation is required for error-free communication and data processing. Semiconductor disk lasers (SDLs) are compact light sources that have shown potential for inexpensively generating intense but focusable ultrashort light pulses of a chosen color at gigahertz repetition rates.

In this thesis, the generation of light pulses with SDLs is studied. Different methods for initiating pulsed operation are reviewed. A state-of-the-art high-power picosecond pulse source emitting in the 1.55-$\mu$m telecommunications band is demonstrated by employing wafer fusion technology and advanced heat management in an SDL pulsed with a dilute nitride semiconductor saturable absorber mirror (SESAM). A simple way to generate picosecond pulses from an SDL by feeding frequency-shifted light back to the gain element of the laser is presented. The dominant way to generate pulses from SDLs, using a SESAM to organize the phases of the lasing cavity modes, is studied in detail. Models for pulse shaping in such passively mode-locked SDLs are reviewed. Stable mode locking (ML) at a very low saturation of absorption, relevant for SDLs pursuing high pulse repetition rates, is demonstrated and qualitatively explained. The regime of harmonic ML where multiple pulses circulate in the SDL cavity is reported and investigated both experimentally and numerically. Saturation and fast recovery of the gain are identified as being responsible for the strong ordering of pulses and for the changes in pulse characteristics observed between states with different numbers of pulses in the cavity. Hysteresis in the properties of the optical output is observed and controlled by tailoring the SDL gain element design. The presented results provide a means to precisely manipulate pulse characteristics in SDLs, paving the way for flexible high-speed data transfer and processing.

# Acknowledgments

The results compiled in this thesis represent the essential parts of the work I carried out at the Optoelectronics Research Centre (ORC), Tampere University of Technology, during the years 2007 - 2011. The research was financed through numerous projects funded by the European Commission, the Academy of Finland, and the Finnish Funding Agency for Technology and Innovation (TEKES), to which I wish to express my gratitude. On a personal level I would like to thank the Graduate School of Modern Optics and Photonics, the Finnish Foundation for Technology Promotion, the KAUTE foundation, and the Finnish Academy of Science and Letters for the financial support they have provided.

At the ORC I have had the privilege to work with world-class scientists. I am deeply indebted to my supervisor, Prof. Oleg Okhotnikov, for the sincere guidance he so generously offers to his students and for his ever passionate commitment towards research. Special thanks go to the former longtime director of ORC, Prof. Emeritus Markus Pessa, for initiating my scientific career when hiring me as a summer student back in 2004. I would also like to thank the current director of ORC, Dr. Pekka Savolainen, for keeping the organizational wheels and money taps running smoothly. The development manager Anne Viherkoski and secretary Eija Heliniemi are thanked for the work they do to control the administrative issues. Prof. Mircea Guina deserves big thanks for providing me with a chance to pretend to be a company worker and for being a living example of work drive.

Warm thanks go to the former members of the Ultrafast and Intense Optics (UIO) Group, especially to Dr. Robert Herda for his contributions to the pulse dynamics simulations presented in this thesis, to Drs. Tommi Hakulinen and Samuli Kivistö for all the help in the lab and for the precise nonlinear reflectivity measurements they performed

for my SESAM samples, to Dr. Antti Isomäki for tutoring me with dispersion measurements, and to Dr. Antti Härkönen for letting me to draw upon his vast expertise on everything related to research, or not related. I am grateful to Dr. Lasse Orsila and Jari Nikkinen for the top-quality work with the simulation and deposition of dielectric coatings. A special thanks goes to Dr. Charis Turtiainen for improving the English of my writing.

The pre-examiners of this thesis, Prof. Markku Sopanen and Dr. Stéphane Calvez, are thanked for their insightful comments.

The present members of the UIO group, Antti Rantamäki, Alexander Chamorovskiy, Dr. Jussi Rautiainen, Juho Kerttula and Regina Gumenyuk, thank you for sharing with me life as a PhD student in the UIO Group and for your companionship in and outside the lab.

The long hours the semiconductor crystal growers have spent fine tuning the reactors for the ultimate performance manifest themselves in the results presented in this thesis. Huge thanks to you, Dr. Jari Lyytikäinen, Dr. Soile Suomalainen, Janne Puustinen, and others.

I thank all the colleagues at the ORC, especially those who are unjustly left unacknowledged, for the inspiring working atmosphere.

The collaborators at the École Polytechnique Fédérale de Lausanne are gratefully acknowledged for their superior expertise in fusing wafers.

The role of dear fellow MSc students in my decision to pursue a PhD in Hervanta cannot be overestimated. Thank you, all the members of the #bukkis group.

Finally, I would like to express my gratitude to my family, mother Raija, father Reima, little sister Essi, and grandma Liisa, for the never-ending support and love. Comparable recognition is given to all other relatives and close friends who have had faith in me during the years.

Last, I thank Miru for the light she has brought me.

*Tampere, April 2012*
*Esa J. Saarinen*

# Contents

# List of publications

This thesis is a compendium, which contains some unpublished material, but is mainly based on the following papers published in open literature. These publications are included as appendices and in the text they are referred to as [P1]...[P6].

[P1] E. J. Saarinen, J. Puustinen, A. Sirbu, A. Mereuta, A. Caliman, E. Kapon, and O. G. Okhotnikov, "Power-scalable 1.57 $\mu$m mode-locked semiconductor disk laser using wafer fusion," *Optics Letters*, vol. 34, no. 20, pp. 3139–3141, 2009.

[P2] E. J. Saarinen, J. Nikkinen, and O. G. Okhotnikov, "Semiconductor disk laser with frequency-shifted feedback," *IEEE Photonics Technology Letters*, vol. 23, no. 9, pp. 567–569, 2011.

[P3] E. J. Saarinen, J. Nikkinen, and O. G. Okhotnikov, "Mode-locked semiconductor disk lasers with weakly saturated absorbers," *Optics Communications*, vol. 285, no. 10–11, pp. 2688–2692, 2012.

[P4] E. J. Saarinen, A. Härkönen, R. Herda, L. Orsila, T. Hakulinen, M. Guina, and O. G. Okhotnikov, "Harmonically mode-locked VECSELs for multi-GHz pulse train generation," *Optics Express*, vol. 15, no. 3, pp. 955–964, 2007.

[P5] E. J. Saarinen, R. Herda, and O. G. Okhotnikov, "Dynamics of pulse formation in mode-locked semiconductor disk lasers," *Journal of the Optical Society of America B*, vol. 24, no. 11, pp. 2784–2790, 2007.

[P6] E. J. Saarinen, J. Lyytikäinen, and O. G. Okhotnikov, "Hysteresis and multiple pulsing in a semiconductor disk laser with a saturable absorber," *Physical Review E*, vol. 78, no. 1, p. 016207, 2008.

# Author's contribution

The work presented in this dissertation is essentially teamwork. The author's role in these joint efforts has been to process the semiconductor samples, to design and build the semiconductor disk laser setups and test beds for laser characterization, to collect the data and to perform part of the simulations needed for analysis of the results. A summary of the author's contribution to research work and to manuscript preparation for the scientific papers included in the thesis is given in the table below.

Table 1: Author's contribution to the papers included in the thesis

| Paper # | Contribution to research work | Contribution to writing the paper |
|---|---|---|
| P1 | Group work (60 %) | Main author |
| P2 | Group work (80 %) | Main author |
| P3 | Group work (80 %) | Main author |
| P4 | Group work (50 %) | Main author |
| P5 | Group work (60 %) | Main author |
| P6 | Group work (80 %) | Main author |

# Supplementary publications

The following supplementary papers are related to this work, but are not included in this thesis. In the text, these publications are referred to as [S1]...[S8].


[S1] E. J. Saarinen, A. Härkönen, S. Suomalainen, and O. G. Okhotnikov, "Power scalable semiconductor disk laser using multiple gain cavity," *Optics Express*, vol. 14, no. 26, pp. 12868–12871, 2006.

[S2] E. J. Saarinen, J. Lyytikäinen, and O. G. Okhotnikov, "Optimization of resonant periodic gain structure for power scaling of semiconductor disk lasers," in *The 19$^{th}$ International Laser Physics Workshop 2010 (LPHYS'10)*, Foz do Iguaçu, Brazil, 5-9 July, 2010, seminar 4, p. 206.

[S3] E. J. Saarinen, J. Lyytikäinen, J. Rautiainen, V.-M. Korpijärvi, A. Sirbu, A. Mereuta, A.Caliman, E. Kapon, and O. G. Okhotnikov, "1.57 $\mu$m passively mode-locked wafer-fused semiconductor disk laser," in *CLEO Europe 2009*, Münich, Germany, 14-19 June, 2009, paper CB5.4.

[S4] E. J. Saarinen, J. Lyytikäinen, and O. G. Okhotnikov, "Bistable mode-locking in a semiconductor disk laser," in *CLEO 2008*, San Jose, USA, 4-9 May, 2008, paper CFP4.

[S5] E. J. Saarinen, A. Härkönen, R. Herda, S. Suomalainen, L. Orsila, T. Hakulinen, M. Guina, and O. G. Okhotnikov, "Harmonically mode-locked semiconductor disk lasers with multi-GHz repetition rate," in *CLEO Europe 2007*, Münich, Germany, 17-22 June, 2007, paper CB13-2-THU.

[S6] E. J. Saarinen, A. Härkönen, M. Guina, and O. G. Okhotnikov, "Power scalable semiconductor disk laser using multiple gain cavity," in *CLEO 2007*, Baltimore, USA, 6–11 May, 2007, paper CThEE6.

[S7] A. Rantamäki, E. J. Saarinen, J. Lyytikäinen, and O. G. Okhotnikov, "Multiple gain cavity for power scaling in passively mode-locked semiconductor disk laser," *Proceedings of SPIE*, vol. 7822, 782209, 2010.

[S8] O.G. Okhotnikov, A. Härkönen, E. Saarinen, J. Rautiainen, and M. Guina, "Advances in power scalable, tunable and mode-locked semiconductor disk lasers," *Proceedings of SPIE*, vol. 6451, 64510B, 2007.

# List of Abbreviations and Symbols

| | |
|---|---|
| AlAs | Aluminium-arsenide |
| AlGaAs | Aluminium-gallium-arsenide |
| AlGaSb | Aluminium-gallium-antimonide |
| AOM | Acousto-optic modulator |
| APM | Additive pulse mode locking |
| AR | Antireflective |
| AuSn | Gold tin |
| CW | Continuous wave |
| DBR | Distributed Bragg reflector |
| EC | External compression |
| EP | Electrically-pumped |
| FS | Fused silica |
| FSF | Frequency-shifted feedback |
| FWHM | Full width at half maximum |
| GaAs | Gallium-arsenide |
| GDD | Group delay dispersion |
| GaInAsSb | Gallium-indium-arsenide-antimonide |
| GaInNAs | Gallium-indium-nitride-arsenide |
| GaSb | Gallium-antimonide |
| GTI | Gires-Tournois interferometer |
| HML | Harmonic mode locking |
| HR | High-reflection |

| | |
|---|---|
| ICHS | Intracavity heat spreader |
| InGaAs | Indium-gallium-arsenide |
| InP | Indium-phosphide |
| MBE | Molecular beam epitaxy |
| ML | Mode locking |
| MOVPE | Metalorganic vapor phase epitaxy |
| OC | Output coupler |
| ORC | Optoelectronics Research Centre |
| PL | Photoluminescence |
| QD | Quantum dot |
| QW | Quantum well |
| RF | Radio frequency |
| RoC | Radius of curvature |
| RPG | Resonant periodic gain |
| RT | Room temperature |
| SDL | Semiconductor disk laser |
| SESAM | Semiconductor saturable absorber mirror |
| $SiO_2$ | Silicon dioxide |
| SSDL | Solid-state disk laser |
| $TeO_2$ | Tellurium dioxide |
| $TiO_2$ | Titanium dioxide |
| TPA | Two-photon absorption |
| VECSEL | Vertical-external-cavity surface-emitting laser |

# Symbols, Greek alphabet

| | |
|---|---|
| $\alpha_0$ | Nonsaturable losses |
| $\alpha_G$ | Linewidth enhancement factor of the gain element |
| $\Delta R$ | Modulation depth |
| $\lambda$ | Wavelength |
| $\tau_A$ | Recovery time of absorption |
| $\tau_{FWHM}$ | Full width of the pulse at half of its maximum height |
| $\tau_G$ | Gain recovery time |
| $\Phi$ | Phase of the complex slowly varying electric field envelope |

# Symbols, other

| | |
|---|---|
| $A$ | Complex slowly varying electric field envelope |
| $D_2$ | Second order dispersion |
| $D_3$ | Third order dispersion |
| $E_A$ | Saturation energy of the absorber |
| $E_G$ | Saturation energy of the gain |
| $F_2$ | Inverse slope of two-photon absorption |
| $F_A$ | Saturation fluence of the absorber |
| $F_p$ | Pulse fluence |
| $g$ | Power gain coefficient |
| $g_0$ | Small-signal gain coefficient |
| $l_G$ | Intrinsic losses of the gain element |
| $M^2$ | Beam quality factor |
| $q$ | Power loss coefficient |
| $q_0$ | Unsaturated loss |
| $S$ | Saturation parameter $F_p/F_A$ |
| $T$ | Time in the rest frame of the pulse |
| $\tilde{z}$ | Normalized position |

# Chapter 1

# Introduction

People derive benefit from pulsed lasers in a variety of ways, of which high-speed data manipulation and transfer is the preeminent example. A major part of the bits forming the information exchanged around the world is carried by optical pulses in long-haul communication systems. In the near future, optical connections are expected to advance globally from intercontinental and metropolitan networks to local area networks, and eventually even to replace electrical wires inside computers.

Among all laser types, semiconductor lasers have been proven to be the most flexible, providing the required emission wavelength for numerous applications, along with a compact size and ease of use. When disk geometry is applied to a semiconductor laser having an external cavity, the optical power of the device can be scaled up to watt level without having to compromise the beam quality. A laser with such performance, producing ultrashort optical pulses at gigahertz repetition rates, makes a powerful tool for optical clocking via photonic interconnects between multicore microprocessors. Other interesting applications for this kind of laser include two-photon excitation microscopy for medical diagnostics, frequency comb generation for metrology, and terahertz time domain spectroscopy for material characterization.

Generation of optical pulses from a semiconductor disk laser (SDL), also known as a vertical-external-cavity surface-emitting laser (VECSEL), was already demonstrated in the early days of SDL research in 1990 [1]. The first SDLs – like most state-of-the-art SDLs today – took advantage of optical instead of electrical pumping, since uniform distribution of excited carriers over the whole gain area is easier to achieve by optical absorption than by current injection. In these early experiments the pump light was pulsed

and the gain sample was usually cooled down with liquid nitrogen, which resulted in a complicated and expensive system. Pulses generated by passive means, i.e., without external modulation of loss or gain, were not attained from SDLs until ten years later [2, 3] with the new tide of SDL research initiated by Kuznetsov et al. [4]. Since then, the pulse duration obtained from SDLs has reached the sub-ps level [5], the pulse repetition rate has been pushed beyond 100 GHz [6], and the average output power in pulsed operation has been scaled up to several watts [7].

The rapid progress in pulse generation from SDLs has been possible in part because the technology for pulse formation, readily available for the broadly studied solid-state lasers based on gain crystals doped with rare earth or transition metal ions [8, 9], could be transferred to SDLs with only minor modifications. In particular, the conceptual similarities SDLs share with solid-state disk lasers (SSDLs), at present the dominant pulse source for applications requiring high average power and pulse energy [10], have resulted in fruitful hand in hand development of both types of ultrafast oscillators [3, 11–13].

Although SDLs resemble SSDLs in terms of laser geometry and set-up, the characteristic properties of the semiconductor gain medium differ considerably from other solid-state gain materials. This has a notable impact on the design of an SDL pulse system. Specifically, the interplay of nonlinear effects taking place in the semiconductor elements in the SDL adds to the complexity of the system dynamics. The strong tendency of the semiconductor medium for stimulated emission, together with the short lifetime of excited carriers, results in inherently fast variations of gain and loss in pulsed operation. The shape, number and position in time of the laser pulses can be distinctly manipulated by these effects. Figure 1.1, adapted from Ref. [14], shows a simplified net of relations between some of the most significant parameters and effects in a typical semiconductor disk laser pulse system. The parameters presented in the figure will be discussed in more detail in the following chapters.

## 1.1 Incentives and aim of the thesis

The basis of the analysis of pulse formation in SDLs largely relies on the work conducted on pulsed lasers in general as early as the 1970's [15–19]. Many of the studies concerning the behavior of pulsed solid-state lasers carried out at the turn of the millenium can also be exploited to generate pulses from SDLs [20–22], provided that the nonlinearities

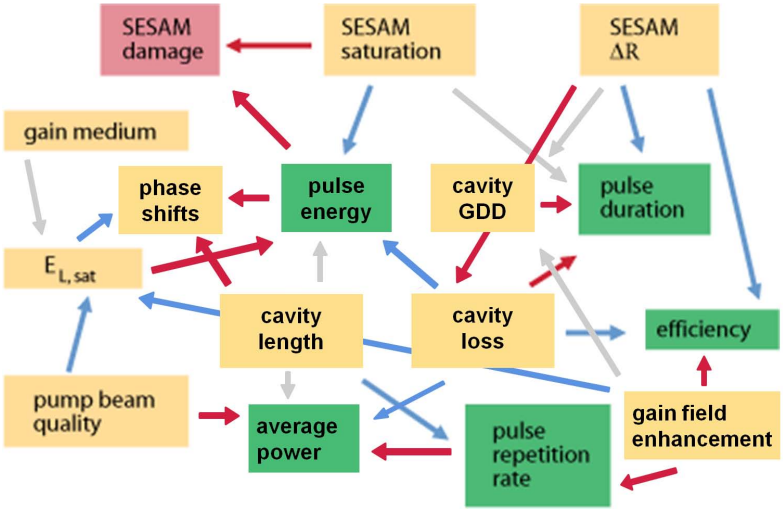


Figure 1.1: Simplified relations between operation parameters of a semiconductor disk laser pulse system, modified from Ref. [14]. Red, blue and grey arrows indicate positive, negative and twofold relations, respectively.

in the gain element of the laser due to strong gain saturation are taken into account. At the time when this doctoral work was initiated, a number of analyses had been published describing pulse generation in SDLs [13, 23, 24]. However, no experimental work had been conducted to systematically examine the pulse formation dynamics in these lasers.

It is the aim of this thesis to push the limits of pulse generation with SDLs. Novel technological approaches are implemented to demonstrate state-of-the-art picosecond SDLs. By means of systematic experimental studies, supported by numerical simulations, the relations between the operation parameters of pulsed SDLs are recognized and clarified. The objective is to gain a better understanding of the behavior of these ultrafast oscillators, and to allow the design and realization of optimized SDL pulse systems for each emerging application.

## 1.2 Thesis outline

This thesis is organized as follows. Chapter 2 discusses the general concept of an optically-pumped semiconductor disk laser. Emphasis is put on the design of the gain structure and on power scaling. Chapter 3 reviews the methods for pulse generation from

SDLs, concentrating on passive mode locking. A wafer-fused 1.57-$\mu$m picosecond SDL producing 0.86 W of average output power is introduced as an example of a state-of-the-art pulse source in the telecommunications band. A simple way to generate pulses using frequency-shifted feedback in an SDL is presented. Chapter 4 deals with the pulse formation and shaping processes in passively mode-locked SDLs. Mode locking in the regime of weak saturation of absorption, harmonic mode locking, pulse dynamics and hysteresis of the output characteristics are investigated. Concluding remarks are given in Chapter 5.

# Chapter 2

# Semiconductor disk lasers

In a nutshell, an optically-pumped semiconductor disk laser is a brightness converter that can be tailored to transform the multimode light from commercial low-cost pump diodes to a high-quality, single transverse mode beam at almost any wavelength from the visible to mid-infrared regime. Through frequency conversion, the spectral coverage of SDLs spans further to ultraviolet light. The basics of operation of SDLs, together with extensive reviews on the results obtained at the wavelengths demonstrated to date, can be found in scientific literature [25–33]. The next sections describe the architecture of the gain element and power scaling of SDLs with regard to aspects relevant to pulse generation. The SDL gain designs and power scaling methods used in this work are presented.

## 2.1 Gain structure design

The standard approach used to achieve efficient stimulated emission from optically-pumped semiconductor gain elements is to implement a resonant periodic gain (RPG) structure, where quantum wells (QWs) are positioned with the help of pump absorbing spacer layers and a carrier diffusion blocking window layer at antinodes of the signal optical field enhanced by a subcavity formed between a bottom distributed Bragg reflector (DBR) and the top surface of the structure [34–36, P6]. The length of the resonant subcavity is equal to a multiple of half the signal wavelength. The RPG design maximizes the overlap between the QWs and the optical field and increases the effective light-matter interaction length of the signal photons inside the gain section, resulting in high unsat-

urated and differential gain [26, 37, P6]. The QWs are often compressively strained to lower the threshold for lasing [38, 39]. Moreover, to facilitate uniform pumping of the wells and thereby further decrease the threshold, the QW distribution can loosely follow the density of excited carriers set by the nearly exponential decay of pump intensity in the semiconductor structure, with several QWs positioned at each antinode near the structure surface, and some QWs omitted from antinode sites deeper inside the structure where carrier density is low [40].

### 2.1.1 Optimization of the number of QWs in an RPG element

Typically, the number of quantum wells in the RPG section of an SDL varies between 2 and 20 [25,30]. The optimal number of QWs depends on the overall cavity design and is guided by constraints set by the application. For a given output coupling in continuous wave (CW) operation, one can estimate the most suitable number of QWs for achieving maximum output power at a given pump power from the equations for carrier density in semiconductor lasers [41, 42]. However, the simplified model presented in Ref. [42] assumes uniform carrier density over the QWs and does not take into account any thermal effects, making the model of little use for real-world devices whose performance is usually limited by thermal roll-over.

A large number of wells may be needed for efficient capture of excited carriers at high pumping levels, or in order to obtain increased single pass gain when dealing with challenging material systems or with lossy intra-cavity elements. On the other hand, a large number of wells implies a thick structure, which is difficult to pump uniformly. The gain may broaden due to unequal excited carrier density in the QWs, but if the overall laser cavity design does not allow for extremely short pulse durations the available excess frequency components can disturb generation of a clean pulse train [43, 44]. Furthermore, for a thick structure dispersion is increased and the gain bandwidth peaks sharply at subcavity resonances [13, 26].

A low number of QWs and the consequent thin gain section decreases nonlinear phase changes in the gain that may otherwise broaden pulses [23, 24, 45, 46]. The downside of the thin structure and the low number of QWs is pump leakage to the DBR, a reduced single pass and differential gain and the lower slope efficiency which limit maximum average output power and the use of such gain designs in applications involving high-loss cavities [32, 42, 47].

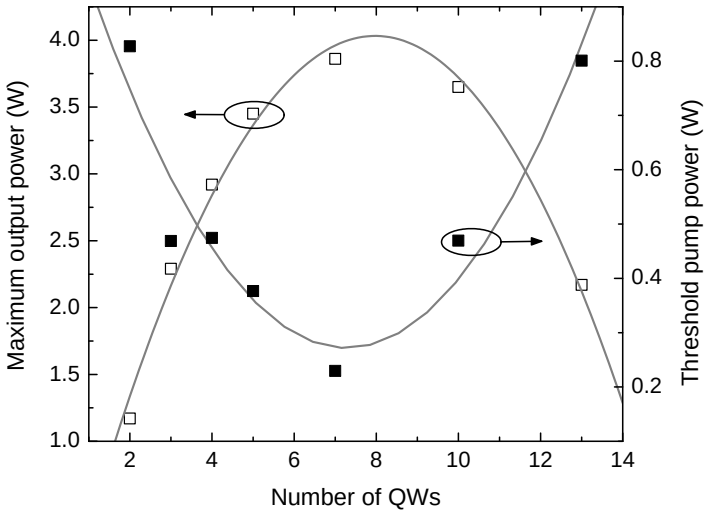


Figure 2.1: Maximum output power and lasing threshold with 3 % outcoupling versus number of QWs placed one per antinode in an RPG structure.

In Fig. 2.1 the experimental maximum average output power (open squares) and lasing threshold (filled squares) are plotted with respect to the number of quantum wells in an RPG structure having one QW per antinode of the standing wave optical field. The RPG design under study with a uniform distribution of QWs and pump absorbing spacer layers results in a pump intensity profile that decays exponentially with distance from the surface of the structure. Pump absorption in the gain section varies from around 50 % for the thinnest structure to close to 100 % for the structure with the largest number of QWs. A more detailed description of the assembly and design of the gain element used in the experiment can be found in [P5] and [S2]. The series of RPG structures were grown by molecular beam epitaxy (MBE), processed, and tested at 15 °C with an output coupler (OC) of 3 %. Scattering of the datapoints around the eye-guiding polynomial fittings can be attributed to the variation in detuning of the QW gain peak from the subcavity resonance wavelength at room temperature (RT) in the range of 10 – 29 nm between the gain samples due to fluctuations in growth. With an increase in temperature, the QW gain peak and the subcavity resonance in GaAs-based SDLs shift to longer wavelengths at rates of $\sim$0.3 nm/K and $\sim$0.1 nm/K, respectively, due to changes

in bandgap and refractive index [48–51]. A detuning optimized for maximum output power allows the QW gain and subcavity resonance to coincide close to the maximum pumping level and at the consequent elevated temperature. The threshold pump power in Fig. 2.1 shows a predictable dependence on the number of QWs. For a low number of QWs a notable part of the pump light is not absorbed in the gain section because of the thin absorbing region. Furthermore, the wells saturate quickly with increasing pump power and cannot efficiently produce the gain required for lasing. An increase in the number of wells enhances pump absorption and gain, which lowers the threshold pump power until at a certain number of QWs the losses associated with a thick structure, largely induced by signal absorption in the inadequately pumped bottom most wells, start to raise the threshold. The opposite trend can be observed in the dependence of the maximum output power on the number of QWs. The slope efficiency rises with the QW number, which amounts to a higher output power when the QW number is increased. However, thermal impedance and the decrease of gain at high pump powers due to shifting of the QW gain peak away from the resonance escalate with a thick structure, causing the maximum output power to drop at large QW numbers. From Fig. 2.1 one can conclude that for a standard RPG element in an SDL and for setups with outcoupling close to 3 %, approximately 7 or 8 QWs provide the best combination resulting in both a low threshold and high CW output performance. A design with either a lower or higher number of QWs could be considered for pulse generation or in applications requiring high power and a large tolerance for losses, respectively.

### 2.1.2 Manipulation of the single pass gain with a top DBR

The etalon formed in an RPG element between the bottom DBR and the semiconductor-air interface is essentially a Gires-Tournois interferometer (GTI) that can be modified by applying a partially reflective mirror on the surface of the semiconductor structure [52]. This enhances the optical field at the resonance wavelength and increases both gain and differential gain, enabling access to applications that require high tolerance for losses [32, P2]. Figure 2.2 shows the output characteristics with various OCs for an RPG element similar to those described in [P2] and [P5] with 5 QWs and a 66 % reflective dielectric coating deposited on its surface. As can be seen in the figure, with such a design losses of up to 20 % can be overcome, instead of the few percent observed for structures without a top mirror. The drawback of the design is the reduced gain band-

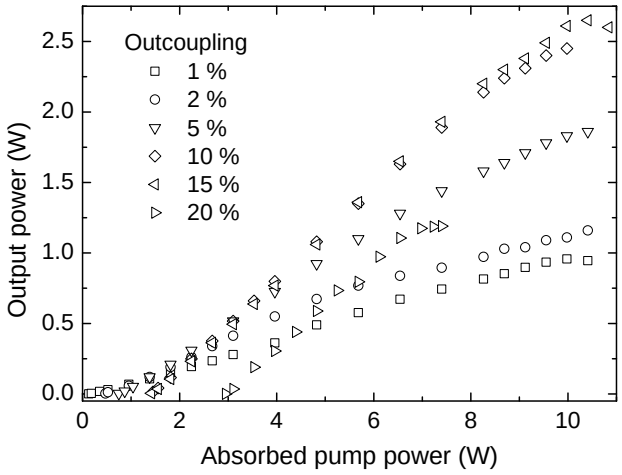


Figure 2.2: Average output power as a function of absorbed pump power for a 5-QW RPG element with 66 % reflectivity of the top surface and different OCs.

width and wavelength tunability, and the consequent increased sensitivity to the thermal shift of the QW gain maximum with respect to the narrow-linewidth resonance peak. The desired operating conditions occur within a limited range of pump power around the optimal point, beyond which thermal roll-over begins to lower the performance [13].

### 2.1.3 Subcavity effects on pulsed operation of SDLs

Adjustment of the GTI properties of the gain element by tailoring the gain section thickness or the reflectivity of the top surface of the gain element has a strong impact on various parameters relevant to pulse generation.

First, with an increase in the top reflectivity, a lower saturation fluence of the gain is expected, which together with the high differential gain results in a tendency for a pulsed SDL to switch to a higher number of pulses circulating inside the cavity for a more complete depletion of the fast recovering gain [P5, P6].

Second, an enhanced subcavity raises the gain only in a narrow spectral range that may not be able to support ultrashort pulses [13].

Third, the variations in the group delay dispersion (GDD) around the resonance wavelength build up with an increase in the top reflectivity or subcavity length, which

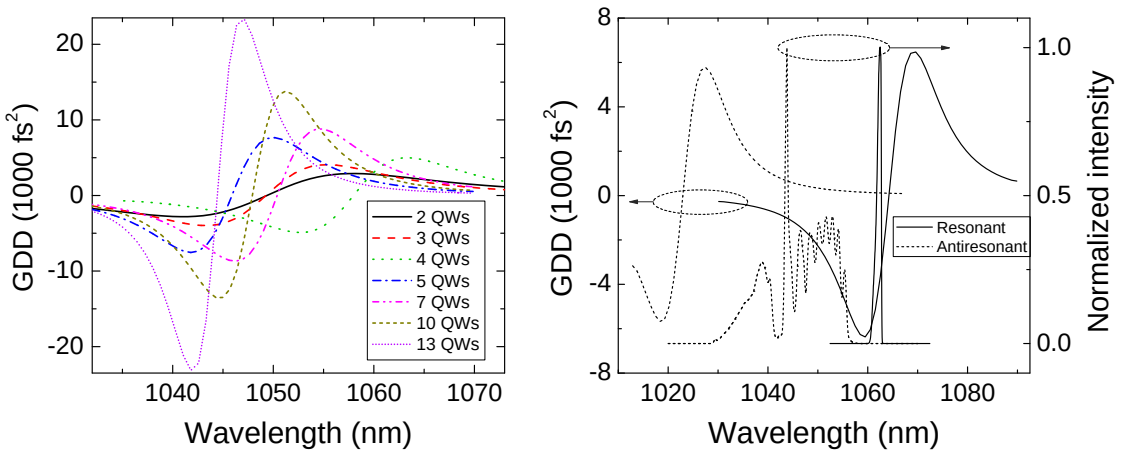


(a) (b)

Figure 2.3: (a) GDD for the RPG structures with different number of QWs. (b) GDD and optical spectrum at lasing threshold for an RPG structure with 5 QWs (solid lines) and a similar but antiresonant gain structure (dotted lines).

makes it challenging to avoid stretching of pulses in time when using gain structures with a strongly enhanced resonant subcavity [53]. Figure 2.3(a) shows GDD for a series of RPG structures with a different number of QWs. The design of the RPG samples is identical apart from the QW number and the thickness of the gain section defined by the number of QWs positioned one per antinode of the optical field. The GDD was extracted from the measurements of optical path length in the structure in reflection as a function of wavelength using a method similar to that described in Ref. [54]. Measurements were performed in the absence of optical pumping and laser action. It is apparent from Fig. 2.3(a) that the GDD for the resonant structures closely follows that expected for a GTI, with relatively small amplitudes around resonance measured for thin samples, and large amplitudes for thick samples.

Fourth, the nonlinear phase shifts associated with the refractive index changes during the pulse transit escalate with enhanced subcavity resonance and can cause pulse broadening and instabilities in pulsed operation if they are not properly balanced [55].

The resonance effects can be suppressed with an antireflective (AR) coating or by setting the thickness of the GTI subcavity such that a node of the optical field occurs at the surface of the gain element. With this kind of antiresonant design the scattering

losses due to non-vanishing surface roughness of the gain sample are decreased because of the low intensity of the optical field at the surface [26]. Furthermore, the effective gain bandwidth of such a device can be even broader than the intrinsic gain bandwidth of the QWs, since the subcavity resonances on both sides of the QW gain maximum enhance the wings of the gain peak [56]. However, the absolute optical field magnitude at the QWs will be much lower than with a resonant structure, resulting in low gain, low differential gain, and high threshold [56]. In Fig. 2.3(b) the GDD measured for a resonant (solid line) and antiresonant (dotted line) gain structure with 5 QWs is plotted together with the optical spectra recorded in pulsed operation close to threshold pump power. The designs of the gain structures are identical apart from the thickness of the cap layer used to adjust the subcavity length. For the antiresonant structure, the output wavelength of the laser is largely determined by the QW gain peak. For the resonant structure, the output wavelength is strongly bound to the subcavity resonance and follows the QW gain peak only to a certain extent. The subcavity resonance determines the point where the GDD turns from negative to positive with increasing wavelength. From Fig. 2.3(b) one can conclude that with an increase in pump power, the dispersion experienced by a pulse in the antiresonant structure gradually decreases when the QW gain peak thermally redshifts away from the resonance, whereas in the resonant structure the dispersion will undergo substantial variations with thermal changes in detuning.

### 2.1.4 Gain elements used in this doctoral work

Most of the semiconductor gain structures exploited in the experiments compiled in this thesis were RPG structures sharing a similar basic design with either one or two QWs placed per antinode of the optical field, starting from the first antinode below the surface of the structure [P1–P6]. In part of the experiments the GTI resonance inside the structure was either enhanced or suppressed with a top DBR or with an AR coating, respectively [P2–P4, P6]. This provided a simple but flexible configuration to study the fundamental effects related to gain saturation and their impact on pulse dynamics in SDLs [P3–P6]. Furthermore, with straightforward control of the differential gain, the design allowed easy access to high numbers of pulses in the laser cavity, thus enabling manipulation of pulsing conditions and pulse properties [P4–P6]. The high tolerance to losses of the structures exhibiting an enhanced resonance effect was essential for the experiments including highly nonlinear mirrors or a frequency shifter [P2, P3]. When

operating in the technologically difficult wavelength regime of 1.57 $\mu$m, the RPG design allowed substantial output powers to be reached [P1]. In [P6] an antiresonant gain structure was employed to assess the role of differential gain in the formation of multiple equally spaced pulses in the cavity.

## 2.2 Power scaling of SDLs

### 2.2.1 Design guidelines for a high-power SDL

Due to the external cavity mirror of the SDL, the fundamental transversal mode diameter on the gain element can be flexibly adjusted. In particular, the mode diameter together with the pumping area can be increased with very little effect on beam quality, allowing output power in a single transverse mode to scale up with the pump area when the pump intensity is kept constant. However, a large pump spot comes at the expense of decreased lateral heat dissipation from the center of the pumped gain area, which at intense pumping levels results in a large temperature rise through the quantum defect and non-radiative recombination [57–60]. The associated refractive index and bandgap changes at the center of the pumped area of the semiconductor gain mirror initiate thermal roll-over and prevent further power scaling. The decrease in the three-dimensional heat extraction characteristics can be suppressed to a certain extent with a heat spreader of very high thermal conductivity or by choosing a super-Gaussian or top-hat spatial pump distribution instead of the conventional Gaussian pump profile, but it nonetheless sets an upper limit of about 1 mm for the pump spot diameter [57–60].

A general guideline for the design of a high-power SDL gain structure would be to minimize the quantum defect and cavity losses, to maximize pump absorption and to either optimize detuning for a zero mismatch at high operating temperature or suppress subcavity resonance in favor of large temperature tolerance, depending on application [34, 42, 61].

### 2.2.2 Design considerations for a high-power short-pulse SDL

Design guidelines for reaching high average power are not in direct conflict with the laser design requirements set by short pulse generation. For example, flattening the GDD of the gain chip with an AR section does not have a serious effect on maximum output

power if the decreased gain is balanced by proper output coupling [61, 62]. Power scaling of SDLs in the ultrashort pulse regime is challenging, however, because the carrier density-dependent nonlinear phase shifts induced by the pulse at the gain element and absorber increase with pulse fluence and make it preferable to avoid strong saturation of cavity elements in order to achieve sub-ps pulse durations [5]. This becomes increasingly difficult when pulse duration approaches the timescale of carrier scattering in semiconductors, for which saturation fluence is decreased by spectral hole burning [63]. Moreover, power scaling via a large transverse mode size at the gain element implies a large temperature difference between the center and outer parts of the pumped gain region, which results in inhomogeneous gain broadening which may disturb clean pulsing [62]. The tendency of SDLs to switch to many pulses circulating in the cavity for minimized losses due to gain saturation, spontaneous emission between consecutive pulses and two-photon absorption (TPA) further limits the peak power of the pulses [64, P4, P5].

The highest average output power to date from a short-pulse SDL has been achieved with a semiconductor structure where a quantum dot (QD) absorber and a QW gain section are integrated in one chip and separated by a pump blocking DBR [7]. Management of dispersion and nonlinear phase effects in such a structure is very difficult and sensitive to errors during growth. This reflects on the pulse duration which has been tens of picoseconds for integrated structures [7, 65, 66]. Proposals for an improved gain design for high-power sub-ps SDLs include, for example, a gain section with a graded barrier bandgap profile that promotes carrier drift towards QWs and suppresses pump absorption saturation problematic for thin gain sections [67]. However, the average output power demonstrated in the fs regime with such a design has been on the order of 10 mW. A series of thin DBRs instead of one thick DBR in the gain element has been proposed to enable a reduction of pulse width by a factor of two through minimization of chirp [68]. The downside of this approach is the increased sensitivity of the design to growth errors. Spontaneous mode locking shows potential for sub-ps pulse generation at watt-level average output powers with a compact cavity configuration and supposedly a standard RPG structure tolerant to growth errors [69]. A drawback for this method is the high threshold, caused by the thick gain section required for establishing saturable absorption.

In Section 2.2.4 a method for power scaling an SDL based on distribution of thermal load between multiple gain elements is described and its applicability to short pulse generation is analyzed.

### 2.2.3 Thermal management

The temperature-coupled phenomena affecting the performance of SDLs have been thoroughly investigated in scientific literature [25, 26, 30, 49, 50, 70–73].

The temperature-sensitive nature of semiconductors makes it difficult to engineer a gain element impervious to the changes in temperature detrimental to the high-power performance of SDLs. Therefore, most of the approaches to scale up the power of SDLs attempt to impede the temperature increase in the gain element by transferring the heat away from the gain chip as efficiently as possible. These methods will be discussed in the next subsections.

Other cavity elements of a pulsed SDL, such as nonlinear mirrors, usually operate at off-resonance and are not heated by the pump beam but only by absorption of the intracavity signal optical field. Thus they do not require as stringent thermal management as the gain mirror [51]. With proper cavity design antiresonant nonlinear mirrors, for example, are damaged due to heating only at intracavity average powers above several tens of watts [74, 75, P1]. However, the methods for thermal management of the gain chip discussed below can be applied to control temperature increase and prevent thermal damage in other cavity elements as well [75].

#### Flip-chip method

The conventional heat management approach, in which the substrate is removed to reduce thermal impedance leaving only a few $\mu$m thick semiconductor gain chip bonded to a heat spreader below, is referred to as the flip-chip method [4]. The flip-chip approach requires the gain section to be grown before the DBR on the substrate, which is thinned, and after bonding of the DBR side of the chip to the heat spreader, removed by chemical etching with the help of etch-stop layers grown very first on the substrate. Disregarding the extensive post-growth processing, the possibility to use low-cost heat spreaders, and the lack of problems related to spectral filtering by the etalon effect present in assemblies with an intracavity heat spreader, makes the flip-chip method attractive for SDLs intended for pulse generation. Diamond-copper composite or synthetic diamond heat spreaders can be used provided that appropriate bonding techniques are implemented [76, P5]. In this work, most of the gain chips were processed using the flip-chip approach. The flip-chip gain samples were bonded to diamond-copper composite heat spreaders with AuSn solder and further bonded to copper heat sinks with indium

solder [P5].

In the 1-$\mu$m wavelength regime, where excellent crystal quality GaAs/AlAs DBRs with low thermal impedance can be employed, the performance of the flip-chip method exceeds that of other heat management methods for large (>400 $\mu$m) pump spot diameters [25,59], allowing access to record high output powers from SDLs [34,77]. However, in wavelength regimes away from 1 $\mu$m, where material systems other than InGaAs have to be used, the thermal conductivity of the bottom mirror decreases considerably, resulting in diminished heat extraction [59]. At long wavelengths, the increased thickness and consequent high thermal impedance of the DBR further limits the performance of the flip-chip method [78, 79].

One of the major drawbacks of the flip-chip method has been that a soft solder has to be used for bonding of the semiconductor chip to a diamond heat spreader because of the large difference in the thermal expansion coefficients of the semiconductor and diamond. The tension imposed on the chip at the end of the bonding process, when the assembly has cooled down from the melting temperature of the solder, easily breaks the chip if a hard solder is used [80]. A junction bonded with a soft solder like indium degrades over time and cannot sustain high operating temperatures for long, making soft solder unsuitable for industrial applications [81]. A bonding procedure that could be performed close to RT using a substance of proven long-term reliability would allow the use of diamond heat spreaders even in industrial applications. The author has followed successful investigations of such methods closely and is confident that these efforts will bear fruit in the near future.

### ICHS method

The intracavity heat spreader (ICHS) method relies on heat extraction through a transparent heat spreader placed directly on the top surface of the semiconductor gain structure [59, 82, 83]. Capillary bonding with water can be used to attach the heat spreader to the gain chip [84, 85]. The advantage of the ICHS method is the close contact of the heat spreader to the gain section where the heat is generated. The ICHS approach bypasses the thermal impedance of the gain DBR, which makes it a superior heat transfer method in spectral regimes outside the 1-$\mu$m wavelength regime which benefits from the mature InGaAs material system [25, 59]. Usually, either natural or synthetic diamond heat spreaders are preferred due to their excellent heat conductivity and high transparency in

a wide spectral range [86, 87]. Synthetic single crystal diamonds grown by chemical vapor deposition can exhibit very low birefringence, which is favorable if the laser cavity includes polarization selective elements. The downside of the ICHS method is the high cost of diamonds of good optical quality and the unproven long-term reliability of the capillary bond.

For pulsed SDLs problems arise from spectral filtering caused by the etalon effect in ICHSs with flat parallel surfaces. The optical spectrum is modulated with a peak spacing corresponding to the optical thickness of the heat spreader, which disturbs the distribution of lasing modes and prevents pulse formation. This effect can be avoided by replacing the flat ICHS with a wedged ICHS [P1]. For a diamond heat spreader 300 $\mu$m in thickness, an angle of about 2° between the top and bottom surfaces is enough to completely remove the disturbing fringes from the spectrum. However, an AR coating should be deposited on the top surface of the diamond to minimize reflection losses for the signal and to further decrease residual reflectivity.

Combining flip-chip and ICHS methods for two-sided heat extraction from the gain structure would also increase SDL output performance [88]. Processing of such an assembly is, however, challenging.

### 2.2.4 SDL with multiple gain elements

The heat load imposed on the gain element by the pump source can be efficiently dissipated when split between multiple gain chips sharing one cavity [S1]. In contrast to beam combining methods conventionally used for power scaling [89], with such a scheme the coherence of light and the excellent beam quality of SDLs is preserved while the output power can be scaled up linearly with the number of gain chips without incurring coupling losses or the need for external phase locking [90, 91, S1]. This power scaling approach is supported by the availability and low price of commercial pump diode modules capable of delivering excess pump powers that cannot be absorbed by a single gain element, without enlarging the pumping area over the limit where power scalability breaks down.

Figure 2.4 shows the output power obtained from an SDL with two gain elements assembled in a Z-shaped cavity with a 6 % OC [S1]. As a reference, output characteristics for single gain chips measured separately in linear cavities with 3 % outcoupling, together with the sum output power composed of the single gain experiments, are plotted in the same figure. Among the available OCs the above mentioned values for outcou-

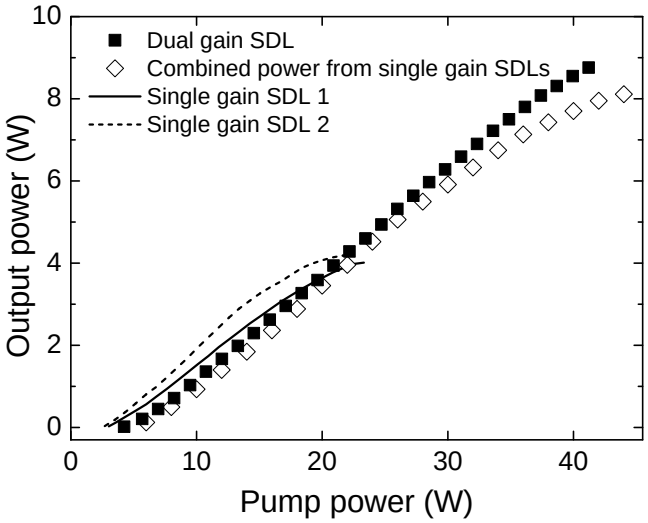


Figure 2.4: Output characteristics of the dual-gain SDL (filled squares) and single gain SDLs (solid and dashed line), and the combined output power from the single gain SDLs (open squares) as a function of incident pump power.

pling were found to give the highest maximum output power. Due to distributed heating the dual gain SDL can sustain two times higher thermal load than the single gain SDL, which results in a delayed thermal roll-over and doubled output power compared to the single chip scheme. The large roundtrip gain obtained with multiple gain elements in one cavity allows larger outcoupling to be used compared to the single gain SDL. Consequently, increased slope efficiency is expected. The dual gain laser exhibits only a minor degradation of beam quality compared to single chip setups. The beam quality factor $M^2$ measured in high-power operation was 1.45/1.28 for the two-gain SDL in horizontal and vertical directions, respectively, and $\sim$1.2/1.2 for the single chip lasers [92, S1].

The multiple gain approach can be applied to scale up the power of pulsed SDLs [S7]. Nevertheless, problems may arise from gain filtering if intracavity heat spreaders are used for thermal management of the gain elements. Even wedged heat spreaders can introduce fringes to the optical spectrum if the etalon effects originating from each heat spreader couple together. Another problem stems from the summed birefringence of the heat spreaders which may disturb the polarization of the laser. With flip-chip processed gain elements power scalability in pulsed operation is preserved [S7]. The rise in output

power is often accompanied by an increase in the number of pulses circulating in the multiple gain cavity. In practice, the dimensions of the cavity elements require the cavity to be rather long, thus favoring multiple pulsing.

To achieve short pulses in a multiple gain cavity, adjustment of the laser wavelength might be needed, because the dispersion of the gain elements may sum up to stretch the pulses. The wavelength of the pulsed multiple gain SDL can be tuned to a low-dispersion regime with a thin intracavity fused silica (FS) etalon, for example [S7].

# Chapter 3

# Methods for pulse generation from SDLs

This chapter discusses the pulse generation methods applied to SDLs. The advantages and disadvantages and the state of the art of each method are reviewed. As examples of cutting edge pulse sources demonstrated using different methods, a 1.57-$\mu$m high-power SDL with a saturable absorber and a picosecond SDL with frequency-shifted feedback are presented.

## 3.1 The prior art

Traditionally, techniques for generating optical pulses have been categorized as active and passive [93, 94]. Active methods rely on external modulation of the amplitude or phase of the laser light at a frequency synchronized with the roundtrip frequency of the laser, whereas in passive methods the required modulation is induced by the light field itself. The shortest pulses to date emitted directly from lasers have been obtained through passive mode locking (ML), a method discussed in more detail in the next chapter [95, 96]. In a mode-locked laser the separation of the phases of adjacent longitudinal laser cavity modes is fixed. The superposition of a set of such frequency components corresponds to a pulse in the time domain.

### 3.1.1 Active methods

The first pulsed SDLs were demonstrated with *synchronous pumping* [1], i.e. by pumping the SDL with another laser delivering pulses at a repetition rate adjusted to match the inverse of the SDL roundtrip time. With this method no pump energy is wasted between pulses, making it suitable for SDLs intended for pulse generation at low repetition rates and high peak power levels, for which regime the incapability of the semiconductor material to store energy for a long period of time, originating from the short excited carrier lifetime, becomes more pronounced with CW pumping. Average output powers of hundreds of milliwatts and pulse durations on the order of tens of picoseconds have been achieved directly from the SDL with synchronous pumping [97–99]. External compression of the pulses has lead to pulse durations as short as 21 fs, indicating high linear chirp of the pulses. The peak power of the pulses after compression can exceed 1 kW, making them suitable for supercontinuum generation, for example. However, unless synchronization of the SDL with an external clock is required by the application, or the SDL emits at a wavelength allowing commercial telecommunications components to be utilized for building of the pulsed pump source [100], the complexity and cost of the system often surpasses the advantages gained.

External amplitude or phase modulation provides a straightforward way to generate pulses from SDLs. The first pulsed SDL operating near RT was demonstrated by inserting an acousto-optic modulator (AOM) into the laser cavity to vary resonator losses at the fundamental cavity repetition rate [101]. The performance of lasers pulsed with this approach is intrinsically limited by the modulator characteristics, particularly by the width of the low-loss time window, spectral filtering in the modulator, and the speed of the driving electronics, making it difficult to reach sub-ps pulse durations [94]. Furthermore, stabilization of the cavity length to the modulator frequency is needed. The author is not aware of studies reporting pulses shorter than $\sim$100 ps from SDLs pulsed via *active modulation*.

*Gain switching* by a pulsed pump laser has resulted in the highest pulse energies and peak powers obtained directly from SDLs, with average output powers in the 100 mW range, pulse durations on the order of tens of nanoseconds and repetition rates in the 10-kHz range, amounting to pulse energies and peak powers on the order of tens of microjoules and 1 kW, respectively [102–104]. Laser pulses with these characteristics are of interest particularly at eye-safe wavelengths longer than 1.4 $\mu$m for applications includ-

ing remote sensing, laser radars and active imaging [105–108]. Although less compact, in this wavelength regime SDLs can challenge Q-switched solid-state microchip lasers as sources of high-energy pulses [109, 110].

The high intracavity optical power associated with continuously pumped SDLs, together with the fast and stable recovery of the intracavity field due to the large gain cross section and the short carrier lifetime in the gain medium, permits energetic nanosecond pulses to be extracted from the SDL cavity in a controlled way at repetition rates of several MHz when the intracavity light is deflected from the cavity with the help of an AOM, for example [111]. The advantage of such a *cavity dumping* approach is that the wavelength and repetition rate of the $\mu$J-pulses can be widely tuned without affecting other pulse parameters significantly.

*Additive pulse ML (APM)*, which benefits from the effects of nonlinear interactions on the interference of colliding pulses from two coupled cavities, has been applied to shorten pulses in an SDL [112–115]. The pulse width was decreased from 19 to 6 ps in a synchronously pumped SDL combined with an auxiliary cavity exhibiting Kerr nonlinearity, which worked as an artificial saturable absorber for the colliding pulses and favored high-intensity radiation provided by pulse shortening [112]. However, the length of the auxiliary cavity has to be actively adjusted to match the length of the laser cavity, thereby diminishing the practical value of this method.

### 3.1.2 Passive methods

Passive methods for pulse generation rely on an intensity-dependent loss mechanism, i.e. on the action of a saturable absorber, for which an increase in the incident light intensity results in a decrease in absorption. The dominant way to implement a saturable absorber inside the SDL cavity is to replace one of the cavity mirrors with a semiconductor mirror that has been integrated with a semiconductor saturable absorber, hence the name of the device, semiconductor saturable absorber mirror (SESAM) [9]. The absorption properties of this device, originally developed in the 1990's for solid-state lasers, can be fine tuned for optimized pulse operation with a given laser gain medium and gain element design [116–118]. The shortest pulses [63], highest average output powers [7], and highest repetition rates [6] obtained from SDLs have been achieved using SESAMs to mode-lock the optically-pumped laser. *SESAM ML* has been successfully applied to electrically-pumped SDLs as well, albeit with modest output powers in

the mW range [119–121]. Femtosecond pulse sources operating in the multigigahertz regime accessible via SESAM ML are ideal for delivering intense clock signals which can be widely distributed to multicore microprocessors.

If the light circulating in the laser cavity to generate stimulated emission is regularly shifted in frequency at every roundtrip before re-entering the gain section, in the presence of an appropriate amount of nonlinearity and spectral filtering in the laser cavity, a train of short pulses can form from the superposition of the frequency-shifted waves at the output of the laser [122–126, P2]. Generation of picosecond pulses from an SDL with such *frequency-shifted feedback (FSF)* is discussed in the last section of this chapter. The FSF method provides a simple and robust means to generate pulses regardless of the design specifications of the laser gain or cavity [127, P2].

Other passive methods with potential for short-pulse generation with SDLs include Kerr-lens ML, which is based on a lensing effect via the Kerr nonlinearity which in certain cavity arrangements reduces resonator losses or increases amplification for high-intensity light, and ML with a variable-reflectivity mirror, which relies on reduced out-coupling losses for high-intensity radiation through the combined effect of a nonlinear crystal and a dichroic mirror exhibiting higher reflectivity for light at the second harmonic than fundamental frequency [128, 129]. However, the author is not aware of reports of pulsed SDLs utilizing these methods that have been published in open scientific literature.

## 3.2 The state of the art

Some of the most impressive results in terms of various laser output parameters obtained to date directly from SDLs pulsed using the methods discussed in the previous section are given in Table 3.1. SDLs passively mode-locked with a SESAM constitute a major part of the results with ultrashort pulse durations, reflecting the dominant role of this pulse generation method in the SDL research community. Indeed, the apparent advantages of SESAM ML that arise from the design flexibility of the semiconductor saturable absorber give little room for other methods for short pulse generation, save for applications that require high pulse energies and peak powers, which are easiest to achieve with gain switching or cavity dumping.

The performance of passively mode-locked SDLs is further illustrated in Fig. 3.1, which shows the average output powers and pulse durations with respect to wavelength

Table 3.1: Overview of SDLs employing different pulse generation techniques.

| Method | Laser wavelength | Pulse duration | Average output power | Repetition rate | Comments | Year and reference |
|---|---|---|---|---|---|---|
| Synchr. pumping | 885 nm | 14 ps | 14 mW at RT | 80 MHz | 324 fs with EC | 1992 [130] |
| | 980 nm | 40 ps | 40 mW at RT | 80 MHz | 185 fs with EC | 2006 [99] |
| | 1.50 $\mu$m | 36 ps | 260 mW at -196 °C | 100 MHz | 21 fs with EC | 1991 [97, 98] |
| | 1.50 $\mu$m | 7.7 ps | 15 mW at -196 °C | 100 MHz | 710 fs with EC | 1991 [1] |
| | 2.01 $\mu$m | 240 ps | 80 mW at 15 °C | 460 MHz | 2.8 GHz via HML | 2008 [100] |
| Active modulation | 856 nm | 100 ps | 26 mW at 0 °C | 336 MHz | | 1999 [101] |
| Gain switching | 1.37 $\mu$m | 11 ns | 90 mW at RT | 5 kHz | $P_{peak}$ =1.5 kW | 2006 [103] |
| | 1.53 $\mu$m | ~25 ns | 3.12 W at 15 °C | 200 kHz | $P_{peak}$ =0.56 kW | 2012 [104] |
| | 1.56 $\mu$m | ~17 ns | ~200 mW at 9 °C | 20 kHz | $P_{peak}$ =0.52 kW | 2009 [102] |
| | 2.00 $\mu$m | 210 ns | 17 mW at RT | 1 kHz | $P_{peak}$ =70 W | 2009 [131] |
| Cavity dumping | 1.05-1.08 $\mu$m | 30 ns | 170 mW at 6 °C | 100 kHz | $P_{peak}$ =57 W | 2010 [111] |
| APM | 1.55 $\mu$m | 6 ps | 60 mW at -196 °C | 100 MHz | | 1993 [112] |
| SESAM ML | 489 nm | 3.9 ps | 6 mW at 0 °C | 1.88 GHz | Frequency doubled | 2005 [132] |
| | 832 nm | 15.3 ps | 5 mW at -33 °C | 1.9 GHz | | 2008 [133] |
| | 959 nm | 28 ps | 6.4 W at -15 °C | 2.47 GHz | Integrated structure | 2010 [7] |
| | 959 nm | 3.3 ps | 102 mW at 5 °C | 50 GHz | | 2006 [134] |
| | 960 nm | 784 fs | 1.05 W at -20 °C | 5.4 GHz | | 2011 [135] |
| | 980 nm | 15 ps | ~30 mW at RT | 15 GHz | EP | 2011 [120] |
| | 999 nm | 335 fs | 120 mW at -22 °C | 1 GHz | $P_{peak}$ =315 W | 2010 [64] |
| | 1.02 $\mu$m | 198 fs | 31 mW at 15 °C | 92 GHz | via HML | 2011 [5] |
| | 1.03 $\mu$m | 107 fs | 3 mW at 15 °C | 5.14 GHz | | 2011 [5] |
| | 1.04 $\mu$m | 60 fs | 35 mW at 0 °C | 1 GHz | | 2009 [63] |
| | 1.04 $\mu$m | 400 fs | 300 mW at 10 °C | 175 GHz | via HML | 2012 [6] |
| | 1.06 $\mu$m | 778 fs | 2.35 W at 25 °C | 2.17 GHz | Spontaneous ML | 2011 [69] |
| | 1.22 $\mu$m | 5 ps | 275 mW at 15 °C | 840 MHz | | 2008 [136] |
| | 1.31 $\mu$m | 6.4 ps | 100 mW at 15 °C | 910 MHz | | 2010 [137] |
| | 1.52 $\mu$m | 6.5 ps | 13.5 mW at -8 °C | 1.34 GHz | | 2003 [138] |
| | 1.55 $\mu$m | 3.2 ps | 120 mW at -22 °C | 2.97 GHz | Thin ICHS | 2005 [139] |
| | 1.56 $\mu$m | 902 fs | 10 mW at 0 °C | 2 GHz | | 2011 [140] |
| | 1.57 $\mu$m | 16 ps | 860 mW at 15 °C | 2.58 GHz | HML, wedged ICHS | 2009 [P1] |
| | 1.96 $\mu$m | 384 fs | 25 mW at 15 °C | 890 MHz | | 2011 [141] |
| FSF | 1.06 $\mu$m | 29 ps | 32 mW at 15 °C | 300 MHz | | 2011 [P2] |

APM, additive pulse ML; EC, external compression; EP, electrically-pumped; HML, harmonic ML; ICHS, intracavity heat spreader; ML, mode locking; RT, room temperature.

(column (a), filled circles) and pulse repetition rates and durations with respect to average output power (column (b), filled circles) achieved to date from SESAM-mode-locked SDLs. For comparison, results from Refs. [142–150] obtained with state-of-the-art diode-pumped solid-state lasers (open circles) representing a traditionally dominant pulse source at high repetition rates are plotted in the same figure. It can be seen that

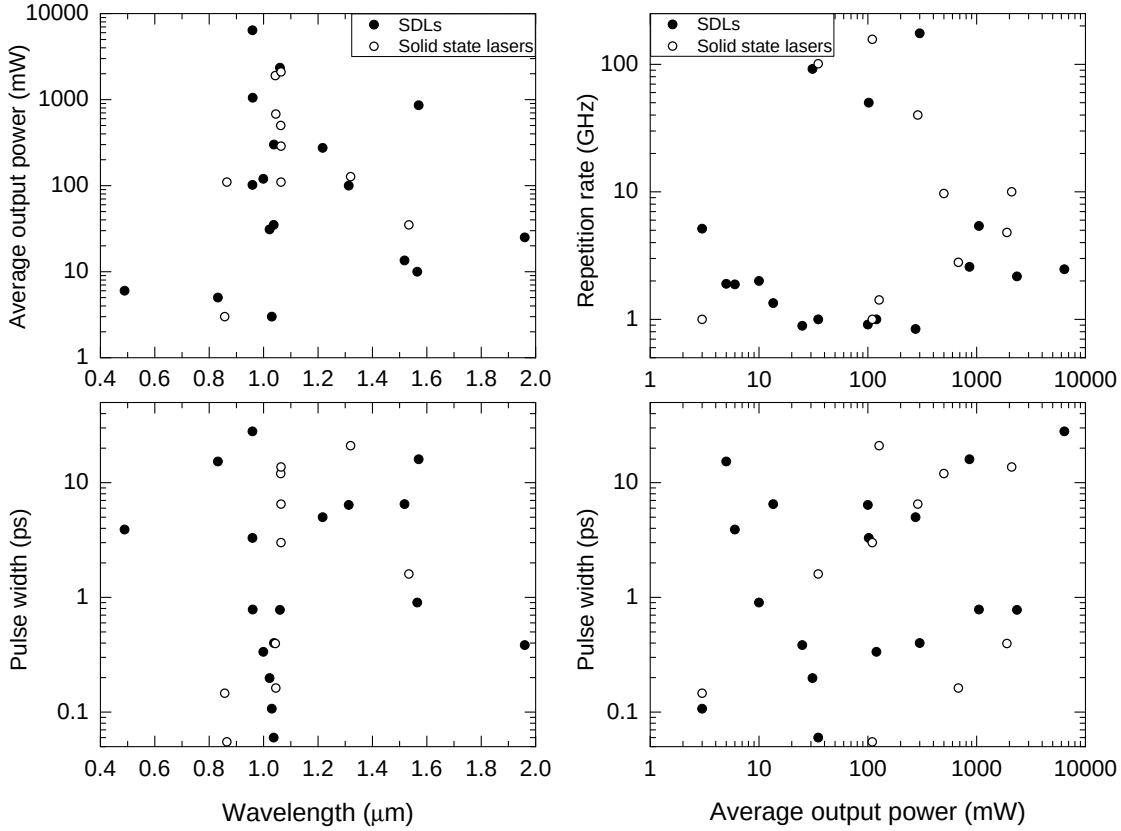


(a) (b)

Figure 3.1: (a) Average output power (top) and pulse width (bottom) vs. wavelength for state-of-the-art SESAM-mode-locked SDLs (filled circles) and diode-pumped solid-state lasers (open circles). (b) Pulse repetition rate (top) and width (bottom) vs. average output power for state-of-the-art SESAM-mode-locked SDLs (filled circles) and diode-pumped solid-state lasers (open circles).

at present the SESAM-mode-locked SDLs, covering a broader wavelength range than diode-pumped solid-state lasers, can reach and even surpass the power and pulse performance of the diode-pumped solid-state lasers at repetition rates from one to 100 GHz. At repetition rates in the MHz-range, i.e., in a regime not applicable for SDLs due to the short excited state lifetime of semiconductors, more impressive results in terms of average output power, pulse energy and width have been obtained from diode-pumped solid-state lasers [10, 12, 151, 152].

## 3.3 Passively mode-locked high-power wafer-fused SDL at 1.57 $\mu$m

### 3.3.1 Motivation

The low thermal conductivity and low refractive index contrast of semiconductor DBR material compounds of the InP material system routinely used at the 1.55-$\mu$m wavelength regime important for low-loss fiber-optic communication limit the output power of 1.55-$\mu$m SDLs having a monolithically grown gain mirror [138, 153]. For InP-based compounds tens of DBR layer pairs are needed to reach high reflectivity, which results in a thick stack of material with high thermal resistance and an increased risk of light absorbing growth defects. The selection of other semiconductor material systems offering DBRs of better thermal and optical quality and emission at 1.55 $\mu$m is very limited since InGaAs/GaAs and GaInAsSb/GaSb, when grown nearly lattice-matched and with good crystal quality, provide gain only for wavelengths shorter than $\sim$1.2 $\mu$m and longer than $\sim$1.7 $\mu$m, respectively [154, 155]. GaInNAs grown monolithically on GaAs can emit at 1.55 $\mu$m, but the high proportion of nitrogen required to decrease the bandgap and lattice constant disturbs the structure of the lattice and may result in considerable optical losses and poor long-term reliability [154, 156].

Heating of the gain element due to the low thermal conductance of InP-based DBRs can be overcome with the ICHS approach for heat removal, provided that the heat spreader is thin enough to avoid strong spectral filtering [139]. However, a thin ($\leq$50 $\mu$m) heat spreader has a reduced cooling capacity and may bend when being mounted to the heat sink assembly [83].

Metamorphic growth has been proposed for combining an InP-based gain section with a GaAs-based DBR of good thermal and optical quality, but the resulting structure suffers from threading dislocations and roughness of the interface between the two compounds of different lattice constants, which has limited the output power in the range of 100 mW in CW and 15 mW in mode-locked operation [140, 157–159].

The next sections describe a set of procedures for building a high-power 1.55-$\mu$m pulsed SDL. The introduced approaches resulted in the demonstration of a picosecond 1.57-$\mu$m SDL generating 0.86 W of average output power at 15 °C, a record power from a pulsed SDL in the 1.55-$\mu$m spectral region at the time of writing this thesis [P1].

### 3.3.2 Wafer fusion technology

Wafer fusion is a process in which two crystalline wafers, their surfaces cleaned from oxides and activated for bonding by Van der Waals forces, are placed in contact under pressure and fuse together at an elevated temperature due to atomic migration and crystal growth induced by surface energy [160, 161]. Typical process parameters for GaAs and InP wafer fusion are in the range of 3 kPa – 3 MPa, 550–650 °C and ∼30 min for the pressure, peak temperature and the dwell time at the peak temperature, respectively [161]. At such values of pressure and temperature a uniform and smooth contact with covalent bonds between the wafers is formed [162]. Crystals with vastly different lattice constants can be fused together, which considerably alleviates the design constraints associated with monolithic devices that require careful adjustment of material compositions in order to minimize lattice mismatch and control the strain accumulated during growth of disparate materials. In the 1.55-$\mu$m wavelength regime wafer fusion technology allows the best features of the highly mature GaAs and InP semiconductor material systems to be combined, namely a GaAs-based DBR with excellent optical quality and an InP-based gain section capable of generating watt-level output powers [163, 164, P1].

### 3.3.3 Gain chip assembly

A 35-layer-pair GaAs/$Al_{0.9}Ga_{0.1}As$ DBR grown by MBE technology lattice-matched to a GaAs substrate provides a ∼140 nm stopband with peak reflectivity higher than 99.9 % at 1.57 $\mu$m due to the large refractive index contrast of 0.44 between consecutive layers, and exhibits an order of magnitude lower thermal impedance compared to an InP-based DBR of the same reflectivity that would require about three times the amount of layer pairs [25, 165, 166]. The GaAs/AlGaAs DBR was fused with a standard AlGaInAs RPG section grown lattice-matched by metalorganic vapor phase epitaxy (MOVPE) on an InP wafer [164, P1]. The RPG comprised 5x2 QWs barrier-pumped with commercial 980 nm diode bars for high-power emission at 1.55 $\mu$m. The fusion interface was formed at a node of the standing wave optical field in the combined structure to minimize scattering losses. Both the MOVPE and wafer fusion were performed at the Laboratory of the Physics of Nanostructures at the École Polytechnique Fédérale de Lausanne, in Lausanne, Switzerland.

The fusion process of the 2" wafers has been described in Refs. [162, 167–170]. As

the first step, the process includes transfer of the GaAs-based DBR onto a separate InP carrier and removal of the GaAs substrate from the GaAs/DBR/InP wafer stack. The DBR on the InP substrate is then fused in an industrial custom-modified wafer bonding machine to the InP gain wafer under a pressure of $\sim$30 bars at a temperature of $\sim$600 °C. Hence, in the fusion step involving the gain section only InP wafers are fused together, which prevents formation of dark line defects in the gain section. Defect formation is inevitable in a fusion process of two wafers of disparate materials, due to the difference in thermal expansion coefficients of the wafers which introduces stress and results in bending of the wafers when the fused assembly cools down from the fusion temperature to RT [162]. After fusing the DBR and the InP gain wafer, selective wet etching was performed to remove the InP substrate from the gain section. The remaining InP carrier with the DBR and gain section fused together was cut into 2.5x2.5 $mm^2$ chips.

For efficient heat removal from the semiconductor gain region a 3x3x0.3 $mm^3$ single crystal CVD diamond heat spreader with birefringence smaller than $10^{-5}$ and a 2° angle between top and bottom surfaces was capillary bonded with deionized water on top of the gain chip. The wedged diamond avoids both mechanical and spectral problems associated with a thin and/or flat ICHS. The negligible birefringence also prevents distortions to the laser beam and consequently to the mode content of the laser. To enable water cooling of the gain sample, the chip-diamond assembly was mounted between two copper plates, using indium foil between the surfaces for firm contact. The top copper plate had a circular aperture of 1.5 mm in diameter for the pump and signal beams. Finally, a two-layer $TiO_2/SiO_2$ antireflection coating was deposited on the diamond/air interface to ensure a fringe-free spectrum and to reduce reflection losses introduced by the tilted surface of the diamond.

### 3.3.4 SESAM ML of the 1.57-$\mu$m SDL

A GaInNAs SESAM was employed as a pulse favoring element in the laser. The GaInNAs material system allows monolithic growth of deep long-wavelength QWs on an AlGaAs/GaAs DBR and GaAs substrate, thereby avoiding the use of InP-based mirrors of low optical quality [171, 172]. The SESAM comprised a 26-layer-pair AlAs/GaAs DBR and a 0.75-$\lambda$-thick absorber section. For saturable absorption at 1.57 $\mu$m, two highly compressively strained 6-nm-thick $Ga_{0.6}In_{0.4}N_{0.035}As_{0.965}$ QWs surrounded by strain compensating GaAsN layers of 2-nm thickness were placed at the antinode of the

optical field in the antiresonant absorber section. The significant strain in the structure, due to the relatively low nitrogen content needed to decrease nitrogen-induced growth defects and the consequent optical losses in the SESAM, manifested itself as a reduced long-term reliability of the device. In particular, spontaneous cracking of the wafer was observed in the course of the experiment. However, owing to the fast nonradiative recombination centers formed with the addition of nitrogen in the InGaAs lattice, the dilute nitride SESAM inherently has a short recovery time of absorption capable of shaping optical pulses down to the picosecond regime [173, 174]. Therefore, no post-growth treatment was applied to the SESAM.

The Z-shaped cavity configuration used in the experiment, described in detail in [P1], enabled the beam size to be independently adjusted at the gain sample and SESAM for proper saturation level of the absorber and large enough ratio of the beam size at the gain mirror to that at the SESAM to initiate stable mode locking while maintaining a cavity roundtrip time shorter than the gain relaxation time for reduced spontaneous emission between pulses. The mode diameter at the gain sample of 210 $\mu$m ensured delivery of high pump powers with moderate pump intensity. Based on output characteristics measured for the gain chip in a linear cavity in CW operation with OCs available at 1.57 $\mu$m at the time of the study, a 1.5 % OC was chosen for the experiment. However, the CW measurements suggested that, had it been available for the pulse study, an OC of about 2 % would have resulted in better output performance.

Figure 3.2 shows the essential results obtained from the characterization of the 1.57-$\mu$m picosecond SDL. Summing up the power of all beams exiting the cavity, including residual reflections from the AR coated surface of the diamond, leakage through the folding broadband high-reflection (HR) mirror, and the light propagating through the OC, plotted in Fig. 3.2(a), the maximum output power at the 2.6-GHz second harmonic pulse repetition rate amounted to 0.86 W at 15 °C. Such a high power in mode-locked operation is a clear indication of the low scattering losses at the fusion interface of the gain mirror and of the small number of defects induced in the gain mirror by the fusion process. Low nonsaturable losses in the SESAM further contribute to the high output performance. The pulse width, shown in Figs. 3.2(a) and 3.2(b), was maintained around 14 ps with a slight increase from 13 to 15 ps as the incident pump power was increased from 7 to 17 W. However, for pump powers larger than 12 W the number of pulses in the cavity switched from one to two, as depicted in Figs. 3.2(a) and 3.2(c), because the doubled repetition rate allows for more efficient extraction of energy from the gain

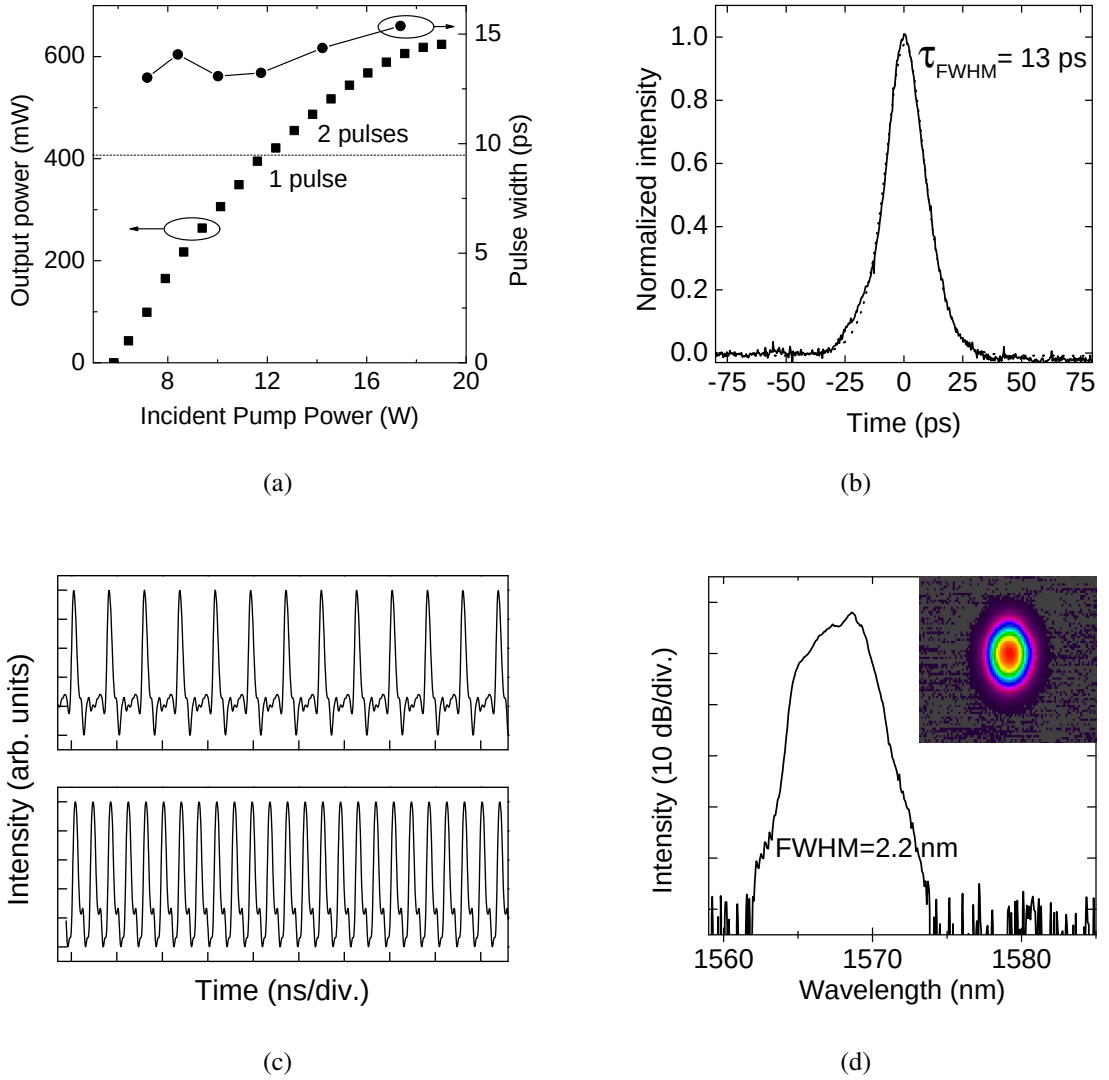


Figure 3.2: (a) Average optical power emitted through the OC (squares) and pulse width (filled circles) with respect to incident pump power for the mode-locked 1.57-$\mu$m wafer-fused SDL. The dotted line marks the transition from the single pulse regime to pulsing at the second harmonic frequency. (b) Autocorrelation measured in the single pulse regime for an average output power of 300 mW (solid line) and sech$^2$ fit (dotted line). (c) Oscilloscope trace for the pulse train with a fundamental (top) and second harmonic (bottom) repetition rate of the picosecond 1.57-$\mu$m SDL. Resolution of the measurement is limited by the 12.5 GHz bandwidth of the photodetector used to record the output signal waveform. (d) Optical spectrum corresponding to the autocorrelation in Fig. 3.2(b). The beam shape at the maximum output power captured with a pyrocamera is shown in the inset.

medium which recovers fast with intense pumping. The center of the relatively broad optical spectrum capable of supporting ∼1.2 ps pulses, as shown in Fig. 3.2(d), redshifted linearly to longer wavelengths with increasing pump power. The above described observations suggest that nonlinear pulse shaping mechanisms in the gain, influenced by pulse fluence, did not play a major role in the laser, but the pulse duration was more likely set by the recovery time of the SESAM or the overall GDD, neither of which was measured due to a lack of equipment and time.

## 3.4 Optical pulse generation from an SDL with frequency-shifted feedback

### 3.4.1 Background

The concept of a laser with frequency-shifted feedback (FSF) was proposed by Streifer et al. as early as 1970 [175]. However, it was not until 1988 that optical pulses were generated from a FSF laser by Kowalski et al. [122]. Since then, the FSF method has been studied extensively for delivering picosecond pulses with pulse energies exceeding 100 nJ from fiber lasers, and pulses with durations on the order of tens of picoseconds from bulk solid-state lasers [124, 126, 176, 177]. Advantages of the method include easy implementation with no need for precise adjustment of the laser pulse system parameters, the robust and self-starting nature of ML, suitability for high-power operation, and the possibility to electrically control the wavelength and duration of the pulses and the shape of the spectrum, which allows for flexible integration of the FSF laser into a given system or application [126, 127, 176, 178]. The first SDL with FSF was described in [P2].

### 3.4.2 Theory of FSF lasers

A comprehensive review of FSF lasers and a thorough theoretical analysis of pulse generation with FSF is provided in Refs. [125] and [123], respectively. In an FSF laser the frequency of the light circulating in the laser cavity is shifted by a small discrete amount for every roundtrip [122]. FSF is usually set up via the Doppler effect with an AOM operating in CW mode to shift the first order diffracted light fed back to the gain medium by an amount equal to the acoustic frequency of the AOM [122, 179, 180]. A periodic pulse waveform builds up from the constructive interference of the set of phase-coupled

frequency components circulating in the laser cavity, with the constant frequency separation between them corresponding to the shift in frequency induced by the intracavity frequency shifter. Due to the repeated shifting of the spectrum towards one end of the gain profile shaped by a bandpass filter needed to trap the optical pulse in the frequency domain, stable pulsed operation requires that new frequency components are generated by nonlinear processes at the other end of the gain spectrum [123,181]. In a semiconductor medium the nonlinearities related to the changes in excited carrier density induced by the intracavity field may create these new spectral components, which are then amplified while crossing the gain peak after consecutive passes through the frequency shifter, and act as a phase-seeding mechanism which establishes a slowly varying phase distribution throughout the laser spectrum, constituting a pulse in the time domain [23, 123, 182]. In parallel, this results in energy transfer from the center of the optical pulse to its wings, which compensates for the one-directional energy transfer due to the frequency shift.

### 3.4.3 Experiment

The experimental setup for the FSF SDL, described in detail in [P2], is shown in Fig. 3.3(a). The single pass gain of the InGaAs/GaAs RPG mirror used in the study was enhanced by a top dielectric coating with 66 % reflectivity to manage losses caused by the $\sim$90 % diffraction efficiency of the $TeO_2$ AOM operating at +1 diffraction order in the long arm of the V-shaped laser cavity. The AOM available did not allow the frequency shift generated in one roundtrip to be tuned. The traveling acoustic wave in the $TeO_2$ cell at a frequency of 80 MHz was oriented to give an up shift of 160 MHz for the intracavity light at every roundtrip. Relatively large laser cavity dimensions were chosen to suppress reflection of the zero order diffracted beam from the cavity end mirror, and with it the feedback having no frequency shift. The combined effect of a 25-$\mu$m-thick fused silica etalon and the enhanced gain subcavity served as an intracavity spectral filter with a bandwidth of a few nanometers around 1.06 $\mu$m, trapping the pulse in the frequency domain while allowing pulse durations in the ps range. A 1-%-reflective end mirror was used in the cavity to couple out a high-quality output beam instead of the low-quality beam from zero order diffraction, which was blocked by the mount of the end mirror.

Careful optimization of the cavity alignment and radio frequency (RF) power applied to the AOM was required to obtain stable ML. However, the optimal cavity alignment

leading to stable pulsing could seemingly be achieved for any given cavity length within the stability range of the cavity, suggesting that the length of the cavity was not a critical parameter of the system. Self-initiated pulsing at the fundamental cavity repetition rate of 300 MHz was observed starting from threshold to up to 70 mW of average output power, beyond which instabilities and a CW component became dominant. The most stable pulse train with the shortest pulses of 29-ps duration, shown in Figs. 3.3(b) and 3.3(c), was obtained at an average output power of 32 mW. The optical-to-optical conversion efficiency of the laser was slightly below 1 %. With a frequency-tunable and electrically-stabilized AOM more suitable for the filter and nonlinearity characteristics of the SDL gain and cavity, shorter pulses with lower jitter at a higher average power could be expected. A ring cavity or a standing wave cavity with the gain chip as a folding mirror could further increase the output power due to halved losses in the AOM and doubled single-pass gain, respectively. Lower losses would allow gain designs with a reduced cavity enhancement to be used and thus decrease broadening of the pulses in time due to higher order dispersion and nonlinear phase changes in the gain element. A more detailed study of the spectral characteristics and chirp of the output of the FSF SDL might also be of interest to the scientific community.

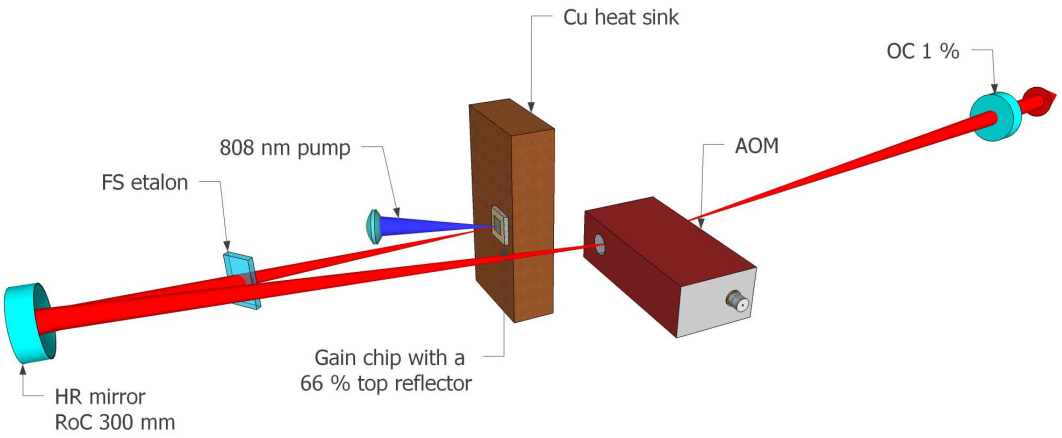


AOM, acousto-optic modulator; FS, fused silica; HR, high-reflection; OC, output coupler

(a)

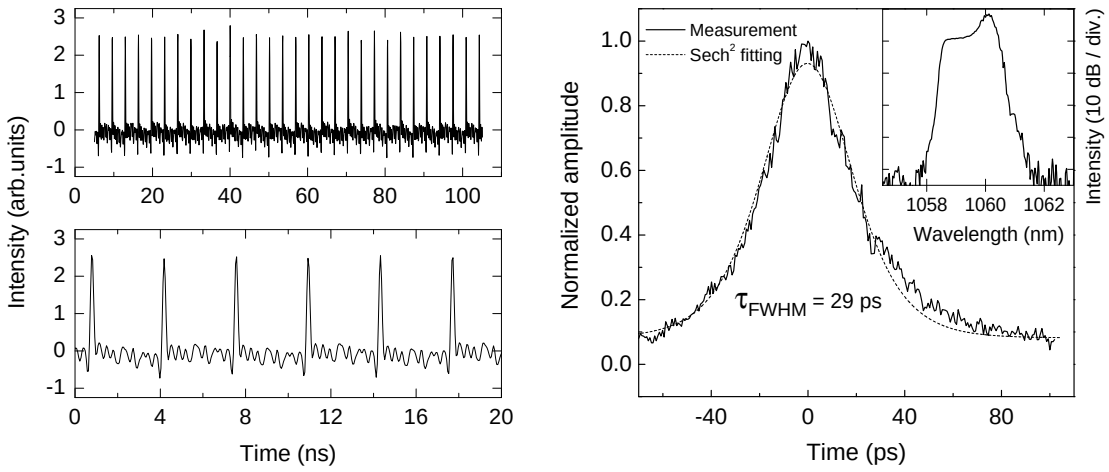


(b) (c)

Figure 3.3: (a) Schematic illustration of the SDL with FSF. (b) Pulse train from the FSF SDL with different time scales as seen on a 2.5-GHz oscilloscope. (c) Noncollinear autocorrelation and corresponding optical spectrum at an average output power of 32 mW.

# Chapter 4

# Pulse formation in SESAM-mode-locked SDLs

Passive ML with a SESAM is the dominant and most successful approach for generating pulses from SDLs. In this chapter pulsed operation in SDLs via SESAM ML is discussed, starting with a description of the SESAM based on the macroscopic parameters relevant to formation of pulses, and continuing with a review of the studies addressing the theory of passive ML. Emphasis is placed on the research and modeling of SESAM-mode-locked SDLs and on the pulse shaping mechanisms related to characteristics of semiconductor material and nanostructures. Next, ML in the regime of weak saturation of SESAM absorption is examined. Finally, pulse formation in picosecond SDLs exhibiting gain perturbations during pulse transit is studied both numerically and experimentally. Observations of harmonic ML, dynamics of pulse characteristics, and hysteresis between different pulse regimes are presented and analyzed. As a result, guidelines for control and manipulation of optical pulses from passively mode-locked SDLs are proposed.

## 4.1 SESAM

A semiconductor saturable absorber mirror (SESAM), usually comprising a DBR topped with a QW or QD absorber section, is characterized by its reflectivity with respect to fluence (defined as energy per area) of the incident light pulse [183]. Absorption observed at low pulse fluences decreases and consequently reflectivity of the SESAM increases

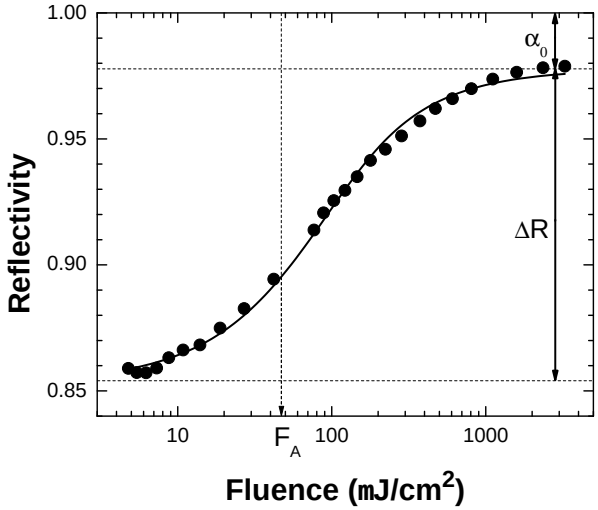


Figure 4.1: Reflectivity versus pulse fluence for a 5-QW near-resonant SESAM

with an increase of the pulse fluence, because the initial states of the absorbing interband transition become depleted while the final states become partially occupied [118, 184]. At very high intensities the reflectivity of the SESAM may drop due to TPA [185, 186]. Reflectivity of the SESAM as a function of pulse fluence can be modeled to reasonable accuracy with a standard two-level system [21, 187]. Figure 4.1 shows a typical reflectivity (filled dots) measured for a 5-QW SESAM as a function of the fluence of a 2-ps pulse detuned -7 nm from the SESAM subcavity resonance wavelength. The fit (solid line) to the data was performed using a formula derived from rate equations of a two-level system (and modified for practical use to include TPA) for reflectivity experienced by a monochromatic square pulse with a fluence $F_p$ and a duration short compared to the recovery time of the absorption [21, 183, 187–189].

### 4.1.1 Macroscopic parameters of the SESAM

The key parameters of the SESAM extracted from the nonlinear reflectivity curve shown in Fig. 4.1 are modulation depth $\Delta R$, i.e. the maximum difference between reflectivity at high and low pulse fluences, saturation fluence of the absorber $F_A$ at which the reflectivity is increased from the low-intensity value by $\Delta R/e$, and nonsaturable losses

$\alpha_0$ mainly caused by defects in the semiconductor lattice and by transmission through the bottom DBR. The inverse slope of TPA $F_2$ determines the fluence at which TPA decreases the reflectivity from the maximum value by a factor $1/e$ [186, 190]. The recovery time of absorption $\tau_A$, which characterizes the relaxation speed of excited carriers can be resolved with a pump-probe reflectivity measurement [191, 192]. The reflectivity observed after the pump pulse usually shows an exponential decay with two time constants, a fast decay component of 10 fs – 1 ps originating from intraband thermalization and cooling of carriers via carrier-carrier scattering and carrier-phonon interactions, and a slow component of 100 fs – 10 ns that results from carrier trapping in impurity states and recombination via recombination centers or by radiation [118, 193, 194]. At a high pulse intensity the optical Stark effect may contribute to the change in absorption, with a recovery time constant on the order of the polarization decay time typically measured in tens of femtoseconds [8, 195–197]. The SESAM parameters and the GDD of the device can be precisely adjusted by various methods reported for example in Refs. [9, 198–200], [199–201], [9, 199, 202, 203], [8, 9, 198, 202, 204–206], [190], and [9, 200, 201, 207–209] for the fine tuning of nonsaturable losses, modulation depth, saturation fluence, recovery time, inverse slope of TPA, and GDD, respectively.

### 4.1.2 SESAM designs

In addition to the type of the absorbing region, SESAMs can be categorized by the approach chosen for tuning of the macroscopic SESAM parameters.

Similarly to tailoring field enhancement in a semiconductor gain structure, the optical field strength inside a SESAM can be tuned by adjusting the thickness and top reflectivity of the effective GTI structure formed by the bottom mirror, absorber section and surface of the SESAM. Depending on the top reflectivity and the detuning of the laser wavelength from GTI resonance wavelength, a distinction is conventionally made between resonant and antiresonant designs. Compared to an equivalent antiresonant design, a resonant SESAM exhibits a large modulation depth and low saturation fluence beneficial for easy start-up of ML [210]. On the other hand, an enhanced resonant character increases nonsaturable losses, limits the bandwidth with suitable SESAM parameters for ML, and lowers the damage threshold [203]. In this doctoral work, mostly antiresonant SESAMs without a top DBR or AR coating were employed to ensure low-loss broadband operation favorable for ultrashort pulse generation in SDLs typically having a low

single pass gain.

SESAMs can also be classified according to whether shortening of the recovery time of absorption is accomplished with fast recombination centers thanks to ion bombardment [204], defective crystal growth [211], or surface states [206], for example, or by the optical Stark effect or carrier thermalization around the exciton resonance in QWs [5, 197, 212].

## 4.2 Principles of passive ML in SDLs

### 4.2.1 Elementary concepts of ML

In this thesis fundamental or one-pulse ML refers to a condition for which all longitudinal cavity modes within the lasing bandwidth are in phase at a certain moment (and position). If this condition is met, it then follows from the fixed frequency separation of one optical cycle per roundtrip between adjacent cavity modes that the phases of the modes coincide repeatedly after every time period (and distance) equal to the roundtrip time (and roundtrip length) of the cavity. In effect, an optical pulse circulates in the laser cavity, the center of the pulse corresponding to the moment (and position) when the modes are in phase. If only every $n^{\text{th}}$ cavity mode is phase-locked in this way, and the other cavity modes between the locked modes are efficiently suppressed to avoid supermode noise, the time period (and distance) required from one coincidence of the phases to the next is $n$ times shorter compared to fundamental ML due to the $n$ times larger separation in frequency of the adjacent locked modes, thus amounting to an $n$ times shorter pulse period [213–216]. In this thesis such a regime where $n$ pulses circulate in the laser cavity is referred to as harmonic ML or operation at the $n^{\text{th}}$ harmonic frequency, repetition rate or order.

In general, a laser adopts the operation regime which minimizes losses [217]. If lower losses are introduced in pulsed operation than in CW operation, the laser may become mode-locked. With a saturable absorber, favoring of pulses occurs naturally due to the intensity-dependent transmission characteristics. A choice between fundamental and harmonic ML is made similarly, based on which operation regime results in the lowest losses [218].

### 4.2.2 Literature on the theory of passive ML

Since the first proposal of pulse generation via ML in the 1960's [219], an extensive amount of studies have been performed to theoretically describe passive ML in different pulse duration regimes and in the presence of various pulse shaping mechanisms, the strength of which change depending on the laser type under examination [17, 19, 220–225]. A comprehensive review of the evolution of the most successful theoretical model of ML, based on the master ML equation developed to a great extent by H. Haus, can be found in Ref. [226]. In search for tutorials and papers that discuss ML from a broad perspective one might look into Refs. [227–229]. A more precise picture of the theoretical models intended for short-pulse solid-state lasers in particular can be obtained from Refs. [20, 22, 230]. For an accurate description of ML in semiconductor lasers, models that take into account strong modulation of gain and loss per roundtrip should be used [224, 231].

The standard description of harmonic ML is based on rate or recursive equations for pulse energy and gain [232, 233]. However, despite the vast number of studies of passive harmonic ML, the principles for transitions between regimes with different numbers of pulses in the laser cavity are still under active research [218, 224, 234–237].

#### Basic schemes of pulse formation in passively mode-locked lasers

Traditionally, the analysis of ML builds upon the time domain description of saturable gain and absorption during pulse transit. Three basic schemes can be distinguished: ML with a fast absorber [17, 221], ML with a slow absorber [19, 22] and ML with a slow absorber and gain saturation [16, 238]. In addition, soliton ML with a slow absorber, where nonlinearities compensate GDD to form close to transform-limited pulses, has been thoroughly investigated [220, 222, 239, 240].

### 4.2.3 Literature on the theory of passive ML in SDLs

Although both the early studies of pulse shaping in actively mode-locked SDLs in the 1990's and the reports of passive ML in SDLs in 2000 discussed pulse shaping, acknowledging the strong chirping of pulses in particular, no systematic investigation of pulse formation in SDLs was performed until 2002 by Paschotta et al. [3, 23, 97, 130]. Like in a report published earlier in the same year by Garnache et al., short pulse opera-

tion was accounted for by a balanced interplay between normal chromatic cavity dispersion and self-phase modulation from refractive index changes in semiconductor structures, showing similarity to soliton ML frequently observed in fiber and bulk solid-state lasers [23, 24, 241].

Since then, a large part of the theoretical considerations have been devoted to explaining the occurrence of sub-ps pulses in SDLs exploiting SESAMs with a near-surface QW typically placed $\sim$2 nm from the semiconductor structure surface of the SESAM to advance fast surface recombination and trapping [196, 212]. Mechanisms such as the optical Stark effect and rapid excitonic recovery of absorption, as reported in Refs. [63, 64, 196, 197, 242, 243] and [5, 46, 67], respectively, have been proposed as being responsible for pulse shortening. These effects are negligible for the picosecond SDLs presented in this thesis, but for completeness they will be covered in more detail in Section 4.2.5. Despite the apparent efforts to understand sub-ps pulse formation in SDLs, no analytical nor numerical approach to model passively mode-locked SDLs that includes all the above mentioned phenomena has been presented. Such a model would require the fast carrier thermalization effects and the inhomogeneous nature of the carrier distribution in the semiconductor elements of the laser to be taken into account [46]. Furthermore, the dominant mechanism behind shortening of pulses into the 100-fs regime still remains unclear, not least because of the large variation of system parameters such as pulse fluence and repetition rate in SDLs where sub-ps pulses have been observed [5, 64].

Fully distributed or simplified analytical time-domain models and simulations that minimize the use of macroscopic phenomenological fitting parameters (that require experimental characterization of semiconductor structures) and instead draw from first principles employing e.g. semiconductor Bloch equations have also been presented for optimization of pulse generation in SDLs [68, 244–247]. However, the heavy calculations inherent to such models reduce their attractiveness for engineering purposes.

In addition, investigations on picosecond pulse dynamics in SDLs in the regime of multiple pulses in the cavity and with weak saturation of absorption have been performed by the author in [P3–P6]. The results obtained from these studies are reviewed in Sections 4.3 and 4.4.

### 4.2.4 Pulse shaping in SESAM-mode-locked SDLs

Considering the large gain cross section of semiconductors and typical pulse durations in SDLs compared to SESAM recovery times, amongst the basic schemes of passively mode-locked lasers ML with a slow saturable absorber in the presence of strong gain saturation best characterizes pulse formation in a SESAM-mode-locked SDL [13, 16, 188, 224]. In this ML scheme the net gain window for a pulse opens if the absorber saturates faster than the gain, i.e., if the saturation energy of the absorber is much lower than that of the gain. The net gain window remains open until the gain is saturated to a level where losses surpass gain. Theory and experiments suggest that for stable ML, the saturation energy of the gain must be about an order of magnitude larger than the saturation energy of the absorber [229, 238, 248]. In the absence of additional pulse shaping mechanisms, the pulse duration relates to the width of the net gain window determined by the interplay of absorber saturation and gain depletion, where, however, the intrinsic absorber recovery time, governed mainly by interband relaxation of carriers, has a major role.

Analysis of pulse shaping in SESAM-mode-locked SDLs has been to a large extent based on numerical simulations, which, although perhaps lacking physical insight compared to bulky analytical models of mode-locked semiconductor lasers [224, 231], are far less limited in applicability and have been proven suitable for engineering purposes [25, 188, 249, P4]. Section 4.2.6 reviews the numerical methods used in this doctoral work.

### 4.2.5 Pulse shaping in fs SESAM-mode-locked SDLs

Pulses much shorter than the interband recombination time of the absorber can be observed in passively mode-locked SDLs if additional mechanisms like the optical Stark effect, spectral hole burning in the SESAM and gain, and rapid carrier thermalization, introduced in the next subsections, contribute to pulse shortening and turn the semiconductor elements into effectively fast pulse shapers [46, 63, 197]. A necessary condition for ultrashort pulse formation is the minimization of the chirp, conveniently provided for SDLs by soliton-like ML, i.e., the interplay of dispersion and self-phase modulation in the semiconductor elements [23].

### Soliton-like ML

In contrast to other solid-state lasers, for which no significant dynamic gain saturation takes place but the gain is saturated to a constant value by the average intracavity intensity, semiconductor lasers can exhibit a large gain depletion during the pulse transit through the gain medium. The dynamic gain saturation is further followed by fast gain recovery between pulses. In a semiconductor saturable absorber, on the other hand, a change of opposite sign compared to that in the gain is generated in the excited carrier density when an optical pulse bleaches the absorber. Changes in the excited carrier density are directly related to changes in the refractive index of semiconductor material through the linewidth enhancement factor derived from Kramers-Kronig transforms connecting the refractive index and absorption of a material [23, 250–252]. Consequently, changes that are nonlinear in time are induced to the phase of the carrier wave of the pulse. When summed up, the net variation in refractive index from gain and absorber saturation in a roundtrip of a pulse typically observed in SDLs corresponds to a phase change that can be compensated for by normal intracavity GDD [23]. Therefore, analogously to soliton ML but with self-phase modulation replaced by phase changes of opposite sign caused by modulation in carrier density, with an appropriate amount of normal GDD pulse broadening effects eliminate each other, and a pulse much shorter than the recovery time of the absorber can be sustained [239, 240].

Soliton-like ML in SDLs results in close to transform-limited $\mathrm{sech}^2$-shaped pulses characteristic of traditional optical solitons; however, the inverse dependence of pulse duration on pulse energy and the independence of pulse duration of the absorber recovery time predicted by the soliton theorem are not fulfilled [46, 253]. The first systematic experimental evidence of soliton-like pulses in SDLs was provided in 2010 by Hoffmann et al. in a study which confirmed the normal cavity dispersion regime to be more favorable for short pulse generation compared to the anomalous regime in SDLs where phase effects in the absorber dominate [254].

### Spectral hole burning and fast carrier thermalization

If the gain bandwidth is broad enough and pulse stretching effects are small, i.e. cavity GDD is minimized or compensated for by nonlinear phase changes, the duration of a pulse may approach the scattering times of electrons and holes in the QWs of the gain structure [46]. The pulse can then burn a spectral hole in the inhomogeneous carrier

distribution of the gain element, as the pulse removes carriers faster than scattering processes can refill the states [63]. This causes loss or reduced gain for the pulse tail, which limits pulse energy and shortens the pulse from the trailing edge [63, 255].

Similarly, when the pulse duration approaches the dephasing time of electron-hole pairs in SESAM QWs, spectral hole burning of the absorption may occur [5]. Electron-hole pairs lose coherence through scattering processes in a time on the order of $\sim$100 fs, giving rise to a recovery mechanism of absorption capable of shaping ultrashort pulses [46, 193, 256]. Comparable dynamics occur with an excitonic resonance in SESAM QWs, for which spectral hole burning due to exciton-exciton bleaching by phase-space filling may occur, if the pulse duration approaches the dephasing time of excitons [257]. Such a saturable absorption mechanism recovers on the $\sim$100-fs timescale of the exciton ionization via interaction with thermal (longitudinal optical) phonons.

Femtosecond pulse generation reported by Klopp et al. in Refs. [5, 46, 67] has been partly accounted for by the carrier thermalization effects leading to rapid recovery of absorption.

### ML assisted by the optical Stark effect

The optical Stark effect refers to the splitting of energy states by an intense optical field, which, within the framework of excitonic absorption in semiconductor QWs and nonresonant excitation, manifests itself as a near-instantaneous spectral shift of the absorbing resonance and an effective fast saturable absorber mechanism [8, 63, 258]. Particularly, if the optical field is applied at a wavelength longer than the exciton resonance, a strong blue shift of the resonance peak associated with the generation of virtual excitons is induced [212, 259]. The virtual exciton populations persist only as long as the exciting pulse, resulting in a recovery of absorption on the timescale of the pulse duration when the resonance shifts back.

The nonresonant optical Stark effect was observed in semiconductors in the mid-80's and explained theoretically soon afterwards [195, 259–262]. In SDLs the influence of the Stark effect on pulse shortening was first proposed by Garnache et al., who exploited a SESAM of the surface recombination type to generate sub-500 fs pulses [24]. Since then, the Stark effect has been claimed to contribute to the fast response of QW-SESAM absorption in numerous studies [63, 64, 196, 197, 242]. Although theoretical investigations on the magnitude and impact on pulse duration of the Stark effect in a saturable absorber

exist, no direct experimental evidence confirming its role in shaping ultrashort pulses in SDLs has yet been presented, mainly because of difficulties in distinguishing between contributions from the different potential pulse shortening mechanisms discussed in this section [197, 242, 243, 249].

According to the latest estimations, at full saturation of the SESAM, the optical Stark effect becomes effective at pulse durations below ∼800 fs (when approaching the polarization decay time) and may shorten the pulse to the point where pulse lengthening due to effects such as gain filtering and GDD compensates it fully [243].

### 4.2.6 Pulse propagation simulation of an SDL

A simulation of a pulse circulating in an SDL cavity can give useful insight into how different parameters of the laser affect the pulse properties and performance of the laser. An analytical approach for describing passive mode locking may require a number of approximations, whereas with numerical simulations more subtle effects including temporal and spectral shape of the pulse and stability of different operation regimes can be investigated [17, 19, 23, 188, 239]. Moreover, simulations provide direct access to the consequences of changing particular setup parameters, presenting a laser engineer with intuitive and fast means to improve the current system design.

Some of the lasers demonstrated in this thesis were simulated using a non-commercial software, which models the optical pulse as a superposition of a few thousand (typically 4096) complex amplitudes oscillating within the roundtrip time period, starting from white noise [210, P4,P5]. The software was originally developed by R. Herda to model fiber lasers [201]. Within the studies presented in this thesis, the software was customized in order to simulate the semiconductor gain element. The model excludes thermal effects due to intense pumping, the optical Stark effect, and ultrafast carrier dynamics in the semiconductor elements of the laser. This reduces the reliability of the model at very high power levels and for pulse durations much below 1 ps. As in a true laser, in the model the pulse propagates sequentially through cavity elements described in the computer program with appropriate operators. Operators are applied to the pulse in either the time or the frequency domain and their impact on the pulse calculated with either analytical or numerical methods, whichever is more suitable. The required elements for modeling an SDL are the saturable gain, saturable absorber, chromatic dispersion and nonlinear phase change in semiconductor structures, and the gain filter. Cavity loss

including output coupling was also incorporated into the model.

The temporal responses to an optical pulse experienced by the semiconductor gain element and absorber are essentially identical; the gain is depleted by the pulse in a similar way that the pulse saturates the absorption. Therefore, for the wavelength independent power gain coefficient $g$ and power loss coefficient $q$ we have rate equations [17, 21–23, 263, P4,P5]

$$\frac{\mathrm{d}g(t)}{\mathrm{d}t} = \frac{g_0 - g(t)}{\tau_G} - \frac{g(t)|A(t)|^2}{E_G} \tag{4.1}$$

and

$$\frac{\mathrm{d}q(t)}{\mathrm{d}t} = \frac{q_0 - q(t)}{\tau_A} - \frac{q(t)|A(t)|^2}{E_A} \,. \tag{4.2}$$

Here, $g_0$ is the small-signal gain coefficient, $\tau_G$ is the gain recovery time, $E_G$ and $E_A$ are the saturation energies for the gain and absorber, respectively, and $q_0$ is the unsaturated loss, which represents the modulation depth of the SESAM. For the instantaneous power of the complex slowly varying electric field envelope $A$ of a pulse after and before transmission through gain and absorber we have the relation [263, 264]

$$|A_{\mathrm{i+1}}(t)|^2 = |A_{\mathrm{i}}(t)|^2 exp[g(t) - q(t)] \,, \tag{4.3}$$

calculated with a first order approximation by the software.

Chromatic dispersion and nonlinear phase change can be modeled with a modified nonlinear Schrödinger equation

$$\frac{\partial A(\tilde{z},T)}{\partial \tilde{z}} = -\frac{i}{2}D_2\frac{\partial^2 A(\tilde{z},T)}{\partial T^2} + \frac{1}{6}D_3\frac{\partial^3 A(\tilde{z},T)}{\partial T^3} + \frac{1}{2}(1 - i\alpha_G)g(\tilde{z},T)A(\tilde{z},T) - \frac{1}{2}l_G A(\tilde{z},T) \,, \tag{4.4}$$

which describes the evolution of the field envelope of a pulse propagating in the gain element [45, 251, 265–270, P5]. Here, $\tilde{z}$ is the normalized position and $T$ represents time in the rest frame of the pulse. $D_2$, $D_3$, $\alpha_G$ and $l_G$ are the second and third order dispersion, linewidth enhancement factor and intrinsic losses for the gain element, respectively. For

pulse propagation in the absorber, a similar equation can be used with the saturable gain replaced by saturable absorption and the other parameters changed accordingly.

Equations 4.1 and 4.2 are solved by approximating the pulse shape with piecewise constant sections [210]. Equation 4.4 is solved numerically with the split-step Fourier transform method [210,266,271]. Gain filtering can be included in the frequency domain step. The gain filter is applied to the pulse by multiplying the Fourier transform of the pulse envelope by a filter function of appropriate shape and bandwidth. Gaussian filtering was used in the simulations.

Alternatively to calculating dispersion and nonlinear phase effects from equation 4.4, a dispersive element can be combined with the gain filter and applied to the pulse in one step in the frequency domain [P4]. The changes in the phase $\Phi$ of the slowly varying pulse envelope induced in the gain are then obtained (in the time domain) from [23]

$$\Delta\Phi(t) = -\frac{1}{2}\alpha_G g(t)\,, \tag{4.5}$$

with $A(t) = |A(t)|exp\{i[\Phi(t) + \Delta\Phi(t)]\}$. In the absorber similar phase changes but of different sign, involving the linewidth enhancement factor of the absorber, occur. Given that the linewidth enhancement factors are positive for semiconductors within the scope of this thesis, contributions to the phase of a pulse due to depletion of the gain and bleaching of the absorption amount to up-chirp and down-chirp, respectively [23, 250, 251].

In simulations shown in this work, the values of the above mentioned model parameters were chosen to closely match the values measured or evaluated for a true laser setup. However, many parameters of an SDL under operation are difficult to determine because of their complex dependence on factors like carrier density, temperature and the quality of semiconductor growth. Examples of typical values for simulation parameters can be found in [P3–P5].

## 4.3 ML with weakly saturated absorbers

### 4.3.1 Incentives

The pursuit of multigigahertz pulse repetition rates and high quality pulses free from pulse broadening nonlinearities in the semiconductor elements of the SDL makes the

regime of operation with a pulse energy comparable to or lower than the saturation energy of the absorber of high practical importance [5, 134]. This regime becomes more critical still when using QW (instead of QD) absorbers, for which a low value of saturation fluence is challenging to achieve without compromising the bandwidth of the device [203, 272].

Results obtained from high-repetition-rate SDLs indicate that stable, clean pulsing may occur at a low level of absorber saturation [273]. In the referenced study it was proposed, however not further analyzed, that a new driving mechanism could be responsible for ML in this regime.

Systematic experimental evidence of how the modulation depth of the SESAM affects the pulse duration in SDLs provides valuable information for engineers aiming to build optimized pulse sources.

The next sections describe and discuss pulsed SDLs operating at a low level of absorber saturation with SESAMs covering a wide range of modulation depths. The development of ML demonstrated with partial bleaching of the SESAMs is explained qualitatively by applying the standard model for saturable gain and absorption to the circumstances of the experiment [P3]. Pulse duration is shown to strongly decrease with an increase in modulation depth.

### 4.3.2 Experiment

The effect of modulation depth on pulse duration was investigated in a SESAM-mode-locked SDL. A detailed description of the experimental setup can be found in [P3]. A number of SESAMs with different modulation depths in the range of 9–16 %, obtained by controlling the enhancement of the subcavity resonance typically detuned a few nm to shorter wavelengths from the laser emission set by the gain resonance at 1058 nm, were tested under operating conditions as similar as possible. The SESAMs had a few-ps recovery time attained by Ni irradiation [274]. For an increased single pass gain matching the losses introduced by the SESAMs, a 5-QW gain element with a 66 %-reflective top coating was employed in the experiment.

Stable, self-starting ML was observed for all the SESAMs, even at pulse energies notably below the saturation energies of the SESAMs. Figure 4.2(a) shows the pulse duration with respect to modulation depth measured at a pulse fluence of 6 $\mu$J/cm$^2$ at the SESAM, corresponding to the saturation parameter S=$F_p/F_A < 0.13$. The experimen-

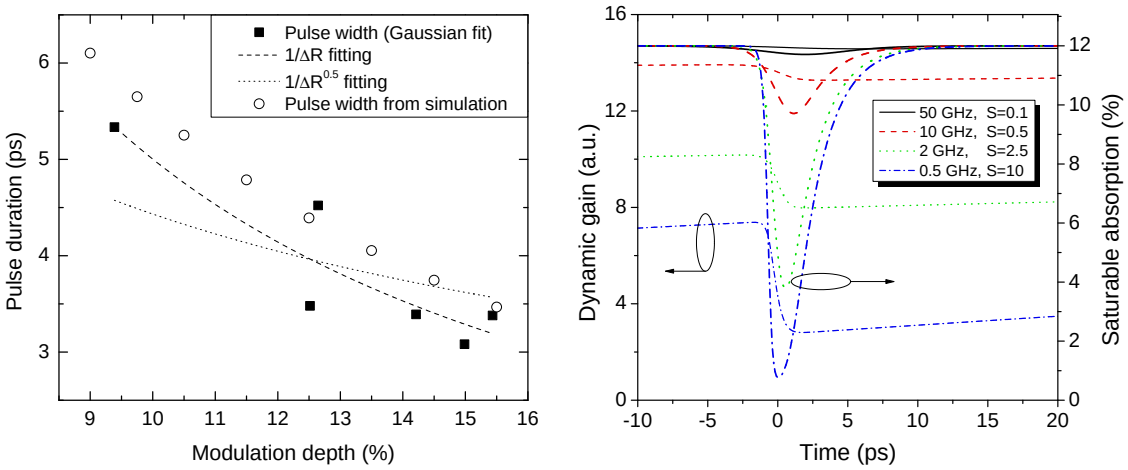


(a) (b)

Figure 4.2: (a) Experimental (filled squares) and simulated (open circles) pulse duration as a function of modulation depth. (b) Gain and absorber dynamics simulated for various cavity lengths and constant output power of the SDL corresponding to different saturation levels of the SESAM with a modulation depth of 12 %.

tal pulse duration (filled squares) decreases with modulation depth and roughly follows a $1/\Delta R$ -dependence supported by numerical simulations (open circles) performed for low-energy pulses (S=0.15) with methods and parameters described in Section 4.2.6 and in [P3], respectively. The $1/\sqrt{\Delta R}$ -fitting acts as a reference representing the guideline for pulse duration derived for solid-state lasers under strong saturation of absorption [22]. Variation in nonsaturable losses and subcavity detuning of the SESAM samples, resulting in unequal pumping conditions and dispersion between experiments with different SESAMs, may explain the scatter in the experimental data. However, according to simulations, even a large variation in dispersion on the order of a few thousand $fs^2$ has little effect on the picosecond pulse duration, which is determined largely by the response of the absorber.

### 4.3.3 Discussion

As class-A lasers, SDLs exhibit low noise and operate in high-Q cavities with negligible spontaneous emission captured by the laser mode [275]. Repetition rates exceeding the

inverse gain relaxation time and pulse energies far below the saturation energy of the gain reduce the distinctive gain excursions by every consecutive pulse characteristic of semiconductor gain medium and drive the gain dynamics closer to those of a slow medium saturated to a nearly unchanged level by the average power. Together these features result in a reduced modulation of absorber loss required to open the net gain window and to initiate and stabilize ML in the regime of low saturation of absorption. There is no need for an additional pulse shaping mechanism. The tendency for the gain and absorption perturbations to diminish with increasing repetition rate or decreasing pulse energy is illustrated in Fig. 4.2(b), where gain and absorber dynamics have been plotted for a high-power SDL with a fundamental cavity repetition rate varying from 500 MHz to 50 GHz. For constant output power the saturation parameter S varies correspondingly, from 10 to 0.1.

ML at low absorber saturation has not been observed with conventional solid-state or fiber lasers because of their tendency for Q-switching (or Q-switched ML in particular) at low pulse energies, which arises from the accumulation of pumped energy in the slowly relaxing medium insufficiently depleted by a single low-energy pulse [21, 276]. SDLs, on the other hand, are almost free from Q-switching instabilities due to the large gain cross section and short relaxation time of the gain, which is comparable to the roundtrip time of typical SDL cavities [13, 21, 134, 277]. Furthermore, with harmonic ML the Q-switching stability criterion for minimum pulse energy is alleviated in direct proportion to the harmonic number [21, 144]. Only in extreme conditions, for a pulse period much shorter than the relaxation time of the gain, has behavior reminiscent of Q-switched ML with slow variations in the amplitude of the pulse train envelope been observed in SDLs [6].

## 4.4 Harmonic ML

### 4.4.1 Background and motivation

Harmonic ML, as defined in the introductory part of the earlier section in this chapter describing the elementary concepts of ML, implies that several equally spaced pulses circulate in the laser cavity [236]. In SDLs mode-locked with a SESAM the physical cavity dimensions set an upper limit of about 50 GHz for the repetition rate of one-pulse ML [134]. Harmonic ML allows repetition rates beyond 100 GHz to be achieved with

relatively long cavities and conventional sample designs [5, 6, 273]. These high pulse repetition rates indicate potential for high-speed optical sampling and clocking, as well as arbitrary waveform generation and data transfer at terahertz bit rates with multiplexing techniques [278–280].

### 4.4.2 Mechanisms of multiple pulse formation in SDLs

In SESAM-mode-locked lasers at intracavity pulse fluences strongly exceeding the saturation fluence of the SESAM, high saturation of the absorber results in reduced discrimination by the SESAM between states with different numbers of pulses in the cavity. At a high enough fluence, reduction of the absorber loss due to more complete bleaching becomes smaller than the increase of loss due to TPA and gain filtering [46, 67, 218]. A state with a higher number of equidistant pulses circulating in the cavity with a smaller fluence may then exhibit lower losses, making a switch to the regime with more pulses likely.

The short gain relaxation time and large gain cross section of semiconductor media favor high pulse repetition rates in SDLs for more efficient extraction of the pumped energy from the gain element [5, 112, 229, 277]. A high pulse repetition rate reduces the energy wasted in spontaneous emission between pulses. Furthermore, the fast gain saturation in the semiconductor for each pulse at a time results in higher gain for low-energy pulses compared to high-energy pulses [187].

In fs-SDLs delivering intense pulses of duration comparable to the intraband carrier thermalization time in QWs, the tendency for harmonic ML or multiple pulse operation is pronounced due to spectral hole burning [5]. The shorter the pulse duration the lower the pulse energy needed for saturation of the absorber, because an increasing part of the absorption bleaching comes from spectral hole burning instead of band filling. The consequent lower saturation fluence manifests as an oversaturated absorber that can no longer suppress additional pulses which use the gain more efficiently and exhibit lower losses from TPA [5]. Analogously, an ultrashort pulse can deplete the gain faster than scattering effects refill the states, which decreases the energy available in the gain for one pulse [63]. Multiple pulsing or harmonic ML is favored for pulses with durations below $\sim$300 fs, as the gain is not depleted by a single pulse but the remaining excited carriers are available for additional pulses after thermalization and cooling of carriers on a $\sim$1-ps timescale [63]. Ultrashort pulses allow very high repetition rates to be achieved.

In Ref. [5] ML at the $18^{\text{th}}$ harmonic repetition rate at 92 GHz was detected.

Coupling the lasing modes to an extracavity frequency-selecting element such as an etalon presents another way to scale up the pulse repetition rate in SDLs independent of the pumping or saturation levels. In Refs. [6, 273] harmonic ML was reported at the $149^{\text{th}}$ and $117^{\text{th}}$ harmonic frequency at 147 and 175 GHz, respectively, with the help of coupling between the laser cavity and the substrate of the SESAM or a diamond heat spreader.

### 4.4.3 Experiment

In the early experiments to mode-lock an SDL at the ORC, a z-cavity configuration was chosen for its straightforward alignment process and independent controllability of mode sizes at the gain element and SESAM. The length of such a cavity is inherently on the order of tens of centimeters for a mode size at the gain mirror matching the typical pump spot size for optical pumping, and that at the SESAM ensuring strong saturation for guaranteed favoring of pulsed over CW regime. Therefore, the cavity roundtrip time approaches or exceeds the $\sim$1-ns relaxation time of the semiconductor gain medium, and at high pumping an increase in the number of pulses in the cavity results in more efficient extraction of the pumped energy for the lasing modes. A resonant gain element was used in the experiments for its high tolerance for losses introduced by the SESAM, cavity and possible mismatch of the pump spot and mode size. Although antireflection coated, the gain chip still exhibited high differential gain, which further increased the likelihood of multiple pulses even at pump powers close to threshold.

Harmonic ML in an SDL was observed in the experiment reported in [P4]. The setup used for characterization of the gigahertz pulse train is described in Ref. [281]. For edge emitting semiconductor lasers the tendency to switch to harmonic ML had been already observed in the eighties, but this was the first time harmonic ML was documented for an SDL [235, 282]. At the onset of lasing one-pulse ML was detected, but with an increase of pump power the number of equidistant pulses circulating in the cavity increased. ML at up to the $6^{\text{th}}$ harmonic frequency of the cavity corresponding to a repetition rate of 2.1 GHz could be achieved. The data obtained from all measurement devices including an oscilloscope and a heterodyne RF analyzer connected to a fast photoreceiver were consistent with the picture of harmonic ML [P4]. Figure 4.3 shows the oscilloscope trace and RF spectrum for ML at the fundamental, second and third harmonic order. The

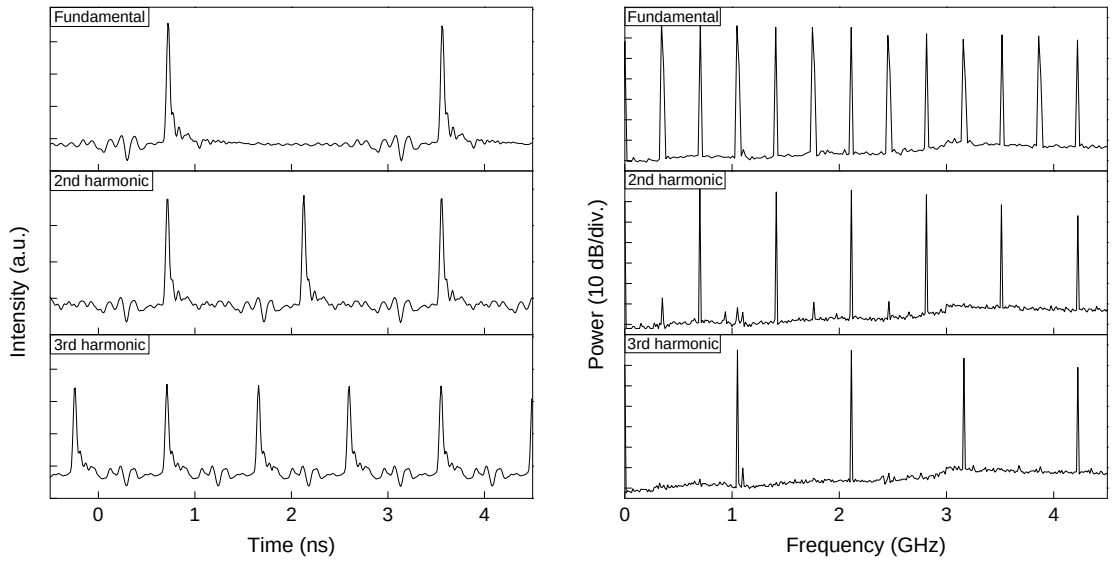


(a) (b)

Figure 4.3: (a) Oscilloscope trace and (b) RF spectrum of the SDL pulse train recorded with a 12-GHz photodiode for fundamental (top), 2nd harmonic (middle) and 3rd harmonic (bottom) ML.

almost complete suppression (by $\sim$60 dB) of the cavity fundamentals in the RF spectra for the harmonic ML is a firm indication of a highly periodic pulse train [233].

The number of pulses circulating in the cavity was found to depend more or less linearly on pump power. This trend was confirmed by numerical simulations performed with methods described in Section 4.2.6. The experimental (filled squares) and simulated (open circles) number of equidistant pulses in the cavity are plotted in Fig. 4.4(a) with respect to absorbed pump power. ML at each harmonic could be observed for a range of pump powers roughly centered around the plotted values where the most stable operation with a nearly constant pulse width and energy of $\sim$15 ps and $\sim 15 \times E_A$, respectively, was attained. Clean pulsing at repetition rates higher than 2.1 GHz was not observed in the experiment, in part due to the oversaturated absorber which allowed noise to develop with an increase in pump power. The differences between the experimental and simulated pulse number can be accounted for by a mismatch between simulation parameters and the parameters of the true laser setup, as no extensive iterations were made to adjust the simulation parameters.

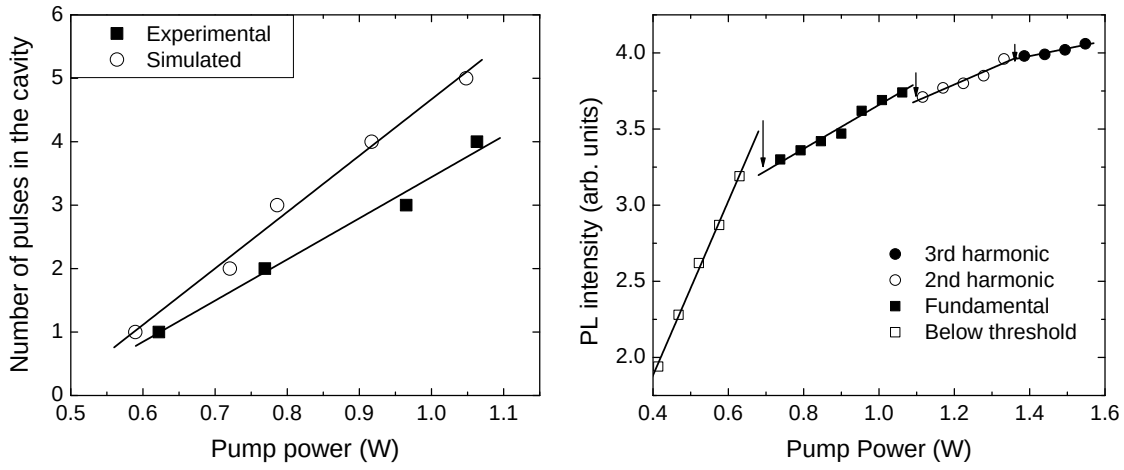


(a) (b)

Figure 4.4: (a) Experimental (squares) and simulated (circles) harmonic order in a SESAM-mode-locked SDL as a function of absorbed pump power. (b) Photoluminescence from the gain element of a SESAM-mode-locked SDL with respect to pump power. The arrows highlight the abrupt drops in the PL signal that correspond to up shifts in the harmonic order.

As expected, shifts to higher harmonics were accompanied by a reduced spontaneous emission level, which can be seen in Fig. 4.4(b) showing the photoluminescence (PL) measured at a large angle to the surface normal of the gain chip to avoid disturbance of the emission by cavity effects in an experiment similar to that reported in [P4]. The improved energy extraction from the gain element by a large number of pulses is observed as a decreased slope of the PL signal with respect to pump power for higher harmonics, as a smaller amount of the increased pump power is wasted in spontaneous emission between pulses.

### 4.4.4 Ordering of pulses

The high periodicity of pulses observed in the experiment described in Section 4.4.3 suggests that a strong pulse ordering mechanism must be present in a harmonically mode-locked SDL. Pulse ordering was studied with numerical simulations by monitoring the formation of pulses from white noise over a long time period corresponding to $\sim 1.5 \times 10^6$ roundtrips in the cavity. In Fig. 4.5(a) the evolution of ML at the $5^{\text{th}}$ harmonic frequency

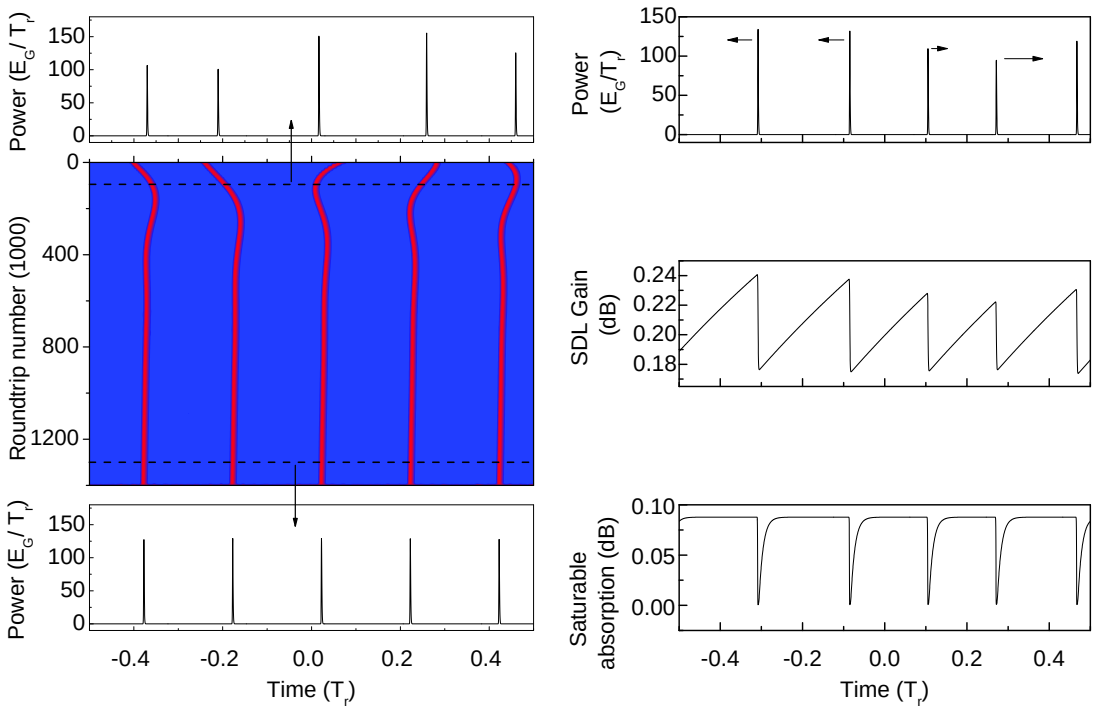


Figure 4.5: (a) Evolution of ML at the 5th harmonic frequency. Power distributions of the pulse sequence within one roundtrip time are shown at an early (top) and late (bottom) stage of pulse train formation. The middle graph illustrates the evolution of the temporal positions of the pulses with respect to roundtrip number. (b) Laser dynamics for non-steady-state 5th harmonic ML developed 40000 roundtrips from white noise. Power distribution, saturable gain and saturable absorption within the roundtrip period are shown in top, middle and bottom panels, respectively. The arrows in the top panel represent the direction and strength of the drifts of pulses relative to each other.

is illustrated, showing a power distribution within one roundtrip time $T_r$ of the SDL cavity for a disordered pulse sequence at an early stage of ML (top), and for a fully ordered pulse sequence (bottom), after $10^5$ and $1.3\times10^6$ roundtrips from the onset of harmonic ML, respectively. The temporal position of the pulses has been plotted within one roundtrip time (on the x-axis) with respect to roundtrip number (on the y-axis) in the middle panel of Fig. 4.5(a). It can be seen that the initially disordered sequence of pulses with diverse intensities evolves to a train of identical pulses within about $4\times10^5$

roundtrips.

Gain saturation with pulse transit and the recovery of the gain on a timescale comparable to or longer than the pulse period were identified as the main mechanisms behind the drift of pulses towards a highly periodic pulse sequence. In the gain element, the leading edge of the pulse undergoes stronger amplification than the trailing edge of the pulse. This manifests itself as an effective shift of the pulse forward in time. The pulse ordering mechanism relies on the fact that the magnitude of the temporal shift experienced by a pulse is essentially determined by the gain available for – or more precisely, the gain depleted by – the pulse at the time of the transit through the gain element [233]. For example, a short period between two pulses and the consequent short time for gain recovery between the pulses results in a low gain level for the second pulse, which thereby experiences a small temporal shift and is left behind relative to the first pulse. As a result, the pulse interval is increased towards a balanced value [283]. Conversely, a long pulse interval provides a strong shift forward in time for the second pulse.

The ordering mechanism is illustrated in Fig. 4.5(b), where the optical power for non-steady-state $5^{\text{th}}$ harmonic ML after having evolved 40000 roundtrips from white noise (top) together with the corresponding SDL gain (middle) and saturable absorption (bottom) are plotted against time spanning one roundtrip period. The direction and length of the arrows in the top panel of Fig. 4.5(b) represent the direction and magnitude of the temporal shifts of the pulses with respect to the average time shift experienced by the pulses.

The contribution of saturable absorption to pulse ordering was found to be negligible, due to the short absorber recovery time compared to the pulse spacing. The drift backwards in time caused by SESAM saturation is constant for all pulses. Furthermore, although influencing the pulse duration, dispersion and nonlinear phase effects were found to have little impact on the strength of pulse ordering for the studied low-power SDL not operating in the soliton regime.

### 4.4.5 Dynamics of pulse characteristics

Harmonic ML in an SDL can be readily observed in the pulse characteristics of the laser with respect to pump and output power. Particularly, the pulse characteristics exhibit notable changes when the laser shifts from one state of operation to another with a different number of pulses in the cavity. In Fig. 4.6 the duration, time-bandwidth product

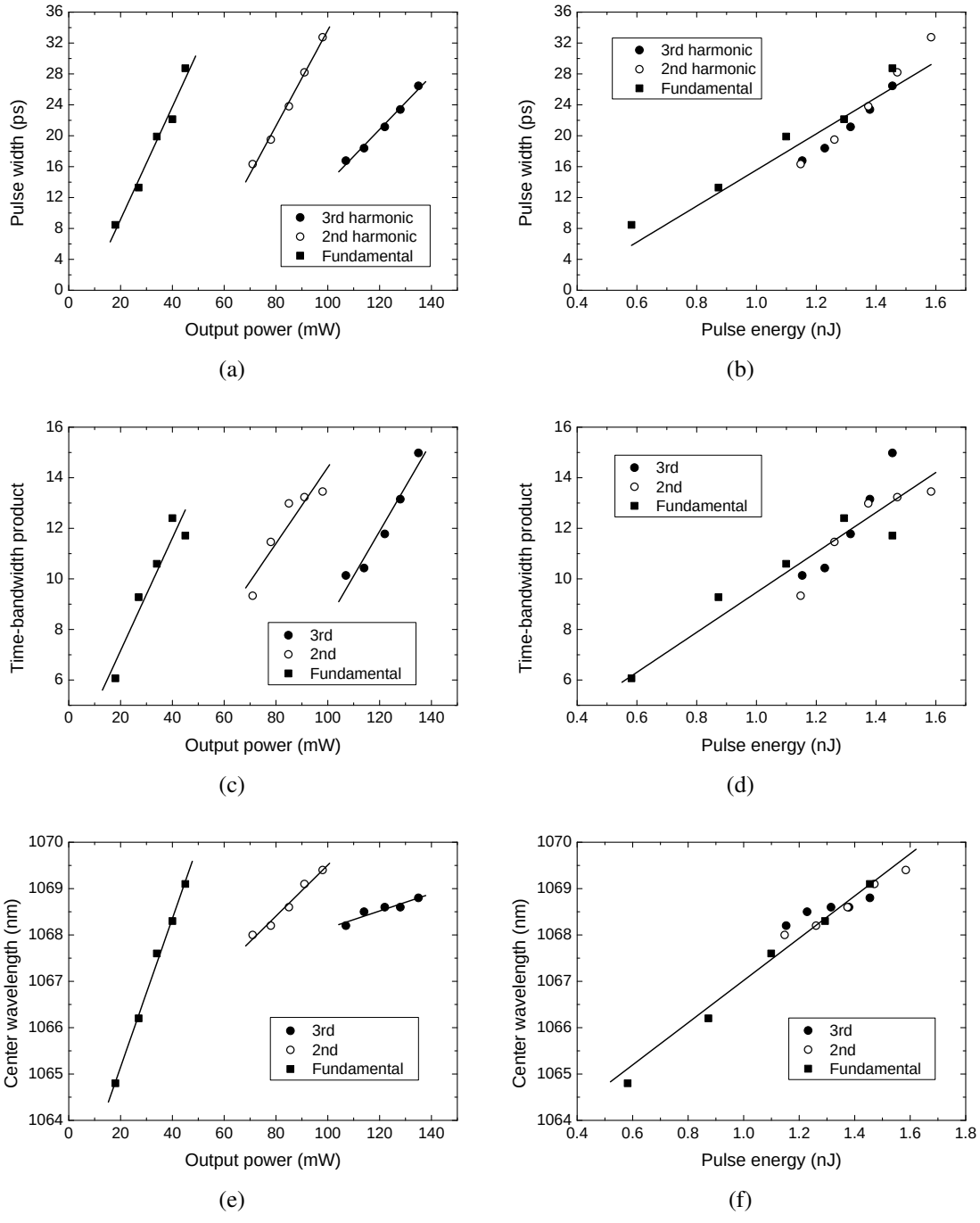


Figure 4.6: Pulse characteristics for ML at the fundamental, second and third harmonic repetition rate. (a) and (b) Pulse width, (c) and (d) time-bandwidth product, (e) and (f) center wavelength with respect to output power and pulse energy, respectively.

and center wavelength of the pulses delivered by a SESAM-mode-locked SDL reported in [P5] have been plotted with respect to output power (left column) and pulse energy (right column). The pulse characteristics versus output power show distinctive differences between ML at the fundamental, second and third harmonic cavity repetition rate of 1 GHz. However, with respect to pulse energy, a regular increase of pulse duration, time-bandwidth product and center wavelength is measured for all the states of operation.

The nonlinear phase changes related to the carrier density changes induced by the pulses in the semiconductor elements – particularly in the gain structure – of the SDL largely explain the observations shown in Fig. 4.6. The phase changes increase with pulse energy, because a more energetic pulse depletes the gain and saturates the SESAM more efficiently. The (negative) phase contribution from the SESAM is not expected to change much with pulse energy in typical SDLs operating at full saturation of the absorber, even for pulses with the lowest energy. Phase changes in the gain element thus dominate, and the pulses are broadened at high pulse energies due to increased up-chirp in the presence of normal dispersion, as shown in Figs. 4.6(a)–(d). Sharp steps in pulse characteristics with respect to output power occur with a change in harmonic number as the pulse characteristics follow the more or less linear dependence on pulse energy. The decreased slope of the pulse broadening with output power for the higher harmonics is because the intracavity energy added with an increase of pump power (amounting to the increase in output power) is divided by a larger number of pulses at the higher repetition rate.

The red shift with output power and pulse energy seen in Figs. 4.6(e) and 4.6(f) cannot be of thermal origin because of its discontinuous dependence on pump and output power. Rather, the center wavelength changes with the amount of gain saturation induced during pulse transit. Specifically, the up-chirped pulses observed in the studied SDL experience a red shift in the gain element because of the larger amplification of the low-frequency spectral components in the leading edge of the pulse compared to that of the high-frequency components in the trailing edge of the pulse. The higher the pulse energy the faster and more complete the gain depletion, and the more pronounced the red shift of the pulse. For example, the abrupt steps to shorter wavelengths with an increase in the pulse repetition rate seen in Fig. 4.6(e) are a result of the weaker red shift in the gain for the pulses with lower energy. The blue shift of the pulse in the SESAM due to the higher reflection of the trailing edge compared to the leading edge of the pulse is not expected

to change much with respect to pulse energy in the studied regime of strong saturation of the SESAM.

Gain dynamics during one roundtrip time simulated for fundamental, second and fourth harmonic ML are shown in Fig. 4.7(a). The simulations were run at a constant pump and output power, resulting in a nearly constant rate of gain recovery between pulses for different harmonics [217, 246]. An increase in the pulse repetition rate then implies less complete gain recovery, a decreased pulse energy and lower pulse-induced gain depletion. Consequently, pulse distortions and wavelength shifts due to gain perturbations are smaller for ML at high harmonics. The strong effect of gain saturation during pulse transit on the center wavelength of the pulse is further illustrated in Fig. 4.7(b) showing optical spectra for different harmonics observed for a SDL reported in [P4]. In contrast to the thermal red shift with increasing pump power usually expected for semiconductor lasers, a blue shift with harmonic number is observed even though the pump and output powers increase with the harmonic number [50]. Figure 4.7(c) shows the SDL input-output light relation corresponding to the pulse characteristics measurements of Fig. 4.6. A small step-like increase in output power can be observed at around 1.1 and 1.35 W of pump power where the laser shifts up in harmonic number and the energy wasted in spontaneous emission is decreased.

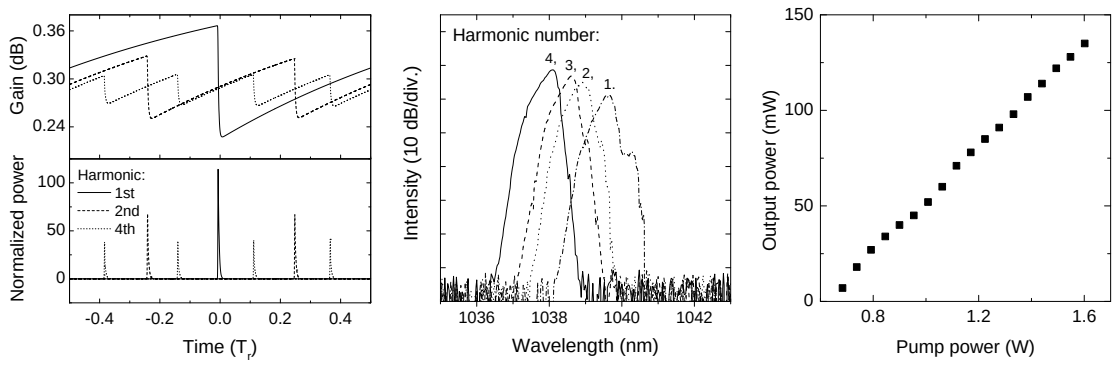


Figure 4.7: (a) Gain dynamics (top) simulated for an SDL delivering mode-locked pulses (bottom) at the fundamental, second and fourth harmonic cavity repetition rate. (b) Optical spectra measured for ML at different harmonics. (c) Input-output light measurement corresponding to the results shown in Fig. 4.6.

### 4.4.6 The effect of dispersion on pulse characteristics

SDLs showing a strong tendency for harmonic ML typically take advantage of gain designs with high differential gain, such as the RPG structures employed in the harmonically mode-locked SDLs studied in this thesis. As discussed in Section 2.1.3, these kinds of gain elements exhibit distinctive variations of dispersion around the subcavity resonance wavelength, which may in part explain the broadening of pulses in time frequently observed in harmonically mode-locked SDLs [P4–P6].

The effect of second and third order dispersion on the pulse characteristics of SESAM-mode-locked SDLs was investigated with numerical simulations [P5]. Particularly, the aim was to identify the dispersion regime responsible for the results shown in Fig. 4.6. Anomalous second order dispersion resulted in time-broadened pulses seeming to correspond to those observed in the experiment. However, unlike in the experiment, regardless of the sign of third order dispersion the pulses blueshifted with an increase in pulse energy, because of the down chirp and the pronounced difference in amplification between the leading edge and the trailing edge of the pulse at high pulse energies. Normal second order dispersion together with zero or negative ($D_3$<0) third order dispersion led to nearly transform-limited pulses with durations much shorter than in experiments. The dispersion regime for which the simulations matched the experimental results was normal second order and positive third order dispersion. Figures 4.8(a) and 4.8(b) show the experimental and simulated optical spectra obtained for fundamental ML at different pulse energies, respectively. The shape and red shift of the simulated spectra closely resemble the measured spectra. With normal second order and positive third order dispersion also the dependence of the simulated pulse duration and time-bandwidth product on pulse energy followed the trends seen in Fig. 4.6 [P5]. Positively chirped pulses can be expected with the specified dispersion regime, as confirmed by an earlier experiment in which pulses from an SDL similar to that reported in [P5] were externally compressed down to 1 ps with anomalous dispersion [P4].

The presented investigation suggests that the large third order dispersion, inherent to RPG structures near the gain resonance, may prevent quasi-soliton pulse formation, and significantly contributes to the pulse broadening observed in the harmonic ML experiments. Shorter pulses could be obtained by tuning the laser wavelength with respect to gain resonance with an intracavity filter or etalon, for example, or by decreasing the field enhancement in the RPG element.

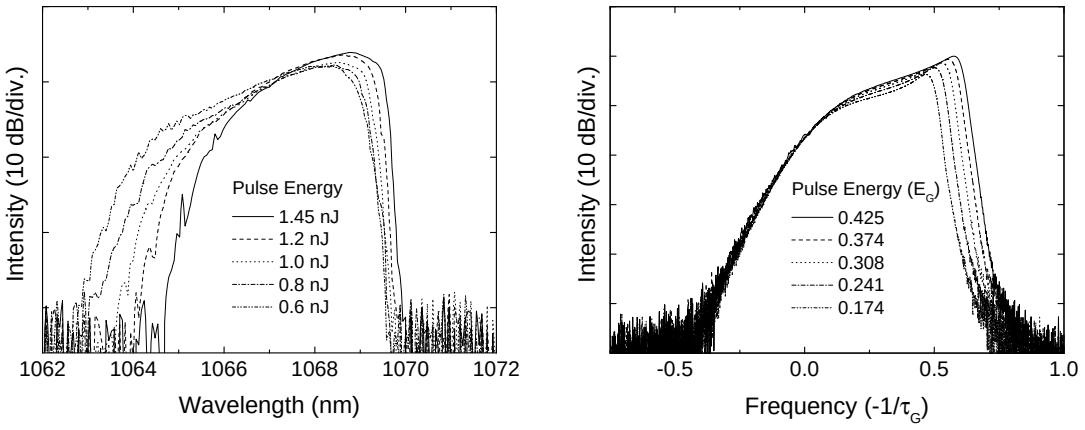


Figure 4.8: (a) Experimental and (b) simulated optical spectra for various pulse energies of a SESAM-mode-locked SDL.

### 4.4.7 Hysteresis and bistability

#### Background and motivation

In SESAM-mode-locked SDLs exhibiting harmonic ML with an increase of pump power the range of pump powers for which a given harmonic is observed can overlap with the pump power ranges for the adjacent regimes having one pulse more or one pulse less circulating in the cavity [P6]. This feature, known from studies for diode lasers, manifests itself as hysteresis and bistability of the SDL pulse characteristics [235, 236, P6]. Tailoring the semiconductor gain characteristics represents a convenient way to control the size and number of hysteresis loops obtained at a given pump power, thus holding promise for future applications in all-optical processing, for example [284, P6].

#### Principles of hysteresis formation

Models for passive ML allow multiple stable solutions for a single pulse or multiple pulses to exist for a given small-signal gain [16, 19, 224, 232, 234, 236, 276, 285].

The hysteresis and bistability observed in SESAM-mode-locked SDLs can be explained by the dependence of the effective amplification of the pulses on pulse energy, analogously to the analysis presented in Refs. [285, 286]. At low pulse energies the

effective amplification increases with increasing pulse energy because of the more complete absorber saturation. However, at high pulse energies, the gain saturates and loss mechanisms arise from TPA in the absorber and from gain filtering. Gain filtering may occur due to a short pulse width resulting from efficient pulse shaping by the absorber, or because of increased chirping due to nonlinear phase effects caused mainly by gain perturbations induced by the energetic pulses. The latter mechanism is further encouraged by the use of a resonant gain element with a decreased bandwidth, increased field enhancement and a tendency for pronounced gain compression. The loss mechanisms cause the effective amplification for existing pulses in the cavity to decrease with pulse energy at high pulse energies, until with increasing pump power at a certain pulse energy amplification for a low-energy pulse, appearing from noise enhanced by the energy accumulating in the gain, exceeds the amplification for the high energy pulses. The low-energy pulse then grows and the high-energy pulses diminish until an energy balance is achieved between pulses. Increased pumping is needed to again reduce the effective amplification for the pulses and further increase the number of pulses. Hysteresis in pulse number with respect to pump power arises because typically for the state with an increased number of identical pulses the absorber and gain are still strongly saturated. Consequently, the effective amplification is increased if pulse energy is decreased, generating a feedback loop that restores the energy to a pulse that loses energy. With decreasing pump power, the pulse drop-out becomes likely only when the effective amplification for the pulses reaches its maximum level, i.e. when the losses due to incomplete saturation of the absorption start to dominate over the less saturated gain. Then, if the energy of one of the pulses decreases due to (random) fluctuations, the pulse experiences lower amplification than the other pulses and continues to diminish.

Hysteresis at the threshold of a mode-locked laser appears due to saturable absorption. For emission with random phases of the longitudinal modes at the onset of lasing the threshold is higher than for a mode-locked pulse that can bleach the absorber.

### Experiment

Three semiconductor gain designs were tested in an SDL mode-locked at 1 $\mu$m by a 3-QW antiresonant SESAM to highlight the role of differential gain in hysteresis loop formation [P6]. Figure 4.9(a) shows the refractive index profiles and corresponding standing wave optical fields for the RPG design, an RPG design with a reduced field

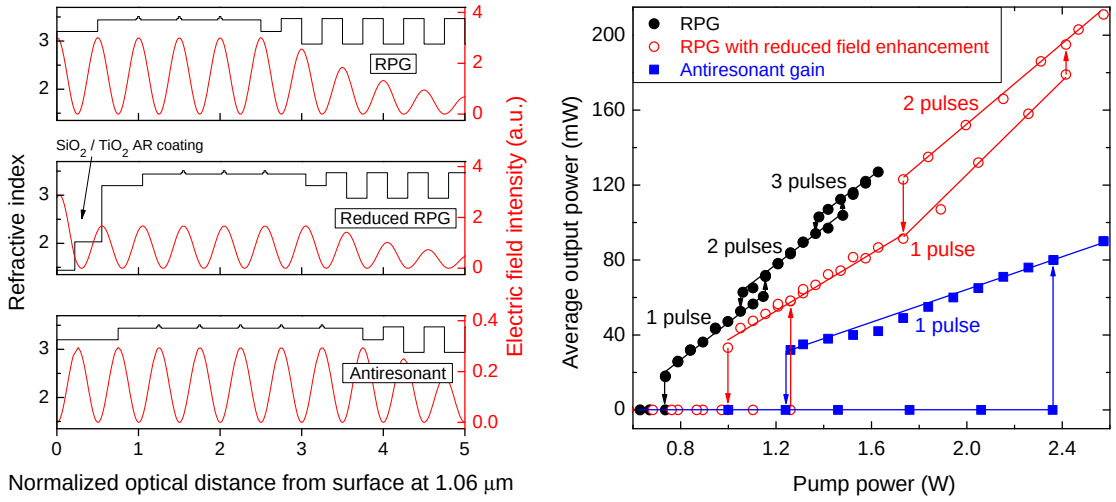


(a) (b)

Figure 4.9: (a) Design schematics for an RPG structure (top), an RPG structure with reduced field enhancement (middle) and an antiresonant structure (bottom). (b) Input-output light curves for ML with the gain designs displayed in (a) showing diverse differential gain characteristics.

enhancement thanks to AR coating, and the antiresonant design used in the study. Figure 4.9(b) shows the power characteristics measured for the gain designs in mode-locked operation. Hysteresis and bistability occurs with all the gain designs, either at threshold or between states with a different harmonic number. Furthermore, the number and size of the hysteresis loops appear to depend on the differential gain. For the RPG structure having the largest differential gain, a small increase of pump power is enough to raise the unsaturated gain and the pulse energy to a level favoring formation of additional pulses. Moreover, the long effective interaction length in the RPG allows for efficient gain saturation at a low pulse energy and enables a small increment in pulse energy to change the effective amplification favorable for an increase in pulse number.

Instead of many small hysteresis loops observed at fairly low pump powers for the RPG structure, the number of the loops occurring in the pump power range of Fig. 4.9(b) is decreased and the size of the loops is increased for the RPG design with a reduced field enhancement and for the antiresonant structure. The largest hysteresis at threshold and operation at the fundamental repetition rate only is observed for the antiresonant structure having the lowest differential gain.

Hysteresis in the output power was accompanied by hysteresis in the pulse characteristics, which had similar tendencies as those seen in Fig. 4.6 for harmonic ML. Figure 4.10 shows the pulse duration and operation wavelength with respect to incident pump power for the RPG design with reduced field enhancement. Pulse duration and red shift scale up with pulse energy due to enhanced gain distortions, and drop down with a shift to a higher harmonic because of the decrease in pulse energy and less complete gain recovery between pulses.

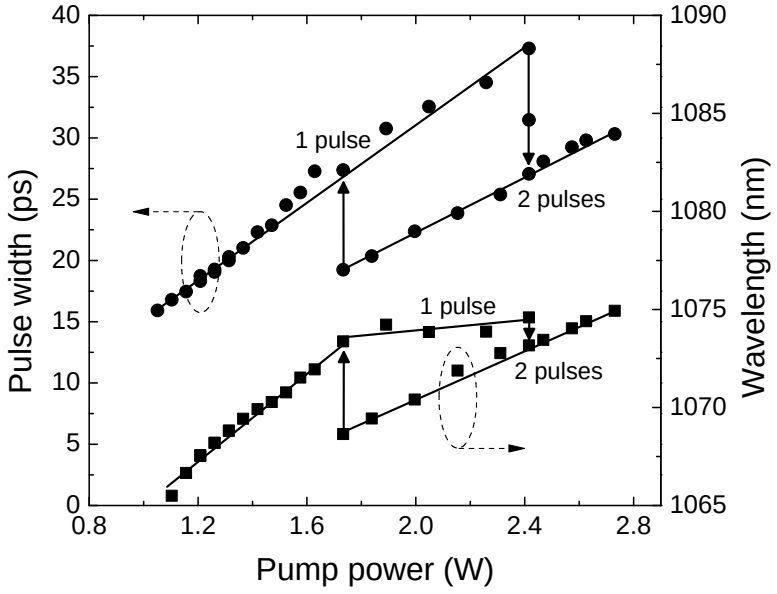


Figure 4.10: Hysteresis in pulse duration and center wavelength associated with a switch between fundamental and second harmonic ML measured for the RPG design with reduced field enhancement.

### 4.4.8 Guidelines for control of pulses from SDLs

The analysis presented in the previous sections gives grounds for simple guidelines for the control of pulse generation from SESAM-mode-locked SDLs.

The pulse repetition rate obtained at a given pump power from a harmonically mode-locked SDL can be controlled by adjusting the gain recovery time [P4]. A short recovery of the gain implies more pulses in the cavity. Low saturation energies of the gain medium and absorber promote high repetition rates [P5]. An RPG structure exhibiting high field

enhancement can be used to increase the number of pulses in the cavity efficiently, even at moderate pump powers [P4-P6].

Hysteresis in the output characteristics of the SDL can be controlled by the choice of gain design [P6]. For a resonant design with a large differential gain, modest pump power modulation can provide a shift in the operation regime. For distinct hysteresis loops an antiresonant gain should be employed. Hysteresis loops are expected to further enlarge with harmonic number, because the increase in pump power needed for a given change in pulse energy increases at high repetition rates when the energy is distributed among many pulses.

The pulse energy can be scaled up while keeping the nonlinear phase effects low by increasing the saturation energies of the gain medium and absorber [P4]. This is readily accomplished by increasing the transverse laser mode size on the gain element and absorber or by decreasing the field enhancement in both the semiconductor elements, which may, however, decrease the efficiency and pulse quality of the laser.

To shorten pulse duration, nonlinearities and dispersion should be controlled in order to achieve a balance between contributions from the gain element and SESAM. Generally, gain perturbations should be kept small in order to avoid high-order dispersion by tuning the field enhancement or by operating at antiresonance [P5]. Large mode sizes at the gain element and absorber help to avoid oversaturation and the consequent pulse broadening due to nonlinearities. Gain filtering and the recovery time of the absorber should be minimized to achieve sub-ps pulses. A large SESAM modulation depth results in more efficient pulse shaping [P3]. In particular, pulse duration for an SDL at weak saturation of the absorber is approximately inversely proportional to the modulation depth. However, a large modulation depth is often accompanied by high nonsaturable losses, which limit the output performance of the laser.

# Chapter 5

# Conclusion

The main achievements of this thesis are as follows:

A high-power (> 0.6 W) passively mode-locked semiconductor disk laser utilizing a wafer-fused gain mirror and a wedged diamond heat spreader was presented. The approach resulted in a picosecond pulse source at the wavelength of 1.57 $\mu$m difficult to access by monolithically grown semiconductor gain structures.

The first frequency-shifted feedback semiconductor disk laser was demonstrated. By using a glass etalon for spectral edge filtering and an acousto-optic modulator to shift up the frequency of the optical radiation at every roundtrip, stable mode locking starting at the laser threshold was obtained. The studied method provided a robust and simple means for pulse formation, alleviating cavity design constraints inherent to SESAM-mode-locked lasers.

Pulse shaping in semiconductor disk lasers in the regime of low absorber saturation was studied. Experiments performed with a wide assortment of SESAMs exhibiting different modulation depths together with numerical simulations confirmed that steady-state mode locking can be achieved at pulse energies well below the saturation energy of the absorber. Pulse duration was shown to decrease strongly with modulation depth. The findings are of practical importance for lasers with multigigahertz repetition rates inclined to partial bleaching of absorption.

Harmonic mode locking for the generation of ultrashort pulses from a semiconductor disk laser at multigigahertz repetition rates was demonstrated and studied in detail both experimentally and numerically. Gain saturation and fast recovery of the gain were found to be responsible for the strong pulse ordering in multiple pulse operation.

Pulse formation in passively mode-locked semiconductor disk lasers was investigated experimentally and by numerical simulations with a particular emphasis on the effect of dynamic gain saturation and dispersion on pulse shaping. Gain perturbation during pulse transit was identified as one of the main mechanisms behind nonlinear pulse distortions. It was suggested that third order dispersion may prevent quasi-soliton formation, thereby limiting pulse shortening in the laser.

Hysteresis and bistability in the output characteristics of a passively mode-locked semiconductor disk laser was reported and studied experimentally. It was shown that the size and number of the hysteresis loops could be manipulated by appropriate design of the gain element. The controllability of the phenomenon may contribute to the development of optical memory applications.

# Bibliography


[1] W. B. Jiang, S. R. Friberg, H. Iwamura, and Y. Yamamoto, "High powers and subpicosecond pulses from an external-cavity surface-emitting InGaAs/InP multiple quantum well laser," *Applied Physics Letters*, vol. 58, no. 8, pp. 807–809, 1991.

[2] R. Haring, R. Paschotta, F. Morier-Genoud, U. Keller, A. Garnache, U. Oesterle, J. Roberts, S. Hoogland, S. Dhanjal, and A. Tropper, "Passively mode-locked diode-pumped surface-emitting semiconductor lasers," in *Conference on Lasers and Electro-Optics (CLEO) 2000*, May 2000, pp. 97–98.

[3] S. Hoogland, S. Dhanjal, A. Tropper, J. Roberts, R. Haring, R. Paschotta, F. Morier-Genoud, and U. Keller, "Passively mode-locked diode-pumped surface-emitting semiconductor laser," *IEEE Photonics Technology Letters*, vol. 12, no. 9, pp. 1135–1137, 2000.

[4] M. Kuznetsov, F. Hakimi, R. Sprague, and A. Mooradian, "High-power (>0.5-W CW) diode-pumped vertical-external-cavity surface-emitting semiconductor lasers with circular $TEM_{00}$ beams," *IEEE Photonics Technology Letters*, vol. 9, no. 8, pp. 1063–1065, 1997.

[5] P. Klopp, U. Griebner, M. Zorn, and M. Weyers, "Pulse repetition rate up to 92 GHz or pulse duration shorter than 110 fs from a mode-locked semiconductor disk laser," *Applied Physics Letters*, vol. 98, no. 7, p. 071103, 2011.

[6] K. G. Wilcox, A. H. Quarterman, V. Apostolopoulos, H. E. Beere, I. Farrer, D. A. Ritchie, and A. C. Tropper, "175 GHz, 400-fs-pulse harmonically mode-locked surface emitting semiconductor laser." *Optics Express*, vol. 20, no. 7, pp. 7040–7045, 2012.

[7] B. Rudin, V. J. Wittwer, D. J. H. C. Maas, M. Hoffmann, O. D. Sieber, Y. Barbarin, M. Golling, T. Südmeyer, and U. Keller, "High-power MIXSEL: an integrated ultrafast semiconductor laser with 6.4 W average power," *Optics Express*, vol. 18, no. 26, pp. 27 582–27 588, 2010.

[8] S. Tsuda, W. Knox, S. Cundiff, W. Jan, and J. Cunningham, "Mode-locking ultrafast solid-state lasers with saturable Bragg reflectors," *IEEE Journal of Selected Topics in Quantum Electronics*, vol. 2, no. 3, pp. 454–464, 1996.

[9] U. Keller, K. Weingarten, F. Kartner, D. Kopf, B. Braun, I. Jung, R. Fluck, C. Honninger, N. Matuschek, and J. Aus der Au, "Semiconductor saturable absorber mirrors (SESAM's)

for femtosecond to nanosecond pulse generation in solid-state lasers," *IEEE Journal of Selected Topics in Quantum Electronics*, vol. 2, no. 3, pp. 435–453, 1996.

[10] T. Südmeyer, C. Kränkel, C. Baer, O. Heckl, C. Saraceno, M. Golling, R. Peters, K. Petermann, G. Huber, and U. Keller, "High-power ultrafast thin disk laser oscillators and their potential for sub-100-femtosecond pulse generation," *Applied Physics B*, vol. 97, no. 2, pp. 281–295, 2009.

[11] J. Aus der Au, G. J. Spühler, T. Südmeyer, R. Paschotta, R. Hövel, M. Moser, S. Erhard, M. Karszewski, A. Giesen, and U. Keller, "16.2-W average power from a diode-pumped femtosecond Yb:YAG thin disk laser," *Optics Letters*, vol. 25, no. 11, pp. 859–861, 2000.

[12] T. Südmeyer, S. V. Marchese, S. Hashimoto, C. R. E. Baer, G. Gingras, B. Witzel, and U. Keller, "Femtosecond laser oscillators for high-field science," *Nature Photonics*, vol. 2, no. 10, pp. 599–604, 2008.

[13] U. Keller and A. C. Tropper, "Passively modelocked surface-emitting semiconductor lasers," *Physics Reports*, vol. 429, no. 2, pp. 67–120, 2006.

[14] R. Paschotta, "Encyclopedia of Laser Physics and Technology," RP Photonics Consulting GmbH, Waldstr. 17, 78073 Bad Dürrheim, Germany. [Online]. Available: http://www.rp-photonics.com/passive_mode_locking.html.

[15] A. Siegman and D. Kuizenga, "Modulator frequency detuning effects in the FM mode-locked laser," *IEEE Journal of Quantum Electronics*, vol. 6, no. 12, pp. 803–808, 1970.

[16] G. New, "Pulse evolution in mode-locked quasi-continuous lasers," *IEEE Journal of Quantum Electronics*, vol. 10, no. 2, pp. 115–124, 1974.

[17] H. A. Haus, "Theory of mode locking with a fast saturable absorber," *Journal of Applied Physics*, vol. 46, no. 7, pp. 3049–3058, 1975.

[18] P. W. Smith, M. A. Duguay, and E. P. Ippen, "Mode-locking of lasers," in *Progress in Quantum Electronics*, J. H. Sanders and S. Stenholm, Eds., vol. 3, pt. 2. Pergamon Press, 1975.

[19] H. Haus, "Theory of mode locking with a slow saturable absorber," *IEEE Journal of Quantum Electronics*, vol. 11, no. 9, pp. 736–746, 1975.

[20] F. X. Kärtner, J. Aus der Au, and U. Keller, "Mode-locking with slow and fast saturable absorbers -what's the difference?" *IEEE Journal of Selected Topics in Quantum Electronics*, vol. 4, pp. 159–168, 1998.

[21] C. Hönninger, R. Paschotta, F. Morier-Genoud, M. Moser, and U. Keller, "Q-switching stability limits of continuous-wave passive mode locking," *Journal of the Optical Society of America B*, vol. 16, no. 1, pp. 46–56, 1999.

[22] R. Paschotta and U. Keller, "Passive mode locking with slow saturable absorbers," *Applied Physics B: Lasers and Optics*, vol. 73, pp. 653–662, 2001.

[23] R. Paschotta, R. Häring, A. Garnache, S. Hoogland, A. Tropper, and U. Keller, "Soliton-like pulse-shaping mechanism in passively mode-locked surface-emitting semiconductor lasers," *Applied Physics B: Lasers and Optics*, vol. 75, pp. 445–451, 2002.

[24] A. Garnache, S. Hoogland, A. C. Tropper, I. Sagnes, G. Saint-Girons, and J. S. Roberts, "Sub-500-fs soliton-like pulse in a passively mode-locked broadband surface-emitting laser with 100 mW average power," *Applied Physics Letters*, vol. 80, pp. 3892–3894, 2002.

[25] O. Okhotnikov (Ed.), *Semiconductor Disk Lasers: Physics and Technology*, 1st ed. Wiley-VCH, Weinheim, 2010.

[26] A. Tropper and S. Hoogland, "Extended cavity surface-emitting semiconductor lasers," *Progress in Quantum Electronics*, vol. 30, no. 1, pp. 1–43, 2006.

[27] S. Calvez, J. Hastie, M. Guina, O. Okhotnikov, and M. Dawson, "Semiconductor disk lasers for the generation of visible and ultraviolet radiation," *Laser & Photonics Reviews*, vol. 3, no. 5, pp. 407–434, 2009.

[28] N. Schulz, J.-M. Hopkins, M. Rattunde, D. Burns, and J. Wagner, "High-brightness long-wavelength semiconductor disk lasers," *Laser & Photonics Reviews*, vol. 2, no. 3, pp. 160–181, 2008.

[29] J. L. A. Chilla, Q. Shu, H. Zhou, E. S. Weiss, M. K. Reed, and L. Spinelli, "Recent advances in optically pumped semiconductor lasers," in *Proceedings of SPIE*, vol. 6451, 645109, 2007.

[30] A. Härkönen, "Optically-Pumped Semiconductor Disk Lasers for Generating Visible and Infrared Radiation," Ph.D. dissertation, Tampere University of Technology, Tampere, Finland, 2008.

[31] T. Leinonen, "The design and fabrication of lasing semiconductor nanostructures employing vertical-cavity geometry," Ph.D. dissertation, Tampere University of Technology, Tampere, Finland, 2007.

[32] S. McGinily, "Optically Pumped Semiconductor Vertical External Cavity Surface Emitting Lasers," Ph.D. dissertation, University of Strathclyde, Glasgow, United Kingdom, 2005.

[33] L. Morton, "Visible and Ultraviolet Vertical External Cavity Surface Emitting Semiconductor Lasers," Ph.D. dissertation, University of Strathclyde, Glasgow, United Kingdom, 2008.

[34] T.-L. Wang, Y. Kaneda, J. Yarborough, J. Hader, J. Moloney, A. Chernikov, S. Chatterjee, S. Koch, B. Kunert, and W. Stolz, "High-power optically pumped semiconductor laser at 1040 nm," *IEEE Photonics Technology Letters*, vol. 22, no. 9, pp. 661–663, 2010.

[35] M. Raja, S. Brueck, M. Osinski, C. Schaus, J. McInerney, T. Brennan, and B. Hammons, "Resonant periodic gain surface-emitting semiconductor lasers," *IEEE Journal of Quantum Electronics*, vol. 25, no. 6, pp. 1500–1512, 1989.

[36] S. W. Corzine, R. S. Geels, J. W. Scott, R. H. Yan, and L. A. Coldren, "Design of Fabry-Perot surface-emitting lasers with a periodic gain structure," *IEEE Journal of Quantum Electronics*, vol. 25, no. 6, pp. 1513–1524, 1989.

[37] S.-S. Beyertt, M. Zorn, T. Kubler, H. Wenzel, M. Weyers, A. Giesen, G. Trankle, and U. Brauch, "Optical in-well pumping of a semiconductor disk laser with high optical efficiency," *IEEE Journal of Quantum Electronics*, vol. 41, no. 12, pp. 1439 – 1449, 2005.

[38] A. Adams, "Band-structure engineering for low-threshold high-efficiency semiconductor lasers," *IET Electronics Letters*, vol. 22, no. 5, pp. 249–250, 1986.

[39] J. Lyytikäinen, "Optically Pumped Semiconductor Disk Lasers Operating at Near Infrared Spectral Range," Ph.D. dissertation, Tampere University of Technology, Tampere, Finland, 2011.

[40] H. Foreman, "Mode-Locked Vertical-External-Cavity Surface Emitting Lasers," Ph.D. dissertation, University of Southampton, Southampton, United Kingdom, 2006.

[41] P. Ilroy, A. Kurobe, and Y. Uematsu, "Analysis and application of theoretical gain curves to the design of multi-quantum-well lasers," *IEEE Journal of Quantum Electronics*, vol. 21, no. 12, pp. 1958–1963, 1985.

[42] M. Kuznetsov, F. Hakimi, R. Sprague, and A. Mooradian, "Design and characteristics of high-power (>0.5-W CW) diode-pumped vertical-external-cavity surface-emitting semiconductor lasers with circular $TEM_{00}$ beams," *IEEE Journal of Selected Topics in Quantum Electronics*, vol. 5, no. 3, pp. 561–573, 1999.

[43] D. Lorenser, "Picosecond VECSELs with repetition rates up to 50 GHz," Ph.D. dissertation, Swiss Federal Institute of Technology, Zürich, Switzerland, 2006.

[44] R. Paschotta, RP Photonics Consulting GmbH, Personal communication, Tampere, Finland, Aug. 2006.

[45] G. Agrawal and N. Olsson, "Self-phase modulation and spectral broadening of optical pulses in semiconductor laser amplifiers," *IEEE Journal of Quantum Electronics*, vol. 25, no. 11, pp. 2297–2306, 1989.

[46] P. Klopp, U. Griebner, M. Zorn, A. Klehr, A. Liero, M. Weyers, and G. Erbert, "Mode-locked InGaAs-AlGaAs disk laser generating sub-200-fs pulses, pulse picking and amplification by a tapered diode amplifier," *Optics Express*, vol. 17, no. 13, pp. 10 820–10 834, 2009.

[47] B. Zhao, T. Chen, and A. Yariv, "The extra differential gain enhancement in multiple-quantum-well lasers," *IEEE Photonics Technology Letters*, vol. 4, no. 2, pp. 124 –126, Feb. 1992.

[48] M. Bertolotti, V. Bogdanov, A. Ferrari, A. Jascow, N. Nazorova, A. Pikhtin, and L. Schirone, "Temperature dependence of the refractive index in semiconductors," *Journal of the Optical Society of America B*, vol. 7, no. 6, pp. 918–922, 1990.

[49] Y. P. Varshni, "Temperature dependence of the energy gap in semiconductors," *Physica*, vol. 34, no. 1, pp. 149–154, 1967.

[50] M. A. Holm, D. Burns, P. Cusumano, A. I. Ferguson, and M. D. Dawson, "High-Power Diode-Pumped AlGaAs Surface-Emitting Laser," *Applied Optics*, vol. 38, no. 27, pp. 5781–5784, 1999.

[51] A. Aschwanden, "High Peak Power Passively Mode-Locked VECSELs," Ph.D. dissertation, Swiss Federal Institute of Technology, Zürich, Switzerland, 2004.

[52] F. Gires and P. Tournois, "Interféromètre utilisable pour la compression d'impulsions lumineuses modulées en fréquence," *Comptes Rendus de l'Académie des Sciences*, vol. 258, pp. 6112–6115, 1964.

[53] J. Kuhl and J. Heppner, "Compression of femtosecond optical pulses with dielectric multilayer interferometers," *IEEE Journal of Quantum Electronics*, vol. 22, no. 1, pp. 182–185, 1986.

[54] M. Beck and I. A. Walmsley, "Measurement of group delay with high temporal and spectral resolution," *Optics Letters*, vol. 15, no. 9, pp. 492–494, 1990.

[55] A. C. Tropper, H. D. Foreman, A. Garnache, K. G. Wilcox, and S. H. Hoogland, "Vertical-external-cavity semiconductor lasers," *Journal of Physics D: Applied Physics*, vol. 37, no. 9, p. R75, 2004.

[56] A. Garnache, A. A. Kachanov, F. Stoeckel, and R. Houdré, "Diode-pumped broadband vertical-external-cavity surface-emitting semiconductor laser applied to high-sensitivity intracavity absorption spectroscopy," *Journal of the Optical Society of America B*, vol. 17, no. 9, pp. 1589–1598, 2000.

[57] A. Chernikov, J. Herrmann, M. Koch, B. Kunert, W. Stolz, S. Chatterjee, S. W. Koch, T.-L. Wang, Y. Kaneda, J. M. Yarborough, J. Hader, and J. V. Moloney, "Heat Management in High-Power Vertical-External-Cavity Surface-Emitting Lasers," *IEEE Journal of Selected Topics in Quantum Electronics*, vol. 17, no. 6, pp. 1772–1778, 2011.

[58] A. Chernikov, J. Herrmann, M. Scheller, M. Koch, B. Kunert, W. Stolz, S. Chatterjee, S. W. Koch, T. L. Wang, Y. Kaneda, J. M. Yarborough, J. Hader, and J. V. Moloney, "Influence of the spatial pump distribution on the performance of high power vertical-external-cavity surface-emitting lasers," *Applied Physics Letters*, vol. 97, no. 19, p. 191110, 2010.

[59] A. J. Maclean, R. B. Birch, P. W. Roth, A. J. Kemp, and D. Burns, "Limits on efficiency and power scaling in semiconductor disk lasers with diamond heatspreaders," *Journal of the Optical Society of America B*, vol. 26, no. 12, pp. 2228–2236, 2009.

[60] R. Häring, R. Paschotta, A. Aschwanden, E. Gini, F. Morier-Genoud, and U. Keller, "High-power passively mode-locked semiconductor lasers," *IEEE Journal of Quantum Electronics*, vol. 38, no. 9, pp. 1268–1275, 2002.

[61] B. Rudin, A. Rutz, M. Hoffmann, D. J. H. C. Maas, A.-R. Bellancourt, E. Gini, T. Südmeyer, and U. Keller, "Highly efficient optically pumped vertical-emitting semiconductor laser with more than 20 W average output power in a fundamental transverse mode," *Optics Letters*, vol. 33, no. 22, pp. 2719–2721, 2008.

[62] A. Aschwanden, D. Lorenser, H. J. Unold, R. Paschotta, E. Gini, and U. Keller, "2.1-W picosecond passively mode-locked external-cavity semiconductor laser," *Optics Letters*, vol. 30, no. 3, pp. 272–274, 2005.

[63] A. H. Quarterman, K. G. Wilcox, V. Apostolopoulos, Z. Mihoubi, S. P. Elsmere, I. Farrer, D. A. Ritchie, and A. Tropper, "A passively mode-locked external-cavity semiconductor laser emitting 60-fs pulses," *Nature Photonics*, vol. 3, no. 12, pp. 729–731, 2009.

[64] K. Wilcox, A. Quarterman, H. Beere, D. Ritchie, and A. Tropper, "High peak power femtosecond pulse passively mode-locked vertical-external-cavity surface-emitting laser," *IEEE Photonics Technology Letters*, vol. 22, no. 14, pp. 1021 –1023, 2010.

[65] D. Maas, A.-R. Bellancourt, B. Rudin, M. Golling, H. Unold, T. Südmeyer, and U. Keller, "Vertical integration of ultrafast semiconductor lasers," *Applied Physics B*, vol. 88, pp. 493–497, 2007.

[66] A.-R. Bellancourt, D. Maas, B. Rudin, M. Golling, T. Sudmeyer, and U. Keller, "Mode-locked integrated external-cavity surface emitting laser," *IET Optoelectronics*, vol. 3, no. 2, pp. 61–72, 2009.

[67] P. Klopp, F. Saas, M. Zorn, M. Weyers, and U. Griebner, "290-fs pulses from a semiconductor disk laser," *Optics Express*, vol. 16, no. 8, pp. 5770–5775, 2008.

[68] D. Love, M. Kolesik, and J. Moloney, "Optimization of ultrashort pulse generation in passively mode-locked vertical external-cavity semiconductor lasers," *IEEE Journal of Quantum Electronics*, vol. 45, no. 5, pp. 439 –445, 2009.

[69] Y. F. Chen, Y. C. Lee, H. C. Liang, K. Y. Lin, K. W. Su, and K. F. Huang, "Femtosecond high-power spontaneous mode-locked operation in vertical-external cavity surface-emitting laser with gigahertz oscillation," *Optics Letters*, vol. 36, no. 23, pp. 4581–4583, 2011.

[70] S. Sweeney, A. Phillips, A. Adams, E. O'Reilly, and P. Thijs, "The effect of temperature dependent processes on the performance of 1.5-$\mu$m compressively strained InGaAs(P)

MQW semiconductor diode lasers," *IEEE Photonics Technology Letters*, vol. 10, no. 8, pp. 1076–1078, 1998.

[71] E. P. O'Reilly and M. Silver, "Temperature sensitivity and high temperature operation of long wavelength semiconductor lasers," *Applied Physics Letters*, vol. 63, no. 24, pp. 3318 –3320, 1993.

[72] J.-Y. Yeh, N. Tansu, and L. Mawst, "Temperature-sensitivity analysis of 1360-nm dilute-nitride quantum-well lasers," *IEEE Photonics Technology Letters*, vol. 16, no. 3, pp. 741 –743, 2004.

[73] N. Bazhenov, K. Mynbaev, V. Ivanov-Omskii, V. Smirnov, V. Evtikhiev, N. Pikhtin, M. Rastegaeva, A. Stankevich, I. Tarasov, A. Shkol'nik, and G. Zegrya, "Temperature dependence of the threshold current of QW lasers," *Semiconductors*, vol. 39, pp. 1210–1214, 2005.

[74] R. Paschotta, J. Aus der Au, G. Spühler, F. Morier-Genoud, R. Hövel, M. Moser, S. Erhard, M. Karszewski, A. Giesen, and U. Keller, "Diode-pumped passively mode-locked lasers with high average power," *Applied Physics B: Lasers and Optics*, vol. 70, pp. S25–S31, 2000.

[75] A. Rantamäki, J. Lyytikäinen, J. Nikkinen, and O. G. Okhotnikov, "Effect of thermal management on the properties of saturable absorber mirrors in high-power mode-locked semiconductor disk lasers," *Quantum Electronics*, vol. 41, no. 9, pp. 786–789, 2011.

[76] S. Ranta, T. Leinonen, M. Tavast, T. Hakkarainen, I. Suominen, and M. Guina, "Strain compensation of InGaAs/GaAs SDL gain mirrors grown by molecular beam epitaxy," in *Proceedings of SPIE*, vol. 8242, 824211, 2012.

[77] J. Chilla, S. Butterworth, A. Zeitschel, J. Charles, A. Caprara, M. Reed, and L. Spinelli, "High-power optically pumped semiconductor lasers," in *Proceedings of SPIE*, vol. 5332, pp. 143–150, 2004.

[78] H. Lindberg, M. Strassner, E. Gerster, J. Bengtsson, and A. Larsson, "Thermal management of optically pumped long-wavelength InP-based semiconductor disk lasers," *IEEE Journal of Selected Topics in Quantum Electronics*, vol. 11, no. 5, pp. 1126–1134, 2005.

[79] A. Kemp, J.-M. Hopkins, A. Maclean, N. Schulz, M. Rattunde, J. Wagner, and D. Burns, "Thermal Management in 2.3-$\mu$m Semiconductor Disk Lasers: A Finite Element Analysis," *IEEE Journal of Quantum Electronics*, vol. 44, no. 2, pp. 125 –135, 2008.

[80] C. Kessel, S. Gee, and J. Murphy, "The quality of die-attachment and its relationship to stresses and vertical die-cracking," *IEEE Transactions on Components, Hybrids, and Manufacturing Technology*, vol. 6, no. 4, pp. 414–420, 1983.

[81] K. Fujiwara, T. Fujiwara, K. Hori, and M. Takusagawa, "Aging characteristics of $Ga_{1-x}Al_xAs$ double-heterostructure lasers bonded with gold eutectic alloy solder," *Applied Physics Letters*, vol. 34, no. 10, pp. 668–670, 1979.

[82] W. J. Alford, T. D. Raymond, and A. A. Allerman, "High power and good beam quality at 980 nm from a vertical external-cavity surface-emitting laser," *Journal of the Optical Society of America B*, vol. 19, no. 4, pp. 663–666, 2002.

[83] A. J. Kemp, G. J. Valentine, J.-M. Hopkins, J. E. Hastie, S. A. Smith, S. Calvez, M. D. Dawson, and D. Burns, "Thermal management in vertical-external-cavity surface-emitting lasers: Finite-element analysis of a heatspreader approach," *IEEE Journal of Quantum Electronics*, vol. 41, no. 2, pp. 148–155, 2005.

[84] Z. L. Liau, "Semiconductor wafer bonding via liquid capillarity," *Applied Physics Letters*, vol. 77, no. 5, pp. 651–653, 2000.

[85] A. Härkonen, S. Suomalainen, E. Saarinen, L. Orsila, R. Koskinen, O. Okhotnikov, S. Calvez, and M. Dawson, "4 W single-transverse mode VECSEL utilising intra-cavity diamond heat spreader," *IET Electronics Letters*, vol. 42, no. 12, pp. 693–694, 2006.

[86] J.-M. Hopkins, S. Smith, C. Jeon, H. Sun, D. Burns, S. Calvez, M. Dawson, T. Jouhti, and M. Pessa, "0.6 W CW GaInNAs vertical external-cavity surface emitting laser operating at 1.32 $\mu m$," *IET Electronics Letters*, vol. 40, no. 1, pp. 30–31, 2004.

[87] F. van Loon, A. J. Kemp, A. J. Maclean, S. Calvez, J.-M. Hopkins, J. E. Hastie, M. D. Dawson, and D. Burns, "Intracavity diamond heatspreaders in lasers: the effects of birefringence," *Optics Express*, vol. 14, no. 20, pp. 9250–9260, 2006.

[88] S. Vetter and S. Calvez, "Thermal Management of Near-Infrared Semiconductor Disk Lasers With AlGaAs Mirrors and Lattice (Mis)Matched Active Regions," *IEEE Journal of Quantum Electronics*, vol. 48, no. 3, pp. 345–352, 2012.

[89] T. Fan, "Laser beam combining for high-power, high-radiance sources," *IEEE Journal of Selected Topics in Quantum Electronics*, vol. 11, no. 3, pp. 567 – 577, 2005.

[90] L. Fan, M. Fallahi, J. Hader, A. R. Zakharian, J. V. Moloney, R. Bedford, W. Stolz, and S. W. Koch, "Multichip vertical-external-cavity surface-emitting lasers: a coherent power scaling scheme," *Optics Letters*, vol. 31, no. 24, pp. 3612–3614, 2006.

[91] L. E. Hunziker, Q. Shu, C. Ihli, G. J. Mahnke, M. Rebut, J. L. A. Chilla, A. L. Caprara, H. Zhou, E. S. Weiss, and M. K. Reed, "Power-scaling of optically pumped semiconductor lasers," in *Proceedings of SPIE*, vol. 6451, 64510A, 2007.

[92] A. E. Siegman, "New developments in laser resonators," in *Proceedings of SPIE*, vol. 1224, no. 1, pp. 2–14, 1990.

[93] G. H. C. New, "The generation of ultrashort laser pulses," *Reports on Progress in Physics*, vol. 46, no. 8, p. 877, 1983.

[94] P. M. W. French, "The generation of ultrashort laser pulses," *Reports on Progress in Physics*, vol. 58, no. 2, p. 169, 1995.

[95] H. W. Mocker and R. J. Collins, "Mode competition and self-locking effects in a q-switched ruby laser," *Applied Physics Letters*, vol. 7, no. 10, pp. 270–273, 1965.

[96] S. Rausch, T. Binhammer, A. Harth, J. Kim, R. Ell, F. X. Kärtner, and U. Morgner, "Controlled waveforms on the single-cycle scale from a femtosecond oscillator," *Optics Express*, vol. 16, no. 13, pp. 9739–9745, 2008.

[97] W. Xiang, S. R. Friberg, K. Watanabe, S. Machida, W. Jiang, H. Iwamura, and Y. Yamamoto, "Femtosecond external-cavity surface-emitting InGaAs/InP multiple-quantum-well laser," *Optics Letters*, vol. 16, no. 18, pp. 1394–1396, 1991.

[98] W. H. Xiang, S. R. Friberg, K. Watanabe, S. Machida, Y. Sakai, H. Iwamura, and Y. Yamamoto, "Sub-100 femtosecond pulses from an external-cavity surface-emitting lnGaAs/InP multiple quantum well laser with soliton-effect compression," *Applied Physics Letters*, vol. 59, no. 17, pp. 2076–2078, 1991.

[99] W. Zhang, T. Ackemann, M. Schmid, N. Langford, and A. Ferguson, "Femtosecond synchronously mode-locked vertical-external cavity surface-emitting laser," *Optics Express*, vol. 14, no. 5, pp. 1810–1821, 2006.

[100] A. Härkönen, J. Rautiainen, L. Orsila, M. Guina, K. Röszner, M. Hümmer, T. Lehnhardt, M. Müller, A. Forchel, M. Fischer, J. Koeth, and O. G. Okhotnikov, "2-$\mu$m Mode-Locked Semiconductor Disk Laser Synchronously Pumped Using an Amplified Diode Laser," *IEEE Photonics Technology Letters*, vol. 20, no. 15, pp. 1332 –1334, 2008.

[101] M. Holm, P. Cusumano, D. Burns, A. Ferguson, and M. Dawson, "Mode-locked operation of a diode-pumped, external-cavity GaAs/AlGaAs surface emitting laser," in *Conference on Lasers and Electro-Optics (CLEO) '99*, May 1999, pp. 153–154.

[102] H. L. Chang, S. C. Huang, Y.-F. Chen, K. W. Su, Y. F. Chen, and K. F. Huang, "Efficient high-peak-power AlGaInAs eye-safe wavelength disk laser with optical in-well pumping," *Optics Express*, vol. 17, no. 14, pp. 11 409–11 414, 2009.

[103] K. W. Su, S. C. Huang, A. Li, S. C. Liu, Y. F. Chen, and K. F. Huang, "High-peak-power AlGaInAs quantum-well 1.3-$\mu$m laser pumped by a diode-pumped actively Q-switched solid-state laser," *Optics Letters*, vol. 31, no. 13, pp. 2009–2011, 2006.

[104] Y.-F. Chen, K. Su, W. Chen, K. Huang, and Y. Chen, "High-peak-power optically pumped AlGaInAs eye-safe laser at 500-kHz repetition rate with an intracavity diamond heat spreader," *Applied Physics B: Lasers and Optics*, pp. 1–5.

[105] N. Hempler, J.-M. Hopkins, A. J. Kemp, N. Schulz, M. Rattunde, J. Wagner, M. D. Dawson, and D. Burns, "Pulsed pumping of semiconductor disk lasers," *Optics Express*, vol. 15, no. 6, pp. 3247–3256, 2007.

[106] S. Huang, H. Chang, K. Su, A. Li, S. Liu, Y. Chen, and K. Huang, "AlGaInAs/InP eye-safe laser pumped by a Q-switched Nd:$GdVO_4$ laser," *Applied Physics B: Lasers and Optics*, vol. 94, pp. 483–487, 2009.

[107] A. J. McGrath, J. Munch, G. Smith, and P. Veitch, "Injection-seeded, single-frequency, Q-switched Erbium:glass laser for remote sensing," *Applied Optics*, vol. 37, no. 24, pp. 5706–5709, 1998.

[108] S. M. Spuler and S. D. Mayor, "Raman shifter optimized for lidar at a 1.5 $\mu$m wavelength," *Applied Optics*, vol. 46, no. 15, pp. 2990–2995, 2007.

[109] G. J. Spühler, R. Paschotta, R. Fluck, B. Braun, M. Moser, G. Zhang, E. Gini, and U. Keller, "Experimentally confirmed design guidelines for passively q-switched microchip lasers using semiconductor saturable absorbers," *Journal of the Optical Society of America B*, vol. 16, no. 3, pp. 376–388, 1999.

[110] R. Häring, R. Paschotta, R. Fluck, E. Gini, H. Melchior, and U. Keller, "Passively q-switched microchip laser at 1.5 $\mu$m," *Journal of the Optical Society of America B*, vol. 18, no. 12, pp. 1805–1812, 2001.

[111] V. G. Savitski, J. E. Hastie, S. Calvez, and M. D. Dawson, "Cavity-dumping of a semiconductor disk laser for the generation of wavelength-tunable micro-Joule nanosecond pulses," *Optics Express*, vol. 18, no. 11, pp. 11 933–11 941, 2010.

[112] K. Watanabe, H. Iwamura, and Y. Yamamoto, "Effect of additive-pulse mode locking on an external-cavity surface-emitting InGaAs semiconductor laser," *Optics Letters*, vol. 18, no. 19, pp. 1642–1644, 1993.

[113] J. Mark, L. Y. Liu, K. L. Hall, H. A. Haus, and E. P. Ippen, "Femtosecond pulse generation in a laser with a nonlinear external resonator," *Optics Letters*, vol. 14, no. 1, pp. 48–50, 1989.

[114] E. P. Ippen, H. A. Haus, and L. Y. Liu, "Additive pulse mode locking," *Journal of the Optical Society of America B*, vol. 6, no. 9, pp. 1736–1745, 1989.

[115] H. A. Haus, J. G. Fujimoto, and E. P. Ippen, "Structures for additive pulse mode locking," *Journal of the Optical Society of America B*, vol. 8, no. 10, pp. 2068–2076, 1991.

[116] U. Keller, W. H. Knox, and H. Roskos, "Coupled-cavity resonant passive mode-locked ti:sapphire laser," *Optics Letters*, vol. 15, no. 23, pp. 1377–1379, 1990.

[117] U. Keller, D. A. B. Miller, G. D. Boyd, T. H. Chiu, J. F. Ferguson, and M. T. Asom, "Solid-state low-loss intracavity saturable absorber for Nd:YLF lasers: an antiresonant semiconductor Fabry–Perot saturable absorber," *Optics Letters*, vol. 17, no. 7, pp. 505–507, 1992.

[118] U. Keller, "Recent developments in compact ultrafast lasers," *Nature*, vol. 424, no. 6950, pp. 831–838, 2003.

[119] K. Jasim, Q. Zhang, A. Nurmikko, A. Mooradian, G. Carey, W. Ha, and E. Ippen, "Passively modelocked vertical extended cavity surface emitting diode laser," *IET Electronics Letters*, vol. 39, no. 4, pp. 373–375, 2003.

[120] K. Jasim, Q. Zhang, A. Nurmikko, E. Ippen, A. Mooradian, G. Carey, and W. Ha, "Picosecond pulse generation from passively modelocked vertical cavity diode laser at up to 15 ghz pulse repetition rate," *IET Electronics Letters*, vol. 40, no. 1, pp. 34–36, 2004.

[121] Q. Zhang, K. Jasim, A. Nurmikko, A. Mooradian, G. Carey, W. Ha, and E. Ippen, "Operation of a passively mode-locked extended-cavity surface-emitting diode laser in multi-ghz regime," *IEEE Photonics Technology Letters*, vol. 16, no. 3, pp. 885–887, 2004.

[122] F. V. Kowalski, S. J. Shattil, and P. D. Hale, "Optical pulse generation with a frequency shifted feedback laser," *Applied Physics Letters*, vol. 53, no. 9, pp. 734–736, 1988.

[123] H. Sabert and E. Brinkmeyer, "Pulse generation in fiber lasers with frequency shifted feedback," *Journal of Lightwave Technology*, vol. 12, no. 8, pp. 1360–1368, 1994.

[124] G. Bonnet, S. Balle, T. Kraft, and K. Bergmann, "Dynamics and self-modelocking of a titanium-sapphire laser with intracavity frequency shifted feedback," *Optics Communications*, vol. 123, no. 4–6, pp. 790–800, 1996.

[125] J. Sousa and O. Okhotnikov, "Short pulse generation and control in Er-doped frequency-shifted-feedback fibre lasers," *Optics Communications*, vol. 183, no. 1-4, pp. 227–241, 2000.

[126] A. M. Heidt, J. P. Burger, J.-N. Maran, and N. Traynor, "High power and high energy ultrashort pulse generation with a frequency shifted feedback fiber laser," *Optics Express*, vol. 15, no. 24, pp. 15 892–15 897, 2007.

[127] J. Porta, A. B. Grudinin, Z. J. Chen, J. D. Minelly, and N. J. Traynor, "Environmentally stable picosecond ytterbium fiber laser with a broad tuning range," *Optics Letters*, vol. 23, no. 8, pp. 615–617, 1998.

[128] J. L. Chilla, B. Resan, and R. R. Austin, "Mode-locked external-cavity surface-emitting semiconductor laser," United States patent US 2009/0290606 A1, Coherent Inc, San Francisco, CA, USA, 2009.

[129] K. Stankov and F. P. Schäfer, "Mode-locked laser," United States patent 4,914,658, Max-Plank-Gesellschaft zur Foerderung der Wissenschaften e.V., Goettingen, Fed. Rep. of Germany, 1990.

[130] W. B. Jiang, R. Mirin, and J. E. Bowers, "Mode-locked GaAs vertical cavity surface emitting lasers," *Applied Physics Letters*, vol. 60, no. 6, pp. 677–679, 1992.

[131] J. M. Yarborough, Y.-Y. Lai, Y. Kaneda, J. Hader, J. V. Moloney, T. J. Rotter, G. Balakrishnan, C. Hains, D. Huffaker, S. W. Koch, and R. Bedford, "Record pulsed power demonstration of a 2 $\mu$m GaSb-based optically pumped semiconductor laser grown lattice-mismatched on an AlAs/GaAs Bragg mirror and substrate," *Applied Physics Letters*, vol. 95, no. 8, p. 081112, 2009.

[132] O. Casel, D. Woll, M. A. Tremont, H. Fuchs, R. Wallenstein, E. Gerster, P. Unger, M. Zorn, and M. Weyers, "Blue 489-nm picosecond pulses generated by intracavity frequency doubling in a passively mode-locked optically pumped semiconductor disk laser," *Applied Physics B: Lasers and Optics*, vol. 81, pp. 443–446, 2005.

[133] K. Wilcox, Z. Mihoubi, S. Elsmere, A. Quarterman, H. Foreman, S. Hashimoto, T. Sudmeyer, U. Keller, and A. Tropper, "Passively modelocked 832 nm vertical-external-cavity surface-emitting semiconductor laser producing 15.3 ps pulses at 1.9 GHz repetition rate," *IET Electronics Letters*, vol. 44, no. 25, pp. 1469–1470, 2008.

[134] D. Lorenser, D. J. H. C. Maas, H. J. Unold, A.-R. Bellancourt, B. Rudin, E. Gini, D. Ebling, and U. Keller, "50-GHz passively mode-locked surface-emitting semiconductor laser with 100-mW average output power," *IEEE Journal of Quantum Electronics*, vol. 42, no. 8, pp. 838–847, 2006.

[135] M. Hoffmann, O. D. Sieber, V. J. Wittwer, I. L. Krestnikov, D. A. Livshits, Y. Barbarin, T. Südmeyer, and U. Keller, "Femtosecond high-power quantum dot vertical external cavity surface emitting laser," *Optics Express*, vol. 19, no. 9, pp. 8108–8116, 2011.

[136] J. Rautiainen, V.-M. Korpijärvi, J. Puustinen, M. Guina, and O. Okhotnikov, "Passively mode-locked GaInNAs disk laser operating at 1220 nm," *Optics Express*, vol. 16, no. 20, pp. 15 964–15 969, 2008.

[137] J. Rautiainen, J. Lyytikäinen, L. Toikkanen, J. Nikkinen, A. Sirbu, A. Mereuta, A. Caliman, E. Kapon, and O. Okhotnikov, "1.3-$\mu$m Mode-Locked Disk Laser With Wafer Fused Gain and SESAM Structures," *IEEE Photonics Technology Letters*, vol. 22, no. 11, pp. 748–750, 2010.

[138] S. Hoogland, A. Garnache, I. Sagnes, B. Paldus, K. Weingarten, R. Grange, M. Haiml, R. Paschotta, U. Keller, and A. Tropper, "Picosecond pulse generation with 1.5 $\mu$m passively modelocked surface-emitting semiconductor laser," *IET Electronics Letters*, vol. 39, no. 11, pp. 846–847, 2003.

[139] H. Lindberg, M. Sadeghi, M. Westlund, S. Wang, A. Larsson, M. Strassner, and S. Marcinkevicius, "Mode locking a 1550 nm semiconductor disk laser by using a GaInNAs saturable absorber," *Optics Letters*, vol. 30, no. 20, pp. 2793–2795, 2005.

[140] Z. Zhao, S. Bouchoule, J. Song, E. Galopin, J.-C. Harmand, J. Decobert, G. Aubin, and J.-L. Oudar, "Subpicosecond pulse generation from a 1.56 $\mu$m mode-locked VECSEL," *Optics Letters*, vol. 36, no. 22, pp. 4377–4379, 2011.

[141] A. Härkönen, C. Grebing, J. Paajaste, R. Koskinen, J.-P. Alanko, S. Suomalainen, G. Steinmeyer, and M. Guina, "Modelocked GaSb disk laser producing 384 fs pulses at 2 $\mu$m wavelength," *IET Electronics Letters*, vol. 47, no. 7, pp. 454–456, 2011.

[142] A. Kemp, B. Stormont, B. Agate, C. Brown, U. Keller, and W. Sibbett, "Gigahertz repetition-rate from directly diode-pumped femtosecond Cr:LiSAF laser," *IET Electronics Letters*, vol. 37, no. 24, pp. 1457–1458, 2001.

[143] L. Krainer, D. Nodop, G. J. Spühler, S. Lecomte, M. Golling, R. Paschotta, D. Ebling, T. Ohgoh, T. Hayakawa, K. J. Weingarten, and U. Keller, "Compact 10-GHz Nd:$GdVO_4$ laser with 0.5-W average output power and low timing jitter," *Optics Letters*, vol. 29, no. 22, pp. 2629–2631, 2004.

[144] L. Krainer, R. Paschotta, S. Lecomte, M. Moser, K. Weingarten, and U. Keller, "Compact Nd:$YVO_4$ lasers with pulse repetition rates up to 160 GHz," *IEEE Journal of Quantum Electronics*, vol. 38, no. 10, pp. 1331–1338, 2002.

[145] S. Lecomte, M. Kalisch, L. Krainer, G. Spuhler, R. Paschotta, M. Golling, D. Ebling, T. Ohgoh, T. Hayakawa, S. Pawlik, B. Schmidt, and U. Keller, "Diode-pumped passively mode-locked Nd:$YVO_4$ lasers with 40-GHz repetition rate," *IEEE Journal of Quantum Electronics*, vol. 41, no. 1, pp. 45–52, 2005.

[146] S. C. Zeller, R. Grange, V. Liverini, A. Rutz, S. Schön, M. Haiml, U. Keller, S. Pawlik, and B. Schmidt, "A Low-Loss Buried Resonant GaInNAs SESAM for 1.3-$\mu$m Nd:YLF Laser at 1.4 GHz," in *Advanced Solid-State Photonics*, Jan. 2006, p. TuA6.

[147] A. E. Oehler, T. Südmeyer, K. J. Weingarten, and U. Keller, "100 GHz passively mode-locked Er:Yb:glass laser at 1.5 $\mu$m with 1.6-ps pulses," *Optics Express*, vol. 16, no. 26, pp. 21 930–21 935, 2008.

[148] S. Yamazoe, M. Katou, T. Adachi, and T. Kasamatsu, "Palm-top-size, 1.5 kW peak-power, and femtosecond (160 fs) diode-pumped mode-locked $Yb^{+3}$:$KY(WO_4)_2$ solid-state laser with a semiconductor saturable absorber mirror," *Optics Letters*, vol. 35, no. 5, pp. 748–750, 2010.

[149] D. Li, U. Demirbas, J. R. Birge, G. S. Petrich, L. A. Kolodziejski, A. Sennaroglu, F. X. Kärtner, and J. G. Fujimoto, "Diode-pumped passively mode-locked GHz femtosecond Cr:LiSAF laser with kW peak power," *Optics Letters*, vol. 35, no. 9, pp. 1446–1448, 2010.

[150] S. Pekarek, A. Klenner, T. Südmeyer, C. Fiebig, K. Paschke, G. Erbert, and U. Keller, "Femtosecond diode-pumped solid-state laser with a repetition rate of 4.8 GHz," *Optics Express*, vol. 20, no. 4, pp. 4248–4253, 2012.

[151] C. R. E. Baer, O. H. Heckl, C. J. Saraceno, C. Schriber, C. Kränkel, T. Südmeyer, and U. Keller, "Frontiers in passively mode-locked high-power thin disk laser oscillators," *Optics Express*, vol. 20, no. 7, pp. 7054–7065, 2012.

[152] U. Keller, "Ultrafast solid-state laser oscillators: a success story for the last 20 years with no end in sight," *Applied Physics B: Lasers and Optics*, vol. 100, pp. 15–28, 2010.

[153] M. Guden and J. Piprek, "Material parameters of quaternary III - V semiconductors for multilayer mirrors at 1.55 $\mu$m wavelength," *Modelling and Simulation in Materials Science and Engineering*, vol. 4, no. 4, p. 349, 1996.

[154] M. Guina, T. Leinonen, A. Härkönen, and M. Pessa, "High-power disk lasers based on dilute nitride heterostructures," *New Journal of Physics*, vol. 11, no. 12, p. 125019, 2009.

[155] A. N. Baranov, Y. Cuminal, G. Boissier, J. C. Nicolas, J. L. Lazzari, C. Alibert, and A. Joullié, "Electroluminescence of GaInSb/GaSb strained single quantum well structures grown by molecular beam epitaxy," *Semiconductor Science and Technolology*, vol. 11, no. 8, pp. 1185–1188, 1996.

[156] S. Sato and S. Satoh, "Room-temperature continuous-wave operation of 1.24-$\mu$m GaInNAs lasers grown by metal-organic chemical vapor deposition," *IEEE Journal of Selected Topics in Quantum Electronics*, vol. 5, no. 3, pp. 707–710, 1999.

[157] J.-P. Tourrenc, S. Bouchoule, A. Khadour, J.-C. Harmand, A. Miard, J. Decobert, N. Lagay, X. Lafosse, I. Sagnes, L. Leroy, and J.-L. Oudar, "Thermal optimization of 1.55 $\mu$m OP-VECSEL with hybrid metal-metamorphic mirror for single-mode high power operation," *Optical and Quantum Electronics*, vol. 40, pp. 155–165, 2008.

[158] A. Khadour, S. Bouchoule, G. Aubin, J.-C. Harmand, J. Decobert, and J.-L. Oudar, "Ultrashort pulse generation from 1.56 $\mu$m mode-locked VECSEL at room temperature," *Optics Express*, vol. 18, no. 19, pp. 19 902–19 913, 2010.

[159] I. Tångring, S. Wang, M. Sadeghi, A. Larsson, and X. Wang, "Metamorphic growth of 1.25–1.29 $\mu$m InGaAs quantum well lasers on GaAs by molecular beam epitaxy," *Journal of Crystal Growth*, vol. 301-302, pp. 971–974, 2007.

[160] Z. L. Liau and D. E. Mull, "Wafer fusion: A novel technique for optoelectronic device fabrication and monolithic integration," *Applied Physics Letters*, vol. 56, no. 8, pp. 737–739, 1990.

[161] A. Black, A. Hawkins, N. Margalit, D. Babic, J. Holmes, A.L., Y.-L. Chang, P. Abraham, J. Bowers, and E. Hu, "Wafer fusion: materials issues and device results," *IEEE Journal of Selected Topics in Quantum Electronics*, vol. 3, no. 3, pp. 943–951, 1997.

[162] A. Sirbu, A. Mereuta, A. Caliman, N. Volet, Q. Zhu, V. Iakovlev, J. Rautiainen, J. Lyytikäinen, O. Okhotnikov, J. Walczak, M. Wasiak, T. Czyszanowski, and E. Kapon, "High-power optically-pumped VECSELs emitting in the 1310-nm and 1550-nm wavebands," in *Proceedings of SPIE*, vol. 7919, 791903, 2011.

[163] R. J. Ram, J. J. Dudley, J. E. Bowers, L. Yang, K. Carey, S. J. Rosner, and K. Nauka, "GaAs to InP wafer fusion," *Journal of Applied Physics*, vol. 78, no. 6, pp. 4227–4237, 1995.

[164] J. Rautiainen, J. Lyytikäinen, A. Sirbu, A. Mereuta, A. Caliman, E. Kapon, and O. G. Okhotnikov, "2.6 W optically-pumped semiconductor disk laser operating at 1.57-$\mu$m using wafer fusion," *Optics Express*, vol. 16, no. 26, pp. 21 881–21 886, 2008.

[165] D. I. Babic and S. W. Corzine, "Analytic expressions for the reflection delay, penetration depth, and absorptance of quarter-wave dielectric mirrors," *IEEE Journal of Quantum Electronics*, vol. 28, no. 2, pp. 514–524, 1992.

[166] C. J. R. Sheppard, "Approximate calculation of the reflection coefficient from a stratified medium," *Pure and Applied Optics: Journal of the European Optical Society Part A*, vol. 4, no. 5, p. 665, 1995.

[167] A. Syrbu, J. Fernandez, J. Behrend, C. Berseth, J. Carlin, A. Rudra, and E. Kapon, "InGaAs/InGaAsP/InP edge emitting laser diodes on p-GaAs substrates obtained by localised wafer fusion," *IET Electronics Letters*, vol. 33, no. 10, pp. 866–868, 1997.

[168] A. Syrbu, J. Fernandez, J. Behrend, L. Sagalowicz, V. Iakovlev, J. Carlin, C. Berseth, A. Rudra, and E. Kapon, "Characteristics of InAsP/InGaAsP edge emitting laser diodes obtained by localised fusion on GaAs substrates," *IET Electronics Letters*, vol. 33, no. 23, pp. 1954–1955, 1997.

[169] A. Syrbu, V. Iakovlev, C.-A. Berseth, O. Dehaese, A. Rudra, E. Kapon, J. Jacquet, J. Boucart, C. Stark, F. Gaborit, I. Sagnes, J. Harmand, and R. Raj, "30 °C CW operation of 1.52 $\mu$m InGaAsP/AlGaAs vertical cavity lasers with in situ built-in lateral current confinement by localised fusion," *IET Electronics Letters*, vol. 34, no. 18, pp. 1744–1745, 1998.

[170] A. Sirbu, E. Saarinen, J. Rautiainen, J. Puustinen, A. Mereuta, J. Lyytikäinen, L. Toikkanen, J. Nikkinen, A. Caliman, V. Iakovlev, O. Okhotnikov, and E. Kapon, "Wafer-fused 1310 nm and 1550 nm mode-locked semiconductor disk lasers," in *the 12th International Conference on Transparent Optical Networks (ICTON) 2010*, July 2010, pp. 1–4.

[171] M. Kondow, T. Kitatani, S. Nakatsuka, M. C. Larson, K. Nakahara, Y. Yazawa, M. Okai, and K. Uomi, "GaInNAs: a novel material for long-wavelength semiconductor lasers," *IEEE Journal of Selected Topics in Quantum Electronics*, vol. 3, no. 3, pp. 719–730, 1997.

[172] O. G. Okhotnikov, T. Jouhti, J. Konttinen, S. Karirinne, and M. Pessa, "1.5 $\mu$m monolithic GaInNAs semiconductor saturable-absorber mode locking of an erbium fiber laser," *Optics Letters*, vol. 28, no. 5, pp. 364–366, 2003.

[173] V. Liverini, S. Schön, R. Grange, M. Haiml, S. C. Zeller, and U. Keller, "Low-loss GaInNAs saturable absorber mode locking a 1.3-$\mu$m solid-state laser," *Applied Physics Letters*, vol. 84, no. 20, pp. 4002–4004, 2004.

[174] A. Rutz, R. Grange, V. Liverini, M. Haiml, S. Schon, and U. Keller, "1.5 $\mu$m GaInNAs semiconductor saturable absorber for passively modelocked solid-state lasers," *IET Electronics Letters*, vol. 41, no. 6, pp. 321–323, 2005.

[175] W. Streifer and J. R. Whinnery, "Analysis of a dye laser tuned by acousto-optic filter," *Applied Physics Letters*, vol. 17, no. 8, pp. 335–337, 1970.

[176] M. P. Nikodem, E. Kluzniak, and K. Abramski, "Wavelength tunability and pulse duration control in frequency shifted feedback Er-doped fiber lasers," *Optics Express*, vol. 17, no. 5, pp. 3299–3304, 2009.

[177] M. W. Phillips, G. Y. Liang, and J. R. M. Barr, "Nd:YLF Laser with Frequency-Shifted Feedback," in *Proceedings of Advanced Solid State Lasers*, vol. 15, p. NL3, 1993.

[178] A. Heidt, G. Bosman, M. Becker, M. Rothhardt, K. Schuster, J. Kobelke, and H. Bartelt, "Prospects of high energy ultrashort pulse generation with frequency shifted feedback fiber oscillators," in *European Conference on Lasers and Electro-Optics 2009 and the European Quantum Electronics Conference (CLEO Europe - EQEC 2009)*, June 2009, p. 1.

[179] J. C. Slater, "Interaction of waves in crystals," *Reviews of Modern Physics*, vol. 30, pp. 197–222, 1958.

[180] D. Auth, "Equivalence of Doppler and quantum frequency shifting in Bragg cells," *Proceedings of the IEEE*, vol. 59, no. 3, pp. 413–414, 1971.

[181] O. G. Okhotnikov, "Multiwavelength picosecond frequency-shifted feedback laser with pulse control by a shaped-gain fiber amplifier," *Optics Letters*, vol. 23, no. 18, pp. 1459–1461, 1998.

[182] S. Alam and A. Grudinin, "Tunable picosecond frequency-shifted feedback fiber laser at 1550 nm," *IEEE Photonics Technology Letters*, vol. 16, no. 9, pp. 2012–2014, 2004.

[183] D. J. Maas, B. Rudin, A.-R. Bellancourt, D. Iwaniuk, S. V. Marchese, T. Südmeyer, and U. Keller, "High precision optical characterization of semiconductor saturable absorber mirrors," *Optics Express*, vol. 16, no. 10, pp. 7571–7579, 2008.

[184] T. Hakulinen, "Towards Stabilized, Short Pulse Q-switched Fiber Lasers," Ph.D. dissertation, Tampere University of Technology, Tampere, Finland, 2010.

[185] E. R. Thoen, E. M. Koontz, M. Joschko, P. Langlois, T. R. Schibli, F. X. Kärtner, E. P. Ippen, and L. A. Kolodziejski, "Two-photon absorption in semiconductor saturable absorber mirrors," *Applied Physics Letters*, vol. 74, no. 26, pp. 3927–3929, 1999.

[186] R. Grange, M. Haiml, R. Paschotta, G. Spühler, L. Krainer, M. Golling, O. Ostinelli, and U. Keller, "New regime of inverse saturable absorption for self-stabilizing passively mode-locked lasers," *Applied Physics B: Lasers and Optics*, vol. 80, pp. 151–158, 2005.

[187] L. M. Frantz and J. S. Nodvik, "Theory of pulse propagation in a laser amplifier," *Journal of Applied Physics*, vol. 34, no. 8, pp. 2346–2349, 1963.

[188] D. J. H. C. Maas, "MIXSELs –A New Class of Ultrafast Semiconductor Lasers," Ph.D. dissertation, Swiss Federal Institute of Technology, Zürich, Switzerland, 2008.

[189] M. Haiml, R. Grange, and U. Keller, "Optical characterization of semiconductor saturable absorbers," *Applied Physics B: Lasers and Optics*, vol. 79, pp. 331–339, 2004.

[190] R. Herda, T. Hakulinen, S. Suomalainen, and O. G. Okhotnikov, "Cavity-enhanced saturable and two-photon absorption in semiconductors," *Applied Physics Letters*, vol. 87, no. 21, p. 211105, 2005.

[191] J. Shelton and J. Armstrong, "Measurement of the relaxation time of the Eastman 9740 bleachable dye," *IEEE Journal of Quantum Electronics*, vol. 3, no. 12, pp. 696–697, 1967.

[192] C. J. Saraceno, O. H. Heckl, C. R. E. Baer, M. Golling, T. Südmeyer, K. Beil, C. Kränkel, K. Petermann, G. Huber, and U. Keller, "SESAMs for high-power femtosecond mode-locking: power scaling of an Yb:$LuScO_3$ thin disk laser to 23 W and 235 fs," *Optics Express*, vol. 19, no. 21, pp. 20 288–20 300, 2011.

[193] J. Shah, *Ultrafast Spectroscopy of Semiconductors and Semiconductor Nanostructures*. Berlin: Springer, 1999.

[194] W. H. Knox, C. Hirlimann, D. A. B. Miller, J. Shah, D. S. Chemla, and C. V. Shank, "Femtosecond Excitation of Nonthermal Carrier Populations in GaAs Quantum Wells," *Physical Review Letters*, vol. 56, pp. 1191–1193, 1986.

[195] W. H. Knox, D. S. Chemla, D. A. B. Miller, J. B. Stark, and S. Schmitt-Rink, "Femtosecond ac Stark effect in semiconductor quantum wells: Extreme low- and high-intensity limits," *Physical Review Letters*, vol. 62, pp. 1189–1192, 1989.

[196] S. Hoogland, A. Garnache, I. Sagnes, J. S. Roberts, and A. C. Tropper, "10-GHz train of sub-500-fs optical soliton-like pulses from a surface-emitting semiconductor laser," *IEEE Photonics Technology Letters*, vol. 17, no. 2, pp. 267–269, 2005.

[197] Keith G. Wilcox, Zakaria Mihoubi, G. J. Daniell, Stephen Elsmere, Adrian Quarterman, Ian Farrer, David A. Ritchie, and Anne Tropper, "Ultrafast optical Stark mode-locked semiconductor laser," *Optics Letters*, vol. 33, no. 23, pp. 2797–2799, 2008.

[198] T. Hakulinen, R. Herda, and O. G. Okhotnikov, "Effect of post-epitaxial-growth processing on the nonlinear response of saturable absorber," *Applied Optics*, vol. 47, no. 9, pp. 1235–1238, 2008.

[199] L. R. Brovelli, U. Keller, and T. H. Chiu, "Design and operation of antiresonant Fabry–Perot saturable semiconductor absorbers for mode-locked solid-state lasers," *Journal of the Optical Society of America B*, vol. 12, no. 2, pp. 311–322, 1995.

[200] A. Jasik, J. Muszalski, K. Pierscinski, M. Bugajski, V. G. Talalaev, and M. Kosmala, "Low-temperature grown near surface semiconductor saturable absorber mirror: Design, growth conditions, characterization, and mode-locked operation," *Journal of Applied Physics*, vol. 106, no. 5, p. 053101, 2009.

[201] R. Herda and O. Okhotnikov, "Dispersion compensation-free fiber laser mode-locked and stabilized by high-contrast saturable absorber mirror," *IEEE Journal of Quantum Electronics*, vol. 40, no. 7, pp. 893–899, 2004.

[202] D. J. H. C. Maas, A. R. Bellancourt, M. Hoffmann, B. Rudin, Y. Barbarin, M. Golling, T. Südmeyer, and U. Keller, "Growth parameter optimization for fast quantum dot SESAMs," *Optics Express*, vol. 16, no. 23, pp. 18 646–18 656, 2008.

[203] G. Spühler, K. Weingarten, R. Grange, L. Krainer, M. Haiml, V. Liverini, M. Golling, S. Schön, and U. Keller, "Semiconductor saturable absorber mirror structures with low saturation fluence," *Applied Physics B: Lasers and Optics*, vol. 81, pp. 27–32, 2005.

[204] E. L. Delpon, J. L. Oudar, N. Bouché, R. Raj, A. Shen, N. Stelmakh, and J. M. Lourtioz, "Ultrafast excitonic saturable absorption in ion-implanted InGaAs/InAlAs multiple quantum wells," *Applied Physics Letters*, vol. 72, no. 7, pp. 759–761, 1998.

[205] S. Suomalainen, M. Guina, T. Hakulinen, O. G. Okhotnikov, T. G. Euser, and S. Marcinkevicius, "1 $\mu$m saturable absorber with recovery time reduced by lattice mismatch," *Applied Physics Letters*, vol. 89, no. 7, p. 071112, 2006.

[206] O. Ostinelli, W. Bächtold, H. Haiml, R. Grange, U. Keller, E. Gini, and G. Almuneau, "Carrier lifetime reduction in 1.5 $\mu$m AlGaAsSb saturable absorbers with air and AlAsSb barriers," *Applied Physics Letters*, vol. 89, no. 7, p. 071114, 2006.

[207] D. Kopf, G. Zhang, R. Fluck, M. Moser, and U. Keller, "All-in-one dispersion-compensating saturable absorber mirror for compact femtosecond laser sources," *Optics Letters*, vol. 21, no. 7, pp. 486–488, 1996.

[208] M. Guina, N. Xiang, and O. Okhotnikov, "Stretched-pulse fiber lasers based on semiconductor saturable absorbers," *Applied Physics B: Lasers and Optics*, vol. 74, pp. s193–s200, 2002.

[209] A. Isomäki, A. Vainionpää, J. Lyytikäinen, and O. G. Okhotnikov, "Semiconductor mirror for dynamic dispersion compensation," *Applied Physics Letters*, vol. 82, no. 17, pp. 2773–2774, 2003.

[210] R. Herda, "Semiconductor Mirrors for Ultrafast Fiber Technology," Ph.D. dissertation, Tampere University of Technology, Tampere, Finland, 2006.

[211] R. Takahashi, Y. Kawamura, and H. Iwamura, "Ultrafast 1.55 $\mu$m all-optical switching using low-temperature-grown multiple quantum wells," *Applied Physics Letters*, vol. 68, no. 2, pp. 153–155, 1996.

[212] F. Saas, G. Steinmeyer, U. Griebner, M. Zorn, and M. Weyers, "Exciton resonance tuning for the generation of subpicosecond pulses from a mode-locked semiconductor disk laser," *Applied Physics Letters*, vol. 89, no. 14, p. 141107, 2006.

[213] R. E. McClure, "Mode locking behavior of gas lasers in long cavities," *Applied Physics Letters*, vol. 7, no. 6, pp. 148–150, 1965.

[214] J. Hirano and T. Kimura, "Multiple mode locking of lasers," *IEEE Journal of Quantum Electronics*, vol. 5, no. 5, pp. 219–225, 1969.

[215] M. Becker, D. Kuizenga, and A. Siegman, "Harmonic mode locking of the Nd:YAG laser," *IEEE Journal of Quantum Electronics*, vol. 8, no. 8, pp. 687–693, 1972.

[216] G. T. Harvey and L. F. Mollenauer, "Harmonically mode-locked fiber ring laser with an internal Fabry-Perot stabilizer for soliton transmission," *Optics Letters*, vol. 18, no. 2, pp. 107–109, 1993.

[217] A. E. Siegman, *Lasers*, 1st ed. Mill Valley, Ca: University Science Books, 1986.

[218] J. N. Kutz and B. Sandstede, "Theory of passive harmonic mode-locking using waveguide arrays," *Optics Express*, vol. 16, no. 2, pp. 636–650, 2008.

[219] W. E. Lamb, "Theory of an Optical Maser," *Physical Review*, vol. 134, pp. A1429–A1450, 1964.

[220] O. E. Martinez, R. L. Fork, and J. P. Gordon, "Theory of passively mode-locked lasers including self-phase modulation and group-velocity dispersion," *Optics Letters*, vol. 9, no. 5, pp. 156–158, 1984.

[221] H. Haus, J. Fujimoto, and E. Ippen, "Analytic theory of additive pulse and Kerr lens mode locking," *IEEE Journal of Quantum Electronics*, vol. 28, no. 10, pp. 2086–2096, 1992.

[222] F. Kärtner, I. Jung, and U. Keller, "Soliton mode-locking with saturable absorbers," *IEEE Journal of Selected Topics in Quantum Electronics*, vol. 2, no. 3, pp. 540–556, 1996.

[223] N. N. Akhmediev, A. Ankiewicz, M. J. Lederer, and B. Luther-Davies, "Ultrashort pulses generated by mode-locked lasers with either a slow or a fast saturable-absorber response," *Optics Letters*, vol. 23, no. 4, pp. 280–282, 1998.

[224] A. G. Vladimirov and D. Turaev, "Model for passive mode locking in semiconductor lasers," *Physical Review A*, vol. 72, p. 033808, 2005.

[225] E. D. Farnum and J. N. Kutz, "Master mode-locking theory for few-femtosecond pulses," *Optics Letters*, vol. 35, no. 18, pp. 3033–3035, 2010.

[226] H. Haus, "Mode-locking of lasers," *IEEE Journal of Selected Topics in Quantum Electronics*, vol. 6, no. 6, pp. 1173–1185, 2000.

[227] P. Smith, "Mode-locking of lasers," *Proceedings of the IEEE*, vol. 58, no. 9, pp. 1342–1357, 1970.

[228] E. P. Ippen, "Principles of passive mode locking," *Applied Physics B: Lasers and Optics*, vol. 58, pp. 159–170, 1994.

[229] F. Kaertner, *Ultrafast Optics Textbook*, 1st ed., 2006, ch. 7. [Online]. Available: http://frog.gatech.edu/prose.html

[230] F. X. Kärtner, L. R. Brovelli, D. Kopf, M. Kamp, I. G. Calasso, and U. Keller, "Control of solid state laser dynamics by semiconductor devices," *Optical Engineering*, vol. 34, no. 7, pp. 2024–2036, 1995.

[231] E. Avrutin, J. Marsh, and E. Portnoi, "Monolithic and multi-gigahertz mode-locked semiconductor lasers: constructions, experiments, models and applications," *IEE Proceedings Optoelectronics*, vol. 147, no. 4, pp. 251–278, 2000.

[232] S. Namiki, E. P. Ippen, H. A. Haus, and C. X. Yu, "Energy rate equations for mode-locked lasers," *Journal of the Optical Society of America B*, vol. 14, no. 8, pp. 2099–2111, 1997.

[233] J. Kutz, B. Collings, K. Bergman, and W. Knox, "Stabilized pulse spacing in soliton lasers due to gain depletion and recovery," *IEEE Journal of Quantum Electronics*, vol. 34, no. 9, pp. 1749–1757, 1998.

[234] C. Ausschnitt, "Transient evolution of passive mode locking," *IEEE Journal of Quantum Electronics*, vol. 13, no. 5, pp. 321–333, 1977.

[235] M. Kuznetsov, D. Z. Tsang, J. N. Walpole, Z. L. Liau, and E. P. Ippen, "Multistable mode locking of InGaAsP semiconductor lasers," *Applied Physics Letters*, vol. 51, no. 12, pp. 895–897, 1987.

[236] S. Sanders, A. Yariv, J. Paslaski, J. E. Ungar, and H. A. Zarem, "Passive mode locking of a two-section multiple quantum well laser at harmonics of the cavity round-trip frequency," *Applied Physics Letters*, vol. 58, no. 7, pp. 681–683, 1991.

[237] M. Nizette, D. Rachinskii, A. Vladimirov, and M. Wolfrum, "Pulse interaction via gain and loss dynamics in passive mode locking," *Physica D: Nonlinear Phenomena*, vol. 218, no. 1, pp. 95–104, 2006.

[238] G. New, "Mode-locking of quasi-continuous lasers," *Optics Communications*, vol. 6, no. 2, pp. 188–192, 1972.

[239] O. E. Martinez, R. L. Fork, and J. P. Gordon, "Theory of passively mode-locked lasers for the case of a nonlinear complex-propagation coefficient," *Journal of the Optical Society of America B*, vol. 2, no. 5, pp. 753–760, 1985.

[240] F. X. Kärtner and U. Keller, "Stabilization of solitonlike pulses with a slow saturable absorber," *Optics Letters*, vol. 20, no. 1, pp. 16–18, 1995.

[241] C. Spielmann, P. Curley, T. Brabec, and F. Krausz, "Ultrabroadband femtosecond lasers," *IEEE Journal of Quantum Electronics*, vol. 30, no. 4, pp. 1100–1114, 1994.

[242] K. G. Wilcox, A. H. Quarterman, H. E. Beere, D. A. Ritchie, and A. C. Tropper, "Repetition-frequency-tunable mode-locked surface emitting semiconductor laser between 2.78 and 7.87 GHz," *Optics Express*, vol. 19, no. 23, pp. 23 453–23 459, 2011.

[243] A. Quarterman, S. Carswell, G. Daniell, Z. Mihoubi, K. Wilcox, A. Chung, V. Apostolopoulos, and A. Tropper, "Numerical simulation of optical Stark effect saturable absorbers in mode-locked femtosecond VECSELs using a modified two-level atom model," *Optics Express*, vol. 19, no. 27, pp. 26 783–26 795, 2011.

[244] M. Bahl, H. Rao, N. C. Panoiu, and J. Richard M. Osgood, "Simulation of mode-locked surface-emitting lasers through a finite-difference time-domain algorithm," *Optics Letters*, vol. 29, no. 14, pp. 1689–1691, 2004.

[245] J. Mulet and S. Balle, "Mode-locking dynamics in electrically driven vertical-external-cavity surface-emitting lasers," *IEEE Journal of Quantum Electronics*, vol. 41, no. 9, pp. 1148–1156, 2005.

[246] M. Kolesik and J. Moloney, "Time-Domain Vertical-External-Cavity Semiconductor Laser Simulation," *IEEE Journal of Quantum Electronics*, vol. 43, no. 7, pp. 588–596, 2007.

[247] J. Hader, S. Koch, and J. Moloney, "Microscopic theory of gain and spontaneous emission in GaInNAs laser material," *Solid-State Electronics*, vol. 47, no. 3, pp. 513–521, 2003.

[248] D. Lorenser, H. Unold, D. Maas, A. Aschwanden, R. Grange, R. Paschotta, D. Ebling, E. Gini, and U. Keller, "Towards wafer-scale integration of high repetition rate passively mode-locked surface-emitting semiconductor lasers," *Applied Physics B: Lasers and Optics*, vol. 79, pp. 927–932, 2004.

[249] Z. Mihoubi, G. Daniell, K. Wilcox, and A. Tropper, "Numerical model of a vertical-external-cavity surface-emitting semiconductor lasers mode-locked by the optical stark effect," in *the International Conference on Numerical Simulation of Optoelectronic Devices (NUSOD) '08*, Sept. 2008, pp. 91–92.

[250] G. Agrawal and C. Bowden, "Concept of linewidth enhancement factor in semiconductor lasers: its usefulness and limitations," *IEEE Photonics Technology Letters*, vol. 5, no. 6, pp. 640–642, 1993.

[251] M. Osinski and J. Buus, "Linewidth broadening factor in semiconductor lasers – An overview," *IEEE Journal of Quantum Electronics*, vol. 23, no. 1, pp. 9–29, 1987.

[252] C. Henry, "Theory of the linewidth of semiconductor lasers," *IEEE Journal of Quantum Electronics*, vol. 18, no. 2, pp. 259–264, 1982.

[253] A. Isomäki, "Ultrafast Fiber Lasers Using Novel Semiconductor Saturable Absorbers and Photonic-Crystal Dispersion Compensators," Ph.D. dissertation, Tampere University of Technology, Tampere, Finland, 2007.

[254] M. Hoffmann, O. D. Sieber, D. J. H. C. Maas, V. J. Wittwer, M. Golling, T. Südmeyer, and U. Keller, "Experimental verification of soliton-like pulse-shaping mechanisms in passively mode-locked VECSELs," *Optics Express*, vol. 18, no. 10, pp. 10 143–10 153, 2010.

[255] A. H. Quarterman, K. G. Wilcox, V. Apostolopoulos, Z. Mihoubi, M. Barnes, I. Farrer, D. A. Ritchie, and A. Tropper, "Gain saturation in 60-fs mode-locked semiconductor laser," in *Conference on Lasers and Electro-Optics (CLEO) and Quantum Electronics and Laser Science Conference (QELS) 2010*, May 2010, pp. 1–2.

[256] J. L. Oudar, D. Hulin, A. Migus, A. Antonetti, and F. Alexandre, "Subpicosecond Spectral Hole Burning Due to Nonthermalized Photoexcited Carriers in GaAs," *Physical Review Letters*, vol. 55, pp. 2074–2077, 1985.

[257] W. H. Knox, R. L. Fork, M. C. Downer, D. A. B. Miller, D. S. Chemla, C. V. Shank, A. C. Gossard, and W. Wiegmann, "Femtosecond Dynamics of Resonantly Excited Excitons in Room-Temperature GaAs Quantum Wells," *Physical Review Letters*, vol. 54, pp. 1306–1309, 1985.

[258] H. Haug and S. W. Koch, *Quantum Theory of the Optical and Electronic Properties of Semiconductors*. Singapore: World Scientific, 2004.

[259] A. V. Lehmen, D. S. Chemla, J. E. Zucker, and J. P. Heritage, "Optical Stark effect on excitons in GaAs quantum wells," *Optics Letters*, vol. 11, no. 10, pp. 609–611, 1986.

[260] A. Mysyrowicz, D. Hulin, A. Antonetti, A. Migus, W. T. Masselink, and H. Morkoç, ""Dressed Excitons" in a Multiple-Quantum-Well Structure: Evidence for an Optical Stark Effect with Femtosecond Response Time," *Physical Review Letters*, vol. 56, pp. 2748–2751, 1986.

[261] S. Schmitt-Rink and D. S. Chemla, "Collective excitations and the dynamical stark effect in a coherently driven exciton system," *Physical Review Letters*, vol. 57, pp. 2752–2755, 1986.

[262] S. Schmitt-Rink, D. S. Chemla, and H. Haug, "Nonequilibrium theory of the optical Stark effect and spectral hole burning in semiconductors," *Physical Review B*, vol. 37, pp. 941–955, 1988.

[263] O. Svelto, *Principles of Lasers*, 4th ed. New York, NY: Plenum Press, 1998.

[264] M. E. Fermann, A. Galvanauskas, and G. Sucha (ed.), *Ultrafast lasers: technology and applications*, 1st ed. New York – Basel: Marcel Dekker, 2003.

[265] J. N. Kutz, B. C. Collings, K. Bergman, S. Tsuda, S. T. Cundiff, W. H. Knox, P. Holmes, and M. Weinstein, "Mode-locking pulse dynamics in a fiber laser with a saturable Bragg reflector," *Journal of the Optical Society of America B*, vol. 14, no. 10, pp. 2681–2690, 1997.

[266] G. P. Agrawal, *Nonlinear Fiber Optics*, 3rd ed. San Diego, CA: Academic Press, 2001.

[267] G. Agrawal, "Effect of gain dispersion on ultrashort pulse amplification in semiconductor laser amplifiers," *IEEE Journal of Quantum Electronics*, vol. 27, no. 6, pp. 1843–1849, 1991.

[268] P. V. Mamyshev and S. V. Chernikov, "Ultrashort-pulse propagation in optical fibers," *Optics Letters*, vol. 15, no. 19, pp. 1076–1078, 1990.

[269] R. H. Stolen, J. P. Gordon, W. J. Tomlinson, and H. A. Haus, "Raman response function of silica-core fibers," *Journal of the Optical Society of America B*, vol. 6, no. 6, pp. 1159–1166, 1989.

[270] L. F. Mollenauer, R. H. Stolen, and J. P. Gordon, "Experimental observation of picosecond pulse narrowing and solitons in optical fibers," *Physical Review Letters*, vol. 45, pp. 1095–1098, 1980.

[271] J. A. C. Weideman and B. M. Herbst, "Split-step methods for the solution of the nonlinear schrödinger equation," *SIAM Journal on Numerical Analysis*, vol. 23, no. 3, pp. 485–507, 1986.

[272] A. Lagatsky, C. Leburn, C. Brown, W. Sibbett, S. Zolotovskaya, and E. Rafailov, "Ultrashort-pulse lasers passively mode locked by quantum-dot-based saturable absorbers," *Progress in Quantum Electronics*, vol. 34, no. 1, pp. 1–45, 2010.

[273] A. H. Quarterman, A. Perevedentsev, K. G. Wilcox, V. Apostolopoulos, H. E. Beere, I. Farrer, D. A. Ritchie, and A. C. Tropper, "Passively harmonically mode-locked vertical-external-cavity surface-emitting laser emitting 1.1 ps pulses at 147 GHz repetition rate," *Applied Physics Letters*, vol. 97, no. 251101, pp. 1–3, 2010.

[274] V. D. S. Dhaka, N. V. Tkachenko, E.-M. Pavelescu, H. Lemmetyinen, T. Hakkarainen, M. Guina, J. Konttinen, O. Okhotnikov, M. Pessa, K. Arstila, and J. Keinonen, "$Ni^{+}$-irradiated InGaAs/GaAs quantum wells: picosecond carrier dynamics," *New Journal of Physics*, vol. 7, p. 131, 2005.

[275] G. Baili, F. Bretenaker, M. Alouini, L. Morvan, D. Dolfi, and I. Sagnes, "Experimental Investigation and Analytical Modeling of Excess Intensity Noise in Semiconductor Class-A Lasers," *Journal of Lightwave Technology*, vol. 26, no. 8, pp. 952–961, 2008.

[276] H. Haus, "Parameter ranges for cw passive mode locking," *IEEE Journal of Quantum Electronics*, vol. 12, no. 3, pp. 169–176, 1976.

[277] D. E. McCumber, "Einstein relations connecting broadband emission and absorption spectra," *Physical Review*, vol. 136, pp. A954–A957, 1964.

[278] G. Keeler, B. Nelson, D. Agarwal, C. Debaes, N. Helman, A. Bhatnagar, and D. Miller, "The benefits of ultrashort optical pulses in optically interconnected systems," *IEEE Journal of Selected Topics in Quantum Electronics*, vol. 9, no. 2, pp. 477–485, 2003.

[279] Z. Jiang, C.-B. Huang, D. E. Leaird, and A. M. Weiner, "Optical arbitrary waveform processing of more than 100 spectral comb lines," *Nature Photonics*, vol. 1, no. 8, pp. 463–467, 2007.

[280] R. Ludwig, "Pushing the speed limit," *Communications Engineer*, vol. 3, no. 5, pp. 14–16, 2005.

[281] E. J. Saarinen, "1 $\mu$m picosecond semiconductor lasers with vertical external cavity: technology and characterization techniques," Master's thesis, Tampere University of Technology, Tampere, Finland, 2006.

[282] P. W. Smith, Y. Silberberg, and D. A. B. Miller, "Mode locking of semiconductor diode lasers using saturable excitonic nonlinearities," *Journal of the Optical Society of America B*, vol. 2, no. 7, pp. 1228–1236, 1985.

[283] J. Kutz, "Mode-locked soliton lasers," *SIAM Review*, vol. 48, no. 4, pp. 629–678, 2006.

[284] D. N. Maywar, "All-Optical Processing of Optical-Network Signals using Distributed Feedback Amplifiers," Ph.D. dissertation, University of Rochester, Rochester, United States, 2000.

[285] A. K. Komarov and K. P. Komarov, "Multistability and hysteresis phenomena in passive mode-locked lasers," *Physical Review E*, vol. 62, pp. R7607–R7610, 2000.

[286] A. Komarov, K. Komarov, and E. Pestryakov, "Multiple pulse passive mode locking in lasers with spectrally inhomogeneous gain," *Optics and Spectroscopy*, vol. 100, pp. 623–630, 2006.

P1

# Publication 1

E. J. Saarinen, J. Puustinen, A. Sirbu, A. Mereuta, A. Caliman, E. Kapon, and O. G. Okhotnikov, “Power-scalable 1.57 μm mode-locked semiconductor disk laser using wafer fusion,” Optics Letters, vol. 34, no. 20, pp. 3139–3141, 2009.

# Publication 2

P2

E. J. Saarinen, J. Nikkinen, and O. G. Okhotnikov, ”Semiconductor disk laser with frequency-shifted feedback,” IEEE Photonics Technology Letters, vol. 23, no. 9, pp. 567–569, 2011.

# Publication 3

P3

E. J. Saarinen, J. Nikkinen, and O. G. Okhotnikov, ”Mode-locked semiconductor disk lasers with weakly saturated absorbers,” Optics Communications, vol. 285, no. 10–11, pp. 2688–2692, 2012.

# Publication 4

E. J. Saarinen, A. Härkönen, R. Herda, L. Orsila, T. Hakulinen, M. Guina, and O. G. Okhotnikov, ”Harmonically mode-locked VECSELs for multi-GHz pulse train generation,” Optics Express, vol. 15, no. 3, pp. 955–964, 2007.



P4

# Publication 5

E. J. Saarinen, R. Herda, and O. G. Okhotnikov, ”Dynamics of pulse formation in mode-locked semiconductor disk lasers,” Journal of the Optical Society of America B, vol. 24, no. 11, pp. 2784–2790, 2007.



P5

# Publication 6

E. J. Saarinen, J. Lyytikäinen, and O. G. Okhotnikov, ”Hysteresis and multiple pulsing in a semiconductor disk laser with a saturable absorber,” Physical Review E, vol. 78, no. 1, p. 016207, 2008.



P6

Tampereen teknillinen yliopisto
PL 527
33101 Tampere

Tampere University of Technology
P.O.B. 527
FI-33101 Tampere, Finland

ISBN 978-952-15-2868-2
ISSN 1459-2045